SELECTIVE MOLECULAR RECOGNITION IN IMPRINTED POLYMERIC ADSORBENTS AND IN BIOLOGICAL MACROMOLECULES

Thesis by

Vidyasankar Sundaresan

In partial fulfilment of the requirements

for the degree of

Doctor of Philosophy

California Institute of Technology

Pasadena, CA

2002

(Submitted September 18, 2001)

To my parents, my first teachers,

Who taught me the value of tireless effort,

persistence and resolution in every undertaking

ACKNOWLEDGEMENTS

Most of this thesis reports the results of work done between 1992 and 1997, in the laboratory of Prof. Frances H. Arnold, but unforeseen circumstances delayed its formal submission. I am grateful to the Department of Chemical Engineering, California Institute of Technology, for having given me an opportunity to present this dissertation, including both my earlier work and new research conducted in 2000-2001.

Various former members of the Arnold research group have taught me how to think about and do chemistry. I am deeply grateful to Dr. Pradeep Dhal, Dr. Robert Johnson, Dr. Sanku Mallik and Dr. Barry Haymore, from whom I learnt about synthetic organic chemistry, polymer chemistry and metal-ligand coordination chemistry. My sincere thanks are also due to Dr. Litian Fu, for her help with isothermal calorimetric experiments for measuring metal ligand binding constants.

I wish to thank Dr. Vijayaraghavan of JPL, the Narayan family in Cerritos, and Guru, Jeremy, Dave, Ravi, Swami and Anupama at Caltech, for their help and support during particularly critical times. I am indeed blessed in having a very loyal brother and no man could ask for a kinder, sweeter and more highly accommodating wife than mine. Kiranavali's patience, strength and support have been crucial to me, and I hope I can reciprocate in future. My everlasting gratitude goes to all my family, for constantly believing in me and for providing the necessary motivation and periodic morale boosts.

ABSTRACT

This thesis describes the synthesis and use of molecularly imprinted polymeric adsorbents for use in ligand-exchange chromatographic separations of structurally similar substrates. A general model of stereoselectivity is also described, which can be applied both to chromatographic adsorbents and to biological receptors.

Crosslinking polymerization of trimethylolpropane trimethacrylate (TRIM), under controlled conditions yields macroporous polymers bearing surface-accessible unpolymerized methacrylate residues. These residues have been utilized for copolymerization with different functional monomers to obtain composite polymer matrices with surface coatings of functional polymer chains. Surface modification has been carried out by molecular imprinting, using ternary Cu^{2+} complexes of [*N*-(4-vinylbenzyl)imino]diacetate and bisimidazole templates, with ethylene glycol dimethacrylate as comonomer. Selectivity characteristics similar to bulk-copolymerized polymers have been observed. The physicochemical characteristics of these functional polymer matrices have been evaluated by ^{13}C NMR, X-ray photoelectron spectroscopy, IR spectroscopy, and scanning electron microscopy.

The ability of molecular imprinting to impart enantioselectivity to polymeric adsorbents has been studied using Cu^{2+} complexes of the achiral monomer [*N*-(4-vinylbenzyl)imino]diacetate and α-amino acids. Crosslinking polymerization with ethylene glycol dimethacrylate as the comonomer yields polymeric adsorbents capable of enantioresolutions of underivatized α-amino acids. Chromatographic adsorbents have been prepared by grafting the imprinted polymer on to silica particles. The observed enantioselectivity increases corresponding to the size of the side chain of the amino acid

used as template, with the best enantioresolutions being obtained for materials imprinted against phenylalanine (~ 1.65 for D,L-phenylalanine enantioresolution). Adsorbents imprinted for alanine show negligible enantioselectivity. Cross-selectivity patterns towards non-template amino acids have been investigated, and the ability of an amino acid imprinted material to resolve analogous chiral amines has been demonstrated.

The mechanisms underlying enantioselectivity in imprinted polymers are discussed in terms of the three-point interaction model. This model has been extended to a stereocenter-recognition (SR) model for substrates with multiple stereocenters. For N stereocenters in a linear chain, it has been demonstrated that a minimum of $N+2$ interactions need to be distributed over all stereocenters, such that three effective interactions exist per stereocenter. The general applicability of the SR model is demonstrated for biological ligand-receptor interactions, by reinterpreting several previous experimental observations.

TABLE OF CONTENTS

Chapter 5. A General Model for Stereoselectivity in Ligand-Receptor Interactions

LIST OF FIGURES

Chapter 1

Chapter 2

Chapter 3

Chapter 5

LIST OF TABLES

Chapter 2

Chapter 3

Chapter 1

Introduction

Symmetry and asymmetry in nature

A structure that lacks a plane of symmetry cannot be superimposed onto its mirror *image* by translation or rotation operations. The human hand is a striking visual example of such an object, and a handedness or chirality can be defined for all such asymmetric objects. Thus, a screw is said to be right-handed if its windings propagate clockwise along the screw axis, and left-handed otherwise. It should be noted that such a definition of handedness presumes at least a three-dimensional geometry. Objects that have specific handedness can be found at all length scales in the universe (Fig. 1. 1), e.g., galaxies, mollusc shells, quartz crystals, the DNA double-helix, secondary structures in proteins, e.g., α-helices and parallel and antiparallel β-sheets, small molecules, e.g., amino acids and sugars, and elementary particles, e.g., neutrinos and antineutrinos.

It is usually assumed that the basic forces of nature cannot distinguish left from right, so that the universe may be expected to be equally effective in either of two enantiomorphic ways (Gardner 1990). While this is true for the structures and interactions of macroscopic objects, the assumption breaks down at subatomic length scales. Neutrinos and antineutrinos have intrinsic parity, being uniquely left-handed and right-handed respectively, but interactions involving the weak nuclear force are known to violate parity conservation. Right-handed neutrinos and left-handed antineutrinos do not exist, so that all atomic nuclei are inherently chiral. However, the energy difference arising from the non-conservation of parity in elementary particles is largely negligible at the length scale of molecular interactions (Barron 1982). For all practical purposes, the two molecular structures that are related by a reflection operation are therefore taken to be energetically equivalent. The consequences of nuclear chirality are also more

significant for heavy atoms than for lighter ones (Bouchiat and Pottier 1986). For biologically important molecules such as amino acids and sugars, which are mostly made up of light atoms like H, C, N and O, both mirror images of asymmetric molecular structures are known to exist. For example, although proteins consist of L-amino acid units, peptides containing D-amino acids have been reported in numerous biological sources, from bacterial cells to vertebrate brains (Jollés 1998).

The biochemical significance of stereochemistry

The theoretical foundations for the structural aspects of chemistry, or stereochemistry, were provided by the tetrahedral carbon model proposed by van't Hoff and Le Bel (Ridell and Robinson 1974). Lord Kelvin (1904) initiated the modern discussion of molecular chirality, by noting out that if four different atoms are covalently bound to a tetrahedral carbon atom, two non-superimposable mirror image arrangements of these atoms are possible. A rigorous system of nomenclature for such molecules was proposed by Cahn, Ingold and Prelog (1966). Experimental observations of optical activity and the differing biological functions of asymmetric molecules have a much older history (Drayer 1993). Pasteur (1901) manually separated two crystal forms of tartaric acid, solutions of which rotated the plane of plane-polarized light in opposite directions, and reported that the mold *Penicillium glaucum* destroyed the *dextro* isomer of ammonium tartrate faster than the *levo* isomer. The importance of chirality was firmly established in biochemistry when it was discovered that amino acids and sugars (Barrett 1985; Lichtenthaler 1992) are chiral molecules, naturally occurring in predominantly one enantiomeric form.

Stereochemistry continues to be centrally important for all aspects of chemistry and biology, both in theoretical research and for practical applications. The preponderance of homochirality in terrestrial biochemistry raises numerous interesting scientific questions (Avalos et al. 2000). Most organic molecules are chiral (Sharpless et al. 1992), and most chiral molecules that are not readily available in enantiopure forms from biological sources are still being synthesized as racemic mixtures (Fig. 1. 2). It is therefore of great interest to develop sensing and separation techniques for a wide variety of chiral molecules. This is particularly felt in pharmacological research, because of the need to minimize or eliminate the undesirable side effects that frequently result from even minor amounts of isomeric impurities of drug molecules (Caldwell 1995; Eichelbaum and Gross 1996). One of the most significant examples of the dependence of drug activity on enantiomeric purity is the case of thalidomide, which was used during the 1960s as an anti-nausea prescription in early pregnancy. However, numerous birth defects resulted, leading to a ban on the drug, and it was later discovered that the *S*-enantiomer of the drug is purely responsible for teratogenic activity (Gaffield et al. 1999). The pure *R*- enantiomer of thalidomide has recently been approved for limited use in treating skin conditions associated with leprosy.

The implications of stereochemistry for medicine and drug action were first reported in Abderhalde and Müller's early investigations of the differential vasopressor effects of epinephrine enantiomers (Casey 1970). These observations also led to the development of the three-point attachment model for enantioselectivity (Easson and Stedman 1933). Although it has long been known that different stereoisomers of the same molecule seldom have equivalent pharmacological properties, most drug molecules

have typically been available only as racemic mixtures. In 1992, the United States Food and Drug Administration instituted guidelines to monitor stereochemical purity in formulations of drug molecules, the different structural isomers of which are not equipotent. In the recent past, 65% of the drugs approved for clinical use have been chiral molecules, with only 10% being approved as racemic mixtures (Fig. 1. 3). Regulatory agencies in many other countries have also instituted similar guidelines for stereochemical evaluation and approval of potential drug candidates. The importance of stereochemical purity is thus being increasingly felt, which creates a pressing need for developing enantioselective synthesis procedures and efficient enantioselective, or more generally, stereoselective separation methods.

Stereoselective separations

The separation of diastereomers of any compound is easily accomplished by physical methods, because diastereomers differ in fundamental physical properties, but enantiomer discrimination is a particularly tough problem. Unique recognition of a particular enantiomer of a chiral molecule typically occurs only in interactions with a pure enantiomer of another chiral molecule. The resultant complexes are diastereomeric adducts, which necessarily differ in physical properties. The molecular interaction between chiral entities can be used for enantiopurity determinations and for configuration assignments of enantiomers, e.g., through the use of chiral additives in NMR techniques (Pirkle 1966). To be of practical use in separation technology, the energies of formation of these diastereomeric adducts should be significantly different, while the mechanism of complex formation should also be easily reversible. Diastereomeric co-crystallization

methods and chromatographic techniques, using chiral adsorbent materials or chiral additives in the eluent, are frequently used for chiral separations. Separations of enantiomers of small molecules were first reported through paper chromatography (Dalgliesh 1952) and gas and liquid chromatography (Gil-Av et al. 1966; Rogozhin and Davankov 1971; Mikes and Boshart 1978; Hare and Gil-Av 1979). A number of chromatographic chiral stationary phases have since been developed, based on π donor-acceptor interactions (Welch 1994), host-guest chemistry in cyclodextrin derivatives (Bates et al. 1992), ligand-exchange mechanisms in transition metal ion complexes (Davankov 1989), and chiral silica phases (Flieger et al. 1994). These techniques successfully apply to separation technology the concept of three-point interactions, which was originally proposed for enantioselectivity in adrenergic receptors (Easson and Stedman 1933) and enantiospecific enzymatic activity on prochiral substrates (Ogston 1948). In turn, chromatographic separations have helped understand many mechanisms of stereoselectivity in biological receptor-substrate interactions (Pirkle and Pochapsky 1986; Davankov 1997).

Biological molecules, such as immobilized enzymes (Cancilla et al. 2000; Liang et al. 2000) and enantioselective antibodies (Hofstetter et al. 1998), have been used to develop novel sensing and separation techniques for enantioresolution. The high degree of regio- and stereoselectivities in biological systems ensures that extremely sensitive measurements and high purity separations are possible. It is difficult to obtain a similar combination of high binding strength and high selectivity in other materials. However, immobilized biomolecules often have altered activities as compared to their behavior in solution, and their labile nature results in loss of activity over time. The use of enzymes

and antibodies for sensing and separation technologies can therefore be extremely expensive. Moreover, biomolecules work efficiently only under controlled environments, and tend to be ill suited for large-scale applications (Mallik et al. 1994). It is therefore desirable to develop artificial molecular recognition materials that have the advantages of low cost and robustness, while mimicking biological macromolecules in their selectivity characteristics. Such materials would be particularly useful as chromatographic supports, for the quantitative and qualitative analysis of raw materials, product purity and yields, process impurities, degradation products, residual solvents and trace compounds.

The technique of molecular imprinting

One method to impart binding selectivity to artificial materials is to synthesize them using the technique of molecular imprinting. In this methodology, a target substrate or a molecular analog of it is used as a template around which functional monomers are assembled in solution. The monomers are chosen based on the known chemistries of the functional groups in the template molecule, and the template-monomer complex is polymerized along with cross-linking comonomers. Specific recognition sites thus get fixed in the resulting polymer, in a three-dimensional pattern that is complementary to the geometry of the substrate (Fig. 1. 4). Subsequent to polymerization, the template molecule is removed, leaving behind the necessary functionalities distributed in binding cavities of defined shape and size. The resulting polymeric material should be capable of selective molecular recognition of the template molecule over other structurally related molecules. This approach is particularly attractive for synthesizing materials for use in separation and sensing applications (Ekberg and Mosbach 1989; Wulff 1993; Sundaresan

and Arnold 1995; Piletsky et al. 2001), or as reagents or catalysts in stereoselective synthesis (Whitcombe et al. 2000; Brunkan and Gagne 2000). Various research groups have used different kinds of molecular interactions for this purpose, including covalent bonds (Wulff 1982; Shea and Sasaki 1989), hydrogen bonds (Ekberg and Mosbach 1989) and coordination interactions with transition metal ions (Dhal and Arnold 1991, 1992).

Of the various mechanisms of molecular association used for assembling functional monomers and template molecules into a complex prior to polymerization, the metal coordination interaction combines a substantially high strength of binding, approaching those of covalent bonds, with reversible and rapid kinetics, comparable to hydrogen bond formation and van der Waals interactions. A variety of molecules possess functionalities that coordinate to transition metal ions. These include small molecules such as amines, carboxylic acids, alcohols and amino acids, as also biological macromolecules such as proteins. Metal-coordination chemistry is widely found in nature, as the functioning of a number of enzymes crucially depends upon specific metal ions. Metal coordination has also been successfully used in chromatographic separation technologies. In such an application, the metal ion is usually immobilized on a solid adsorbent that incorporates metal chelating ligands. It is necessary for the immobilizing ligand to strongly bind to the metal ion, so that it is not leached away by analyte molecules. The solid support may be chosen from a variety of materials, including cellulose based resins, crosslinked polymeric matrices and various kinds of silica. The metal chelating ligands most commonly used for immobilizing metal ions on a solid adsorbent (Fig. 1. 5) are amino acids, iminodiacetate (IDA) and nitrilotriacetate (NTA). These ligands chelate the transition metal ion, leaving one or more coordination sites on

the metal occupied by solvent molecules. In the separation process, metal coordinating groups in analyte molecules displace the bound solvent ligands and occupy these sites. The fast kinetics of ligand exchange and the differential thermodynamics of metal coordination by different analytes contribute to efficient separations. Ligand-exchange chromatography (LEC) has found wide application in the chiral resolution of amino acids and hydroxy acids (Davankov 1989). A similar technique in bioseparations utilizes metal coordination interactions of amino acid residues like histidine (Todd et al. 1994), on the surfaces of proteins, and is called immobilized metal affinity chromatography (IMAC).

Thesis objectives and organization

This thesis investigates the synthesis and use of molecularly imprinted polymers for the selective separations of bis-imidazole substrates that differ only in the structure of the spacer separating two imidazole moieties and for enantioresolutions of underivatized amino acids. The mechanisms of enantioselectivity have been discussed in terms of the three-point model of stereospecificity in biological ligand-receptor interactions. This model has been extended to a general stereocenter-recognition model, in order to address the effect of multiple stereocenters in biologically important substrates.

Molecularly imprinted polymers can be synthesized either as bulk copolymers or as surface coatings on other crosslinked polymer matrices and silica particles. The latter approach provides the researcher greater flexibility in tuning the physical and chemical properties of the resultant materials. Chapter two of this thesis discusses the synthesis and characterization of molecularly imprinted polymer coatings that are covalently bonded to the surfaces of crosslinked polymers prepared using trimethylolpropane

trimethacrylate, a monomer that has three polymerizable double bonds per molecule. The imprinted surface grafts have better stability as compared to bulk-copolymerized materials imprinted for bis-imidazole substrates, but possess comparable selectivity characteristics. Chapter three discusses the synthesis and characterization of enantioselective ligand-exchange adsorbents incorporating Cu^{2+} ions, which can be used for chiral resolutions of underivatized α-amino acids. Adsorbents suitable for use in chromatographic separations have been prepared by synthesizing the imprinted polymer as surface coatings on spherical silica particles. The mechanisms responsible for enantioselectivity are discussed in terms of the consequence of molecular imprinting and in the context of models proposed for conventional chiral ligand-exchange chromatographic adsorbents, which covalently incorporate chiral amino acids like proline and phenylalanine into the adsorbent.

The general scheme of molecular imprinting, as shown in Fig. 1. 4, presumes that the template-monomer assemblies are isolated from one another prior to polymerization, and that binding sites are consequently incorporated in the resultant polymer in a random distribution. This assumption has been questioned in a recent study of molecularly imprinted polymers using hydrogen-binding interactions between monomer and template molecules (Katz and Davis 1999). These issues are discussed in chapter four, as part of an overview of the possible mechanisms involved in the observed selectivity characteristics of molecularly imprinted polymers.

The theoretical basis for chiral selectivity in conventional and imprinted ligand-exchanged adsorbents, as discussed in the third chapter, is derived from a stereochemical model of biological enantioselectivity, which calls for a minimum of three points of

interaction between a chiral ligand and its receptor (Easson and Stedman 1933; Ogston 1948; Davankov 1997). There has been a great amount of debate over the theoretical validity and practical applicability of the three-point model (Bentley 1983). Moreover, recent observations of the binding of isocitrate enantiomers to the enzyme isocitrate dehydrogenase have led to the proposal of a new model, which holds that enantioselectivity is determined by a minimum of four interactions (Mesecar and Koshland 2000) between substrate and receptor. Chapter five of this thesis examines the theoretical foundations of these models, and explicates the important assumptions that have been made in the course their development. A new and general model is proposed for the selectivity of biological receptors towards substrates with multiple stereocenters, taking fundamental stereochemical principles into account. The application of the stereocenter-recognition (SR) model to the molecular recognition of substrates with two stereocenters is demonstrated through the examples of isocitrate binding to isocitrate dehydrogenase, the interactions of adrenaline related drug molecules with adrenergic receptors and the inhibition of carboxypeptidase A by epoxybutanoic acid derivatives.

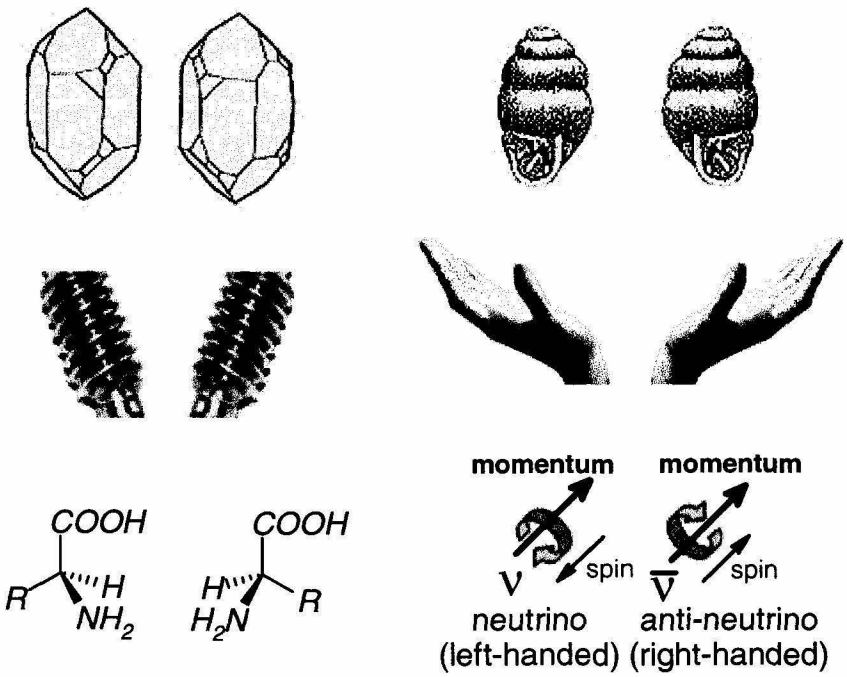

Figure 1. 1. Natural and man-made asymmetric objects. Quartz crystals, mollusc shells, right-handed and left-handed screws, a pair of hands, α-amino acid enantiomers, and elementary particles with intrinsic parity (spin antiparallel or parallel to momentum).

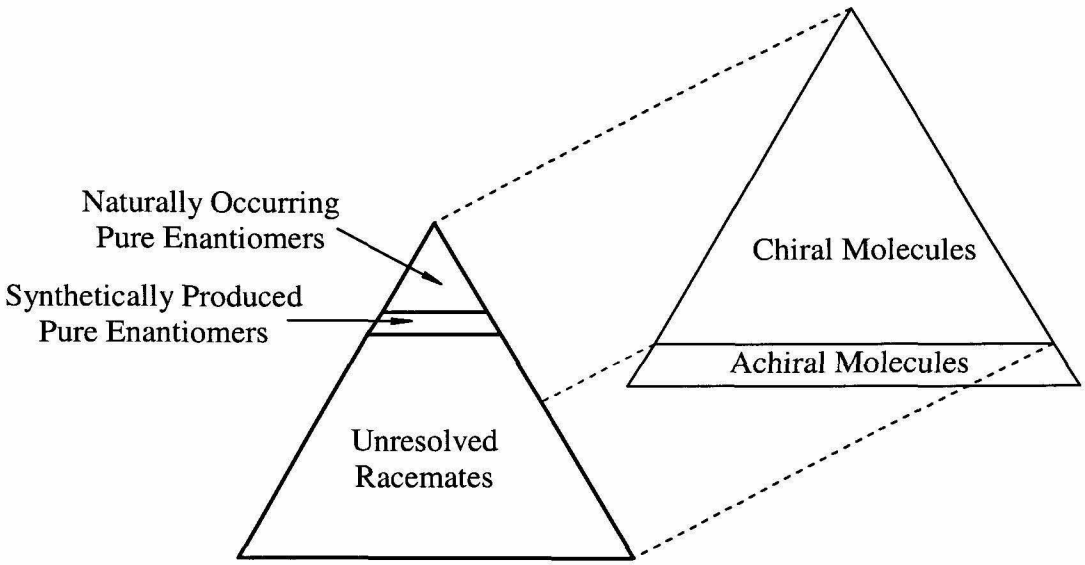

Figure 1. 2. Relative proportions of chiral and achiral organic molecules reported in literature (adapted from Sharpless et al. 1992).

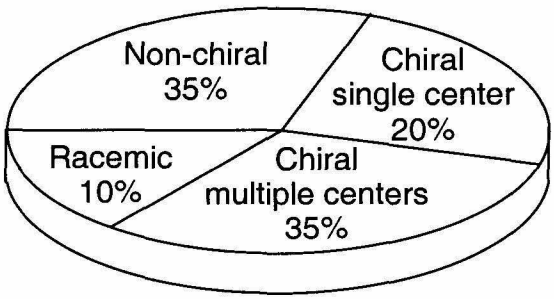

Figure 1. 3. Relative percentages of chiral and achiral drug molecules approved between the years 1998 and 2000. Source: Center for Drug Evaluation and Research, United States Food and Drug Administration (*http://www.fda.gov/cder/guidance/stereo.htm*, and *http://www.fda.gov/cder/rdmt*).

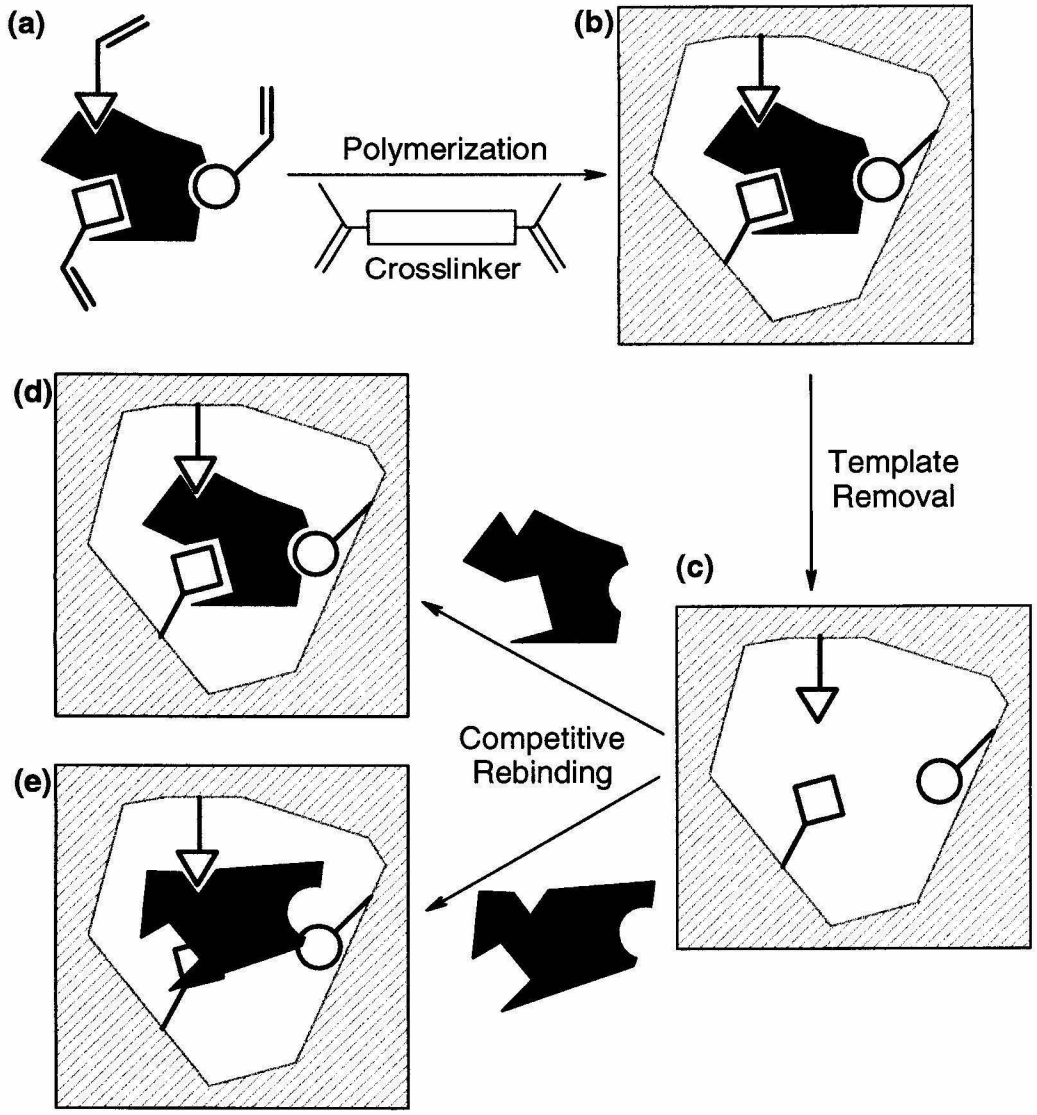

Figure 1. 4. General scheme for molecular imprinting of polymers. A template molecule and functional monomers are assembled in solution (**a**) and polymerized along with cross-linkers (**b**). Template removal results in a polymer (**c**) that has binding functionalities distributed in a three-dimensional pattern that complements the geometry of the template molecule (**d**). The polymer can therefore select for the template over other structurally related molecules (**e**).

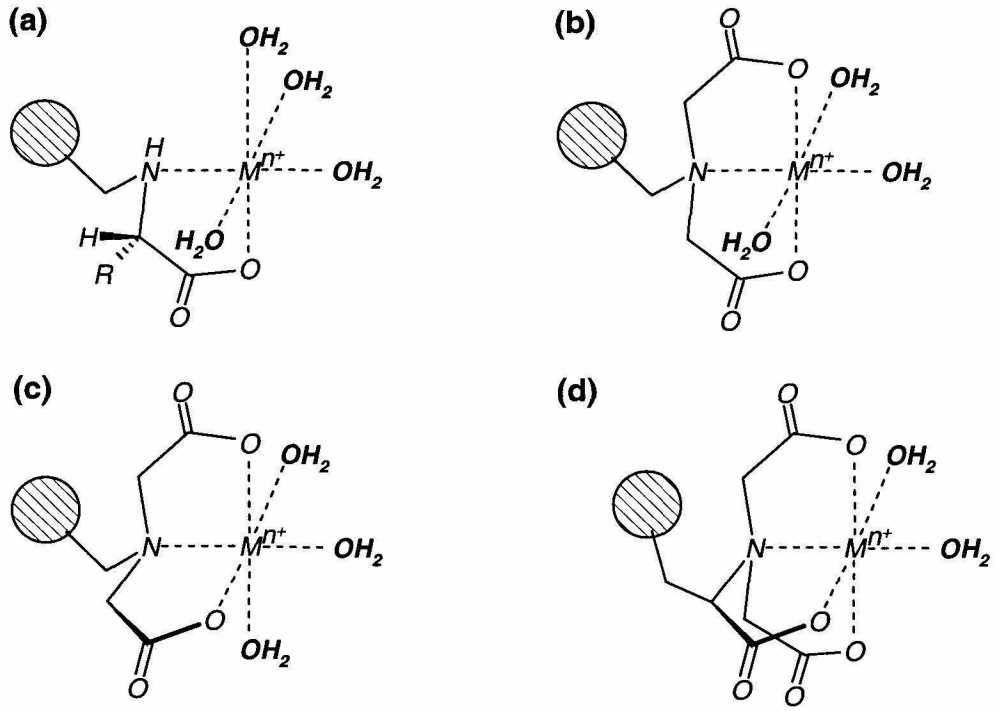

Figure 1. 5. Metal-chelating ligands used in ligand-exchange chromatography (LEC) and immobilized metal-affinity chromatography (IMAC). Typical chemical linkages to an adsorbent surface (shaded circle) are shown, and the transition metal ion (M^{n+}) is assumed to have an octahedral ligand-field. **(a)** α-amino acids leave four coordination sites occupied by solvent molecules. **(b)** Iminodiacetate (IDA) can chelate transition metal ions in meridional (*mer*) geometry, with the carboxylate groups *trans* to each other. **(c)** IDA can also chelate in facial (*fac*) geometry, with the carboxylates *cis* to each other. In both cases, solvent molecules occupy up to three coordination sites. **(d)** The nitrilotriacetate (NTA) complex has solvent molecules occupying two coordination sites in an octahedral ligand-field.

References

Avalos, M., Babiano, R., Cintas, P., Jiménez, J.L. and Palacios, J.C. 2000. *Tetrahedron Asymmetry.* **11:** 2845-2874.

Barrett, G.C. 1985. *Chemistry and Biochemistry of the Amino Acids.* Chapman and Hall, New York.

Barron, L.D. 1982. *Molecular light scattering and optical activity.* Cambridge University Press, Cambridge.

Bates, P.S., Parker, D., and Kataky, R. 1992. *J. Chem. Soc. Chem. Comm.* 153-155.

Bentley, R. 1983. *Trans. NY Acad. Sci. Ser. II* **41:** 5-24.

Bouchiat, M.A. and Pottier, L. 1986. *Science.* **234:** 1203-1210.

Brunkan, N.M. and Gagne, M.R. 2000. *J. Am. Chem. Soc.* **122:** 6217-6225.

Cahn, R.S., Ingold, C., and Prelog, V. 1966. *Angew. Chem. Int. Ed. Engl.* **5:** 385-415.

Caldwell, J. 1995. *J. Chromatogr. A.* **694:** 39-48.

Cancilla, M.T., Leavell, M.D., Chow, J., and Leary, J.A. 2000. *P. Natl. Acad. Sci. U.S.A.* **97:** 12008-12013.

Casey, A.F. 1970. Stereochemistry and biological activity. In *Medicinal Chemistry.* (ed. A. Burger), p. 81. Wiley Interscience, New York.

Dalgliesh, C.E. 1952. *J. Chem. Soc.* **132:** 3940-3942.

Davankov, V.A. 1989. Ligand-exchange phases. In *Chiral Separations by HPLC: Application to Pharmaceutical Compounds.* (ed. A.M. Krstulovich), pp. 446-475. Ellis Horwood, Chichester.

Davankov, V.A. 1997. *Chirality.* **9:** 99-102.

Dhal, P.K. and Arnold, F.H. 1991. *J. Am. Chem. Soc.* **113:** 7417-7418.

Dhal, P.K. and Arnold, F.H. 1992. *Macromolecules.* **25:** 7051-7059.

Drayer, D.E. 1993. The early history of stereochemistry. In *Drug Stereochemistry: Analytical Methods and Pharmacology.* (ed. I.W. Wainer), pp. 1-24. Marcel Dekker, New York.

Easson, L. and Stedman, E. 1933. *Biochem. J.* **27:** 1257-1266.

Eichelbaum, M. and Gross, A.S. 1996. *Adv. Drug Res.* **28:** 1-64.

Ekberg, B. and Mosbach, K. 1989. *Trends Biotechnol.* **7:** 92-96.

Flieger, M., Sinibaldi, M., Cvak, L., and Castellani, L. 1994. *Chirality.* **6:** 547-554.

Gaffield, W., Incardona, J.P., Kapur, R.P., and Roelink, H. 1999. *Cell. Mol. Biol.* **45:** 579-588.

Gardner, M. 1990. *The ambidextrous universe.* W. H. Freeman, New York.

Gil-Av, E., Feibush, B. and Charles-Sigler, R. 1966. *Tetrahedron Lett.* **7:** 1009-1015.

Hare, P.E. and Gil-Av, E. 1979. *Science.* **204:** 1226-1228.

Hofstetter, O., Hofstetter, H., Schurig, V., Wilchek, M., and Green, B.S. 1998. *J. Am. Chem. Soc.* **120:** 3251-3252.

Jollés, P. 1998. ed. *D-amino acids in sequences of secreted peptides of multicellular organisms.* Birkhäuser, Basel.

Katz, A. and Davis, M.E. 1999. *Macromolecules.* **32:** 4113-4121.

Kelvin, Lord. 1904. Appendix H. In *Baltimore lectures on molecular dynamics and the wave theory of light.* Cambridge University Press, Cambridge.

Liang, L.F., Li, Y.T., Yang, V.C. 2000. *J. Pharm. Sci.* **89:** 979-990.

Lichtenthaler, F.W. 1992. *Angew. Chemie. Int. Ed. Engl.* **31:** 1541-1556.

Mallik S.M., Plunkett, S.D., Dhal, P.K., Johnson, R.D., Pack, D. Shnek, D., and Arnold, F.H. 1994. *New J. Chem.* **18:** 299-304.

Mesecar, A.D. and Koshland Jr., D.E. 2000. *Nature.* **403:** 614-615.

Mikes, F. and Boshart, G. 1978. *J. Chromatogr.* **149:** 455-464.

Ogston, A.G. 1948. *Nature.* **163:** 963.

Pasteur, L. 1901. On the asymmetry of naturally occurring organic compounds. In *The Foundation of Stereochemistry: Memoirs by Pasteur, van't Hoff, Le Bel and Wislicenus.* (ed. G.M. Richardson), pp. 1-33. American Book Company, New York.

Piletsky, S.A., Alcock, S., and Turner, A.P.F. 2001. *Trends Biotechnol.* **19:** 9-12.

Pirkle, W.H. 1966. *J. Am. Chem. Soc.* **88:** 1837.

Pirkle, W.H. and Pochapsky, T.C. 1986. *J. Am. Chem. Soc.* **108:** 5627-5628.

Ridell, F.G. and Robinson, M.J.T. 1974. *Tetrahedron.* **30:** 2001-2007.

Rogozhin, S.V. and Davankov, V.A. 1971. *Dokl. Akad. Nauk. SSSR.* **192:** 1288-1290.

Sharpless, K.B., Amberg, W., Bennani, Y.L., Crispino, G.A., Hartung, J., Jeong, K.S., Kwong, H.L., Morikawa, K., Wang, Z.M., Xu, D.Q., and Zhang, X.L. 1992. *J. Org. Chem.* **57:** 2768-2771.

Shea, K.J. and Sasaki, D.Y. 1989. *J. Am. Chem. Soc.* **111:** 3442-3444.

Sundaresan, V. and Arnold, F.H. 1995. *Curr. Opin. Biotech.* **6:** 218-224.

Todd, R.J., Johnson, R.D., and Arnold, F.H. 1994. *J. Chromatogr. A.* **662:** 13-26.

Welch, C.J. 1994. *J. Chromatogr. A.* **666:** 3-26.

Whitcombe, M.J., Alexander, C., and Vulfson, E.N. 2000. *Synlett.* **6:** 911-923.

Wulff, G. 1982. *Pure Appl. Chem.* **54:** 2093-2102.

Wulff, G. 1993. *Trends Biotechnol.* **11**: 85-87.

Chapter 2

Molecular Imprinting I:

Surface Modification of poly(TRIM) Particles

Preface

Part of the following chapter is adapted with permission from the following publication: Dhal, P.K., Vidyasankar, S. and Arnold F.H. 1995. Surface Grafting of Functional Polymers to Macroporous Poly(trimethylolpropane trimethacrylate). *Chem. Mater.* **7:** 154-162.

The research was done in collaboration with Dr. Pradeep K. Dhal. Dr. Dhal and I contributed equally to the material synthesis of poly(TRIM) and graft copolymers, as also to most of the characterization experiments. ^{13}C CP-MAS NMR spectra were obtained by me, while Dr. Dhal obtained the IR spectra of poly(TRIM) and its surface-grafted copolymers. We thank Dr. David Waldman of Polaroid Corporation for help with obtaining XPS spectra.

Abstract

Cross-linking polymerization of a trifunctional methacrylate monomer, trimethylolpropane trimethacrylate (TRIM), under controlled conditions yields macroporous polymers bearing surface-accessible unpolymerized methacrylate residues. These residues have been utilized for copolymerization with different functional monomers to obtain composite polymer matrices with surface coatings of functional polymer chains. Poly(TRIM) modified with methacrylamide, *N,N*-dimethylacrylamide, vinylazlactone, and copper(II) dimethacrylate exhibit useful functional properties that depend on the type of functional monomer used yet retain the desirable physical properties of the original poly(TRIM) matrix. The metal-complexing polymer made by grafting copper(II) dimethacrylate to poly(TRIM) exhibits better accessibility of the metal-coordinating sites compared to its bulk-polymerized counterpart. Similarly, the surface-hydrophilized matrices made by grafting methacrylamide and *N,N*-dimethylacrylamide show good water absorbency yet exhibit better matrix stability to environmental change compared to corresponding bulk-copolymerized materials. The physicochemical characteristics of these functional polymer matrices were evaluated by *13C* NMR, X-ray photoelectron spectroscopy, IR spectroscopy, and scanning electron microscopy. Poly(TRIM) particles surface-modified by template polymerization of a copper(II)-[*N*-(4vinylbenzyl)imino]diacetic acid (6):template complex and ethylene glycol dimethacrylate exhibit selectivity similar to bulk-polymerized templated polymers in rebinding bisimidazole templates.

Introduction

Linus Pauling (1940) proposed that in living organisms, an antigenic molecule acts as a template or an imprint, around which the cellular machinery arranges biological molecules with complementary binding functionalities, in order to construct a macromolecular antibody. Although this has been shown to be incorrect for biological systems, the concept of molecular imprinting has been exploited for synthesizing inorganic and organic solid materials, for use in applications requiring selective molecular recognition. The earliest materials to be prepared using this approach were silica gels that were imprinted for homologues of methyl orange (Dickey 1949). These materials were shown to be capable of selective recognition of their template molecules, but had limited stability (Dickey 1955).

The molecular imprinting approach to imparting selectivity to solid adsorbent materials was first applied to polymerization chemistry by Wulff and Sarhan (1972). Molecular imprinting of polymers involves the preorganization of functional monomers around a template molecule in solution, to form a monomer-template assembly, followed by cross-linking polymerization. This results in a selective binding cavity in which the three-dimensional distribution of binding functionalities is arranged in a pattern that is complementary to the three-dimensional structure of the template. Template removal yields a polymer matrix that can be used to selectively rebind the targeted substrate. The advantage of this approach over the rational design and synthesis of low molecular weight receptors for molecular recognition is that polymers can be imprinted for a large variety of template molecules using similar chemistries. Detailed knowledge of the

structure of the template is not necessary, as the template itself can be made to direct the assembly of complementary binding functionalities in solution, prior to the polymerization reaction. Finally, if the resultant imprinted polymer has the desired material properties, it can directly be employed in such applications as chromatographic separation or heterogeneous catalysis.

The formation of the monomer-template assembly can be achieved through covalently linking the functional monomer to the template moiety or by using non-covalent self-assembly. In the former case, one can expect to design well-defined binding cavities in the imprinted polymer, but template removal requires cleavage of covalent bonds after the polymerization step, which is not always easily accomplished. The subsequent substrate rebinding also involves the reformation of these covalent bonds, so that such materials are frequently observed to be quite inefficient for separation applications (Wulff 1986). Also, recognition involving relatively stable covalent interactions can be kinetically controlled (Shea and Sasaki 1989), so that the selectivity profiles of these materials do not necessarily correspond to what may be expected thermodynamically. Materials exhibiting fast rebinding kinetics, necessary for chromatographic separations or catalysis, have been prepared using rapidly reversible covalent interactions (Wulff 1993). However, the non-covalent self-assembly approach, using hydrogen bonding interactions or electrostatic interactions (Ekberg and Mosbach 1989) or metal coordination interactions (Dhal and Arnold 1991), is more attractive in this regard. The great advantage of the self-assembly approach to forming specific recognition sites in molecularly imprinted polymers is its generality and relative

simplicity. The easy reversibility of non-covalent interactions greatly simplifies the process of template removal and substrate rebinding. Molecularly imprinted polymers have been synthesized for a variety of targets, using hydrogen bond formation between monomer and template (Haupt and Mosbach 1998; Ramström and Mosbach 1999).

The transition metal coordination interaction has been utilized for the synthesis and characterization of polymers molecularly imprinted for bis-imidazole substrates (Dhal and Arnold 1991, 1992). The imidazole moiety in these synthetically designed substrates mimics the histidine residue in proteins, which can enter into coordination interactions with transition metal-ions. Metal-coordination complexes are formed and broken under mild conditions, but the coordination interaction is thermodynamically much more stable than hydrogen bonding and other non-covalent interactions. Furthermore, as the kinetics and the strength of binding vary with the identity of the transition metal ion, an additional degree of control can be incorporated into the material synthesis procedure, and imprinted polymers with tailored binding strengths and kinetic profiles can be obtained for a number of substrates.

The bulk imprinted polymers reported by Dhal and Arnold (1992) were based on ternary coordination complexes of Cu^{2+} with bis-imidazole substrates such as those shown in Fig. 2. 1 (**8**, **9**) and a styrene-based derivative of iminodiacetic acid ([*N*-(4-vinylbenzyl)imino]diacetate, VBIDA). Polymerization of this monomer-template assembly was carried out with excess ethylene glycol dimethacrylate (EGDMA) as cross-linking agent, followed by template and metal-ion removal by acidification and extraction with ethylenediamine tetraacetic acid (EDTA) and 1,4,7-triazacyclononane

(TACN). The imprinted polymers were reloaded with Cu^{2+} and tested for their ability to selectively recognize their template bis-imidazole over other bis-imidazole molecules with closely related structures. It was demonstrated that selectivities in the range of 1. 17 to 1. 24 for different bis-imidazole substrates could be realized using this approach. It should be noted that these substrates differ only by ~4 Å in their imidazole spacing.

However, the techniques used to synthesize these polymeric materials need substantial optimization in many directions. One major goal that yet remains to be realized is the synthesis of imprinted polymers that can differentiate one protein from another. Macroporous imprinted polymers can rebind low molecular weight substrates reversibly and with reasonable efficiency, but the same is not true for macromolecular substrates. Attempts using the imprinting approach to prepare polymers for protein templates have resulted largely in the preparation of immobilized proteins, with considerable loss in the functional activity of the protein. This is probably because the highly crosslinked nature of the imprinted polymer network imposes severe diffusional limitations upon biological macromolecules, leading to significant problems for the crucial template removal step. Another important issue is that the reaction conditions promoting the formation of the monomer-template complex may not be optimum for obtaining desirable structural properties in the polymer. A noticeable problem with the use of the metal (Cu^{2+}) coordination interaction for imprinting bulk-copolymerized materials has been their lack of structural strength. When packed in a chromatographic column, the packing frequently collapses under flow conditions, leading to poor column efficiency and short lifetimes of use. Better column performance has been obtained by

preparing imprinted polymers as surface coats on chromatographic silica particles, and by reloading the material with Zn^{2+} ions instead of Cu^{2+} ions (Plunkett and Arnold 1995). While the use of silica particles as the structural support imparted stability and strength to the chromatographic adsorbent, the incorporation of Zn^{2+} ions in the polymer resulted in shorter retention times and more efficient chromatographic separations.

A parallel effort to address the above issues was to graft copolymerize the monomer-template assemblies to the surface of a solid polymer matrix possessing desirable physical and mechanical properties (Nörrlow 1984). This should also result in localizing binding sites at the solvent accessible surfaces of the polymeric matrix, thereby imposing diminished diffusional limitations on substrate molecules during rebinding studies. Introduction of functional groups by grafting onto a polymer surface (Boven et al. 1990) can yield materials possessing good bulk structural properties as well as desired functional characteristics. This strategy is similar to the synthesis of functional coatings on surface-derivatized porous silica particles for use in chromatographic separations (Unger 1979, Leydon and Collins 1980).

The effectiveness of functional polymers in a range of settings from separations to solid-phase chemical synthesis has generated much interest in developing novel materials with improved thermal and mechanical stability combined with high accessibility of functional groups (Ford 1986, Sherrington and Hodge 1988, Merrifield 1985, Frechet et al. 1988). Functional polymers hold great promise as robust and inexpensive materials for selective substrate recognition and binding, for use in applications involving analytical sensing and separation technologies. Albright (1972) reported that a

crosslinked, macroporous reactive polymer can be synthesized from a trifunctional methacrylate monomer, 2-ethyl-2-(hydroxymethyl)propane-1,3-diol trimethacrylate or trimethylolpropane trimethacrylate (TRIM, Fig. 2. 1, **1**) [Other abbreviations: AIBN, 2,2'-azobisisobutyronitrile; XPS, X-ray photoelectron spectroscopy; SEM, scanning electron microscopy; EGDMA, ethylene glycol dimethacrylate]. Rosenberg and Flodin (1987) later observed that the poly(TRIM) matrix contains residual unreacted double bonds, the concentration of which can be controlled by appropriately controlling parameters such as polymerization time and temperature and the nature and concentration of the porogen (solvent). These polymer-bound double bonds are accessible for subsequent chemical manipulations (Hjertberg et al. 1990, Reinholdsson 1981), and Chromatographic supports for chiral separations have been prepared by grafting chiral polymer chains onto poly(TRIM) particles (Hargitai et al. 1991). TRIM has also been used, instead of EGDMA, as a crosslinking monomer for molecular imprinting using hydrogen bonding interactions (Kempe and Mosbach 1995).

The excellent material properties of macroporous functional copolymer matrices obtained using TRIM as the cross-linker (Verweij et al. 1991, Walenius et al. 1992) prompted us to evaluate their utility as reactive supports for carrying out molecular imprinting polymerization. The high stability of the poly(TRIM) matrix and its relatively low tendency to swell in different solvents suggest that the functionalization could be confined to the porous surface without affecting the bulk mechanical properties. Furthermore, the ease with which methacrylate groups can be copolymerized with

different vinyl monomers (Greenley 1989) should enable a variety of functional polymer chains to be anchored to the poly(TRIM) surface.

To evaluate the reactivity of poly(TRIM) toward grafting with functional polymers, poly(TRIM) was modified with the four different monomers shown in Figure 2. 1: *N*,*N*-dimethylacrylamide (**2**); methacrylamide (**3**); vinylazlactone (**4**) and copper(II) dimethacrylate (**5**). Monomers **2** and **3** would convert the hydrophobic methacrylate surface to a more hydrophilic one, while grafting with **4** would result in a reactive surface amenable to subsequent chemical manipulation (Rasmussen 1988). Copolymerization with **5** would lead to a functional matrix possessing metal coordinating sites. Water absorbency, swelling, accessibility of the new functional groups and changes in surface morphology and other surface properties subsequent to grafting were evaluated. The functional monomers were also copolymerized with TRIM, to allow comparison of matrices with functional groups distributed throughout the bulk polymer to those in which the functional groups are confined to the surface.

The utility of poly(TRIM) as a reactive support for template polymerization was evaluated by grafting polymerizable assemblies of the ternary Cu^{2+} complex of [*N*-(4-vinylbenzyl)imino]diacetate (Fig. 2. 1, **6**) and bis-imidazole template (Fig. 2. 1, **7**), with ethylene glycol dimethacrylate (EGDMA) as a cross-linking agent. The ability of the surface-templated polymer to selectively rebind its template bis-imidazoles was measured and compared to the bulk polymerized templated polymers previously reported (Dhal and Arnold 1991, 1992). A scheme for molecular imprinting using this surface grafting polymerization technique is shown in Fig. 2. 2.

Results and Discussion

Preparation of Reactive Poly(TRIM) Supports and Grafting with Functional Monomers

Variation of the polymerization parameters enables the material properties of poly(TRIM) to be engineered in a systematic fashion (Hjertberg et al. 1990). Polymerization conditions were chosen to yield a macroporous material with desirable morphological characteristics and bearing sufficient residual double bonds for subsequent modification. Polymerization of a 50% (v/v) solution of TRIM in a solvent system of cyclohexane-toluene (70:30 v/v) at 60 °C for 4 h yielded an amorphous, white polymer, which was dried, ground, and sieved.

The different materials prepared by grafting monomers **2-5** onto poly(TRIM) are listed in Table 2. 1. Treatment of poly(TRIM) particles with a monomer solution under reduced pressure should result in adsorption of the monomer on the porous surfaces of the matrix. Polymerization of this heterogeneous mixture of functional monomer and poly(TRIM) particles by free radical initiation at 70-80 °C results in covalent grafting of functional polymer chains to the poly(TRIM) surface. The modified polymer was exhaustively extracted to remove unreacted monomers and ungrafted polymers. It is possible that some amount of polymer remains permanently entangled in the porous network of the poly(TRIM) matrix, instead of being covalently grafted to the surface. The amount of material grafted was estimated from the elemental analyses of the copolymers. Thus, the compositions of the polymers with **2-4** were determined from the nitrogen content of the modified polymers, and the composition of the polymer with **5** was based on the copper content. The extent of grafting depends on the monomer

concentration in the reaction medium, as shown in Fig. 2. 3. The grafting process appears to be efficient, resulting in a large fraction of the monomer grafted onto the polymer particles. A significant amount of functional monomer can be grafted to the polymer surface (~25% w/w). Beyond this, the grafting process leaves soluble polymers, which are removed by extraction.

Unpolymerized methacrylate residues on the poly(TRIM) surface provide anchoring sites to graft new functional groups. The efficiency of the coupling reaction depends on the accessibility of these double bonds. Previous studies using bromine addition, post-polymerization, and NMR relaxation measurements have demonstrated the accessibility and mobility of these polymer bound double bonds (Reinholdsson et al. 1981). The presence of functional polymer chains after exhaustive extraction of these modified polymers with suitable solvents strongly suggests that the functional polymer chains are covalently linked to the poly(TRIM) matrices via the surface exposed unreacted methacrylate residues.

Macroporous poly(TRIM) particles possess permanent pore structures and significant mechanical rigidity and are less sensitive to the surrounding solvent than lightly cross-linked gel-type polymer resins (Hjertberg et al. 1990, Harjitai 1991). Reaction in rigid macroporous polymers is controlled by diffusion of the reactants into the pores rather than swelling of the matrix. Thus, in principle, it should be possible to use either aqueous or organic monomer solutions for modification of poly(TRIM). Methacrylamide can indeed be grafted to poly(TRIM) from an aqueous solution, and only slightly less methacrylamide is grafted to the polymer surface in water than in ethanol

(see Table 2. 1, entries 6-9). Thus, the ability of this reactive polymer is able to graft polymerize in aqueous media can be exploited for immobilization of water-soluble substrates and other, biological substrates that would be sensitive to organic solvents.

To compare the physicochemical behavior of the surface-grafted polymers to materials in which the distribution of functional monomers is homogeneous, the TRIM monomer was copolymerized with the respective monomers at similar molar composition, using an appropriate porogen (see Experimental Section for details). These bulk-copolymerized materials were also exhaustively extracted to remove soluble components.

Spectroscopic Analysis of Surface-Grafted Polymers

The functional polymers prepared by grafting to poly(TRIM) were analyzed using infrared (IR), ^{13}C NMR, and X-ray photoelectron (XPS) spectroscopic techniques. The presence of residual unpolymerized methacrylate residues is evident from the characteristic peak at 1640 cm^{-1} in the IR spectrum of unmodified poly(TRIM) shown in Fig. 2. 4a (Pouchet 1978). Grafting is accompanied by the appearance of new peaks characteristic of the corresponding functional monomers. Thus, the spectrum of methacrylamide-grafted poly(TRIM) (Fig. 2. 4b) contains an intense absorption at 1665 cm^{-1} due to the amide carbonyl stretching vibration as well as a broad peak in the region 3200-3500 cm^{-1} corresponding to N-H stretching. Similarly, the IR spectrum of vinylazlactone-modified particles (Fig. 2. 4c) reveals the presence of new peaks at 1660 and 1825 cm^{-1} characteristic of the azlactone ring (Fazio et al. 1992).

Unmodified poly(TRIM) particles were annealed in ethanol at 80 °C for 30 h in the presence of AIBN in order to assess the reactivity of the residual double bonds. The IR spectrum of this polymer, shown in Fig. 2. 5, is characteristic of a typical methacrylate polymer, with only the ester carbonyl peak at 1735 cm^{-1}. Thus, it appears that complete reaction of the residual double bonds can occur under the conditions of polymerization, in the absence of grafted monomer.

The solid-state ^{13}C NMR spectrum of unmodified poly(TRIM) particles is shown in Fig. 2. 6a. Comparison to the ^{13}C NMR analysis of poly(TRIM) reported previously (Hjertberg et al. 1990) reveals the presence of all expected resonances, including those due to residual double bonds. Resonances due to saturated and unsaturated ester carbonyl carbons appear at 177 and 168 ppm, respectively. The characteristic resonances at 130 (quaternary) and 120 ppm (methylene) also attest to the presence of unpolymerized methacrylate residues. The spectrum of a typical methacrylamide-grafted copolymer (Fig. 2. 6b) is similar to that of bulk-polymerized TRIM-methacrylamide (Fig. 2. 6c). The specific resonances corresponding to the unpolymerized double bonds are largely gone in both materials. Due to the limited resolution of amide and ester carbonyls in this experiment, no peak characteristic of methacrylamide is evident in either spectrum. However, the reduction in the intensity of the unsaturated ester carbonyl peak, concomitant with the increased intensity of the saturated ester carbonyl peak, suggests that the functional polymer chains are grafted to the poly(TRIM) surface.

XPS was used to analyze the chemical nature of the modified surfaces. The advantages of this technique include its element specificity and sensitivity to surface

chemical compositions (Briggs and Seah 1983). XPS has been used to characterize a variety of chemically-modified polymer surfaces (Allcock et al. 1992, Lee and McCarthy 1988). The observable elemental composition of poly(TRIM) comprises only carbon and oxygen. Accordingly, the XPS spectrum of poly(TRIM) shown in Fig. 2. 7a contains only O(ls) and C(ls) peaks at 531 and 290 eV, respectively. The small peaks at 102 and 153 eV, characteristic of Si(2p) and Si(2s), are probably due to contamination by the silicon grease used for vacuum sealing during the polymerization procedure. This is evidently washed away during post-polymerization treatment before grafting a new polymer surface coat, as these peaks are not seen in the grafted samples. Because the functional monomers 2-5 contain elements (i.e., nitrogen and copper) not present in the original poly(TRIM) polymer, the specific peaks in the grafted copolymers corresponding to these elements indicate the presence of functional polymer chains on the surface. The XPS spectrum of a typical copolymer obtained by grafting with methacrylamide (Fig. 2. 7b) shows the N(ls) peak at 395 eV, in addition to the O(ls) and C(ls) peaks. The spectrum of the copper(II) dimethacrylate-grafted copolymer in Fig. 2. 7c reveals the typical Cu(2p) doublet peaks at 932 and 952 eV.

An expanded spectrum of the C(1s) peak of poly(TRIM), shown in Fig. 2. 8a, shows two distinct peaks, centered at 286 and 290 eV. These peaks correspond to backbone and other hydrocarbon carbon and ester carbonyl carbon atoms, respectively. The expanded C(1s) region of the methacrylamide-grafted sample is shown in Fig. 2. 8b. The broadening of these peaks compared to those in poly(TRIM) may be attributed to the amide carbonyl C(1s) peak at 289 eV that overlaps with the ester carbonyl C(1s) peak.

Morphologies of Surface-Grafted Polymers

Anchoring new polymer chains by chemical grafting changes the morphology of the poly(TRIM) particles. The unmodified poly(TRIM) particles are macroporous and possess high surface area (285 m^2g^{-1}), as indicated in Table 2. 1. Further information on the morphology of this material can be obtained by scanning electron microscopy (SEM), which reveals the porous texture of the poly(TRIM) (Fig. 2. 9a). Matrices prepared by simultaneous copolymerization of TRIM with the functional monomers possess surface areas similar to the poly(TRIM) matrix (Table 2. 1). SEM studies of these polymers also show that the macroporous structures are similar, as seen in the micrograph of the bulk copolymer of TRIM with *N*,*N*-dimethylacrylamide (Fig. 2. 9b).

Grafting functional monomers to poly(TRIM) decreases the specific surface area (Table 2. 1). Electron micrographs of the graft copolymers obtained using functional monomers **2** and **3**, shown in Fig. 2. 9c,d, reveal significant changes in the surface morphology upon grafting. The grafted materials have a less open surface texture, with decreased pore volumes, due to incorporation of the new grafted polymer chains in the porous spaces of the poly(TRIM) matrix. This reinforcement leads to more compact structures, while retaining the overall macroporous morphology.

Physicochemical Characteristics of Bulk-Polymerized and Surface-Grafted poly(TRIM)

The surface-grafted metal-complexing polymer made with monomer **5** and the corresponding macroporous polymers with homogeneous distributions of

metal-complexing sites were extracted with a strong Cu(II) chelator, ethylenediamine tetraacetic acid (EDTA). As shown in Table 2. 2, nearly 90% of the total copper could be removed from the surface-grafted polymer in a single extraction step. On the other hand, bulk polymerized samples release only ~65% of the total copper content under similar extraction conditions. While the metal-complexing sites in the surface-grafted material are accessible to EDTA, bulk copolymerization leads to a distribution of metal sites, some of which, presumably in the interior of the matrix, are inaccessible to EDTA. The nonpolar nature of the matrix interior may limit the partitioning of the highly polar chelating agent. This behavior parallels earlier observations with metal complexing templated polymers, which were prepared using ethylene glycol dimethacrylate (EGDMA) as crosslinking monomer. EDTA was unable to completely remove the copper ions from the bulk polymerized EGDMA matrix, while a lipophilic chelating agent (triazacyclononane) was effective (Dhal and Arnold 1992).

Bulk-polymerized and surface-grafted matrices obtained using hydrophilic monomers **2** and **3** do not swell to any significant extent in a non-solvent, hexane. Both the bulk-polymerized and surface-grafted polymers swell appreciably in water, as indicated in Table 2. 3. The swelling is more pronounced for the bulk-copolymerized materials. For example, a surface-grafted polymer containing 18 mol% methacrylamide (P-7) swells to 135% of its dry volume in water, while the corresponding bulk-polymerized matrix containing 15 mol % methacrylamide (P-11) swells to 175% of its original volume. Distribution of the hydrophilic comonomers across the polymer matrices permits greater water penetration and swelling for the bulk-polymerized

materials, while these effects are probably confined to the surface of the grafted copolymers. While grafting with methacrylamide fills the microporous surface regions of the parent poly(TRIM) polymer, the bulk-copolymerized supports possess a porous texture similar to that of poly(TRIM). Copolymerization with a nominal amount of the hydrophilic comonomer does not dramatically influence the polymer morphology. Interaction with water is anticipated to bring about structural rearrangements of the hydrophilic polymer networks, which can be manifested in their morphologies. Furthermore, morphological changes are likely to differ for different structural architectures.

SEM micrographs obtained of the bulk-copolymerized polymer of TRIM with **3** and the corresponding surface grafted support after swelling both materials in water are shown in Fig. 2. 9. A comparison of the surface functionalized material before (Fig. 2. 9d) and after swelling in water (Fig. 2. 10a) shows little change in overall macroporous morphology. In contrast, swelling the bulk-polymerized support in water (Fig. 2. 10b) greatly increases the size of the individual globules and agglomerates and causes a large increase in the interglobular spaces, compared to its dry precursor (Fig. 2. 9b). These observations indicate that the porous morphologies are sensitive to the solvent, but the magnitude of this change depends on the degree to which solvent can penetrate into the polymer matrix. The changes are nominal for the surface-modified matrix, the water penetration being probably confined to the grafted layers on the surface. The greater solvent penetration and overall swelling of the bulk copolymerized material results in more significant morphological rearrangement.

Generating molecularly imprinted binding sites by surface-grafting

The residual methacrylate groups in poly(TRIM) can be utilized to graft a polymerizable monomer-template assembly and cross-linking agent for surface template polymerization. Similar to previously reported template polymerization studies with bulk-polymerized materials (Dhal and Arnold 1991, 1992), the Cu^{2+} complex of [*N*-(4-vinylbenzyl)imino]diacetate (**6**) was used as the monomer, with the templates investigated being 1,4-bis(imidazol-l-ylmethyl)benzene (**8**) and 4,4'-bis(imidazol-l-ylmethyl)biphenyl (**9**). The polymerizable monomer-template assembly, generated by combining methanol solutions of **8** and **6** (mole ratio 6:7 = 2:1), was polymerized with the TRIM matrix and ~ 40 mol % EGDMA (**7**) (for details, see materials and methods section). After polymerization, the light blue polymer was extracted exhaustively with hot methanol to remove any soluble components. Following previously reported procedures (Dhal and Arnold 1992), treatment of the imprinted polymers with acidified aqueous methanol, followed by EDTA extraction, enabled removal of the bis-imidazole template and copper ions. A control polymer with a random distribution of metal centers was prepared under similar polymerization conditions, using 1-benzylimidazole as the template.

Copper ions could be removed to a substantial extent (> 90%) from both these surface-grafted polymers with a single EDTA treatment. The nonpolar chelating agent, 1,4,7-triazacyclononane, necessary to completely remove the copper from the bulk-copolymerized materials, is not required for the surface-grafted materials.

Reloading the polymer with copper ions is achieved by treating the metal free polymers with $CuC1_2$, followed by thorough washing to remove unbound copper ions.

The fidelity with which the placement of metal centers in the polymer mimics or complements the structure of the template should be reflected in preferential binding of the template molecule over other closely related molecules. Competitive rebinding experiments were carried out for the surface-grafted materials using substrates **8** and **9**. The surface-grafted templated polymer prepared using **8** as the template binds its own template bis-imidazole preferentially, with a selectivity ($\alpha_{8/9}$) of 1.30. Similarly, the material prepared against **9** binds to its own template bis-imidazole preferentially, with a selectivity ($\alpha_{9/8}$) of 1. 24. In contrast, the control polymer is unable to distinguish between the two bis-imidazole substrates. The selectivity characteristics of these surface-grafted polymers are similar to those obtained in bulk-copolymerized imprinted materials (Dhal and Arnold 1992), which were prepared using the functional monomer **6** and EGDMA as crosslinking monomer. However, unlike the bulk-copolymerized materials, structural strength is provided by the poly(TRIM) matrix on which the surface graft has been incorporated using the imprinting process.

Conclusions

By controlling the polymerization conditions it is possible to obtain macroporous poly(TRIM) with surface accessible polymerizable double bonds. These reactive double bonds can be used to link functional polymer chains to the surface of the solid support by polymerization in the presence of appropriate functional monomer. Compared to the

macroporous copolymers with a homogeneous distribution of functional groups, confining the functional polymer chains to the surface of the matrix enhances their accessibility for substrate binding. Moreover, as the modifications are confined to the surface regions, solvent effects influencing the functional polymer chains do not compromise the overall matrix integrity. Thus functional polymer surfaces possessing desirable material properties can be obtained. In particular, the poly(TRIM) reactive surface appears to be well-suited for surface template polymerization in order to create highly selective adsorbents, which combine the structural stability of the poly(TRIM) matrix with the binding functionalities incorporated in the polymer surface coating. Moreover, the surface coating technique allows better site accessibility than imprinted polymers prepared by bulk copolymerization.

Experimental Procedures

Instrumentation and analytical techniques

Elemental analyses were performed at Galbraith Laboratories, Knoxville, TN. Melting points were determined on a Büchi melting-point apparatus. IR spectra were recorded in the form of clean KBr pellets using a Perkin-Elmer 1600 FTIR spectrophotometer. Electronic absorption measurements were carried out with a Milton-Roy Array 3000 spectrophotometer. Solution ^{1}H and ^{13}C NMR spectra were recorded on a JEOL GX-400 spectrometer operating at 400 MHz for ^{1}H and at 100 MHz for ^{13}C nuclei. Chemical shifts were recorded relative to tetramethylsilane as an internal reference in the samples. Solid-state CP-MAS ^{13}C NMR spectra were recorded on a

Bruker MSL-200 spectrometer operating at 50.3 MHz. Chemical shifts were calibrated by external reference to aromatic carbon of hexamethyl benzene (132.1 ppm relative to tetramethylsilane). Specific surface areas and pore volumes of the polymers were determined from nitrogen adsorption measurements using an Omnisorp 100 analyzer. Electron micrographs were obtained with a Cam Scan series 2 scanning electron microscope after vacuum coating of the samples with gold. X-ray photoelectron spectra (XPS) of the powder polymer samples were obtained with a VG Scientific Ltd. ESCALAB MK2 electron spectrometer equipped with a VG 5250 data system and a computer controlled translation stage. The spectrometer was operated at a base pressure of about 8.0 x 10^{-11} Torr. The unmonochromatized Mg K_α X-ray source (1253.60 eV) was operated at 15 kV and 20 mA (300 W) and bandpass was set for a resolution of 0.8 eV. Spectra were collected in CAE mode at the appropriate takeoff angles, with the angle defined as that between the sample surface plane and the analyzer axis. Charge compensation was done using a flood gun and referencing of the peaks was carried out by considering the binding energy of hydrocarbon type carbon as 286.0 eV. The samples were dried at 60 °C under high vacuum for 24 h prior to analysis.

Materials and methods

Copper(II) dimethacrylate was synthesized following the procedure of Yici et al. (1991). Methacrylamide and vinylazlactone were obtained from Monomer-Polymer Inc. All other reagents were obtained from Aldrich. Reagents and solvents were purified

following standard methods. 2,2'-azobisisobutyronitrile (AIBN) was recrystallized from ethanol prior to use.

Cu(II)[*N*-(4-vinylbenzyl)imino]diacetate dihydrate (6). The metal chelating ligand [*N*-(4-vinylbenzyl)imino]diacetic acid (5 gm, 20 mmol) was synthesized following the procedure of Morris et al. (1959), and suspended in 30 mL of distilled water. The suspension was treated with 0.1N NaOH, to reach a pH of 7.0, and $CuSO_4.5H_2O$ (5gm, 20 mmol) dissolved in 50 mL of distilled water was slowly added with continuous stirring. The solution was allowed to stir for 3 h, and the solvent removed under vacuum. The residue was treated with 30 mL of methanol and filtered to remove insoluble material. The filtrate was kept at –20 °C, to give bright blue crystals of 6, which were recrystallized from 80:20 ethanol:water solution. Yield: 65%; m.p.: 192-195 °C. Anal. Calculated for $C_{13}H_{17}O_6NCu$: C, 45.02; N, 4.04; H, 4.94. Found C, 44.85; N, 3.92; H, 5.12.

1,4-bis(imidazole-1-ylmethyl)benzene (8). Sodium hydride (1.9 gm, 48 mmol, 60% suspension in mineral oil) was washed with 10 mL of dry THF under nitrogen flow. Dry THF (30 mL) was added, followed by slow addition of 2.85 gm (44mmol) of imidazole in 15 mL of dry THF. After stirring for 30 min, α,α'-dibromo-*p*-xylene (5.3 gm, 20 mmol) dissolved in 20 mL dry THF was added to the suspension. The temperature was raised to 50 °C, and the reaction was conducted under refluxing conditions for 4 h. After cooling, the reaction mixture was treated with 20 mL of ice-cold water and stirred for 20 min. The organic phase was extracted with chloroform (3 x 50 mL) and the combined organic phase was dried over anhydrous sodium sulfate. The

solvent was removed under reduced pressure, and the residue was recrystallized twice from ethyl acetate, to obtain **8**. Yield: 55%; m.p.: 148-150 °C. Anal. Calculated for $C_{14}H_{14}N_4$: C, 70.56; N, 23.51; H, 5. 92. Found C, 70.11, N, 23.36; H, 6.02. ^{1}H NMR ($CDCl_3$) δ 5. 20 (s, 4 H), 6. 85 (s, 2 H), 7.05 (s, 2 H), 7.20-7.24 (m, 4 H), 7.55 (s, 2 H). ^{13}C NMR ($CDCl_3$) δ 49.6, 118.7, 127.3, 129.0, 135.8, 136.7.

4,4'-bis(imidazole-1-ylmethyl)biphenyl (9). Bis(bromomethyl)biphenyl was used instead of the dibromoxylene in the above procedure. All other reaction steps were identical, but the product was obtained as a viscous liquid after removal of solvent under reduced pressure. The viscous liquid solidified after 48 h at –10 °C. Yield: 45%. Anal. Calculated for $C_{20}H_{18}N_4$: C, 76.41, N, 17.82, H, 5.77. Found C, 76.23; N, 17.75; H, 5.70. ^{1}H NMR ($CDCl_3$) δ 5. 20 (s, 4 H), 6. 85 (s, 2 H), 7.05 (s, 2 H), 7.3-7.7 (m, 10 H). ^{13}C NMR ($CDCl_3$) δ 49.8, 119.2, 127.2, 127.8, 129.2, 136.2, 137.0, 139.8.

Preparation of poly(TRIM) support : In a 250 mL round bottom flask, 10 g of TRIM monomer was dissolved in 25 mL of toluene:cyclohexane (30:70 v/v). To this 100 mg of AIBN was added, and the reaction mixture was bubbled with argon gas for 2 h. The sealed flask was kept at 55 °C for 4 h with gentle stirring. The polymer thus obtained was cooled to room temperature, broken into small pieces, and extracted with 250 mL of methanol for 8 h at 37 °C in a shaker bath to remove any unreacted monomer. After filtering, the polymer was dried under vacuum to constant weight, ground, and sieved. Particles in the size range 38-63 μm were used for subsequent experiments.

Preparation of bulk copolymers of TRIM with functional monomers (**2-4**) : A typical procedure is described using **2** as the functional monomer. 4 g of TRIM, 0.6 g of **2**, and 46 mg of AIBN were dissolved in 10 mL of toluene:dioxane (80:20 v/v). The reaction mixture was bubbled with argon for 1 h and polymerized at 70 °C for 12 h and at 80 °C for 15 h. After cooling to room temperature, the polymer was washed with ethanol and dried under vacuum. It was subsequently ground, sieved to the appropriate particle size (63-38 /Cm), extracted with hot methanol overnight, and dried to constant weight under vacuum at 50 °C.

Preparation of bulk copolymer *of TRIM with* **5** : In a typical experiment, a solution of 4 g of TRIM and 50 mg of AIBN dissolved in 6 mL of ethanol was added to 5 mL of ethanolic solution of monomer **5** (0.8 g). After the reaction mixture was bubbled with argon, polymerization and subsequent work up were carried as described above.

Comonomer grafting on poly(TRIM) surface : The general procedure for grafting is described using **2** as the comonomer. Typically, a 50 mL round-bottom flask with a sidearm (outlet) containing 1 g of macroporous poly(TRIM) particles was evacuated for 5 h with gentle stirring. After closing the vacuum connection, a solution of 0.25 g of **2** and 15 mg of AIBN in 5 mL of dioxane was injected slowly (with the system still under vacuum). The resulting mixture was allowed to stir gently under vacuum for 18 h, during which time the monomer solution diffuses inside the pores of the polymer support. After purging with argon for 3 h, the flask was kept at 60 °C for 12 h, at 70 °C for 6 h, and finally at 80 °C for 6 h to ensure complete polymerization. The polymer was cooled to room temperature, washed with 30 mL of methanol, and filtered. The solid residue was

subsequently Soxhlet extracted with refluxing methanol for 24 h to remove ungrafted soluble polymers. After filtering, the polymer was dried to constant weight under vacuum at 50 °C.

Template polymerization by grafting polymerizable monomer-template assembly onto poly(TRIM) : To a stirred solution of 0.6 g of monomer **6** in 5 mL of methanol, 0.21 g of template **8** in 5 mL of methanol was added slowly. After this stirred for 30 min, 0.25 g of EGDMA (**7**) and 25 mg AIBN were added, and the solution was bubbled with a slow stream of N_2 for 30 min. This monomer solution was injected slowly to 3 g of macroporous poly(TRIM) in a 100 mL round bottom flask (evacuated as described above). The resulting suspension was allowed to stir under vacuum for 18 h. Polymerization and work up was similar to the procedure described above for grafting of other functional monomers. A control polymer was prepared in a similar manner, using 1-benzylimidazole instead of **8** as the template. Templates and metal ions were removed, and metal reloading and substrate binding studies were performed following procedures described previously (Dhal and Arnold 1992).

Copper removal : Typically 0.5 g of polymer was suspended in 30 mL of 0.1 M aqueous EDTA (pH 7.0) and was kept in a shaker bath at 37 °C for 36 h. After the polymer was filtered and thoroughly washed, the amount of copper extracted to the aqueous phase was estimated spectrophotometrically.

Polymer swelling : The swelling measurements of these polymer particles were carried out following a literature procedure (Shea et al. 1990). A given volume of dry polymer (typically 2 cm^3) was transferred to a 10 mL graduated centrifuge tube,

graduated to each tenth of a milliliter. The polymer was allowed to pack properly with the help of a vortex vibrator, and the exact dry volume was noted. Excess solvent (approximately 5 times) was added, and any trapped air bubbles were removed by vibration. The polymer was kept at 37 °C in a shaker bath for 24 h. After centrifugation, the final volume of the solvent swollen polymer was noted. Values of the dry and swollen volumes of the polymer were used to calculate percent swelling of the polymer (percent swelling = 100 x change in volume/volume dry polymer). The values reported are an average of three measurements, which have a mutual variation of less than 5%.

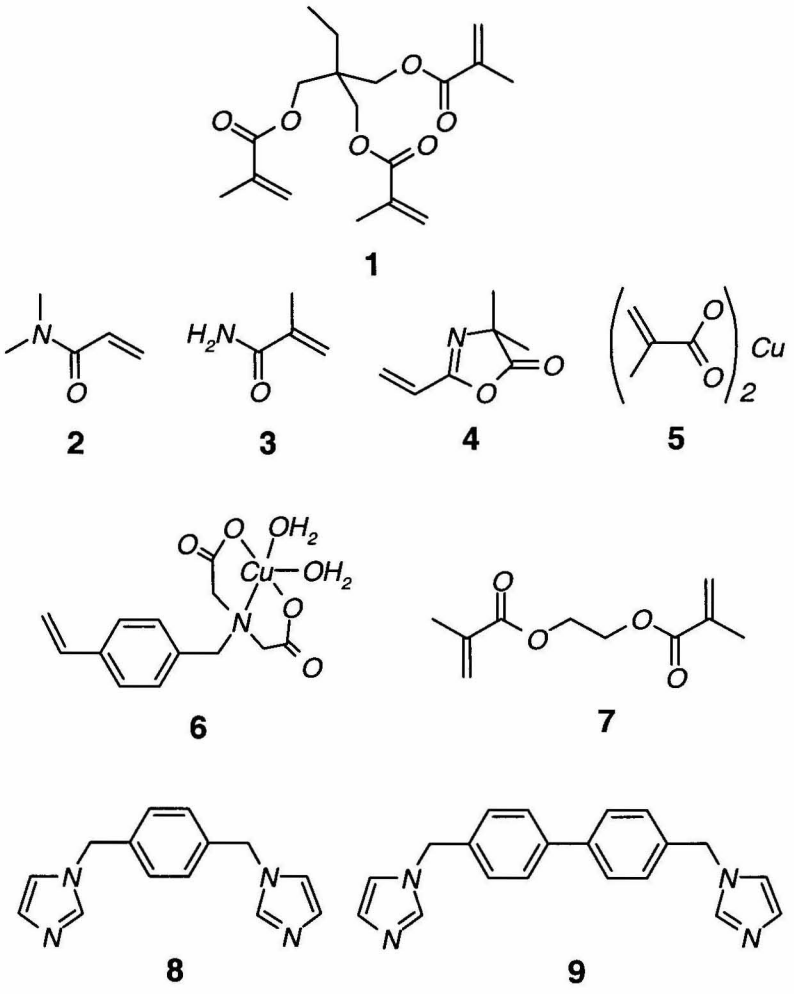

Figure 2. 1. Functional monomers and templates investigated in the study.

1. 2-ethyl-2-(hydroxymethyl)propane-1,3-diol trimethacrylate (trimethylolpropane trimethacrylate, TRIM); **2**. *N*,*N*-dimethylacrylamide; **3**. methacrylamide; **4**. vinylazlactone; **5**. Cu(II) dimethacrylate; **6**. Cu(II)-[*N*-(4-vinylbenzyl)imino]diacetic acid (Cu(VBIDA)); **7**. ethylene glycol dimethacrylate (EGDMA); **8**. 1,4-bis(imidazol-l-ylmethyl)benzene; **9**. 4,4'-bis(imidazol-l-ylmethyl)biphenyl.

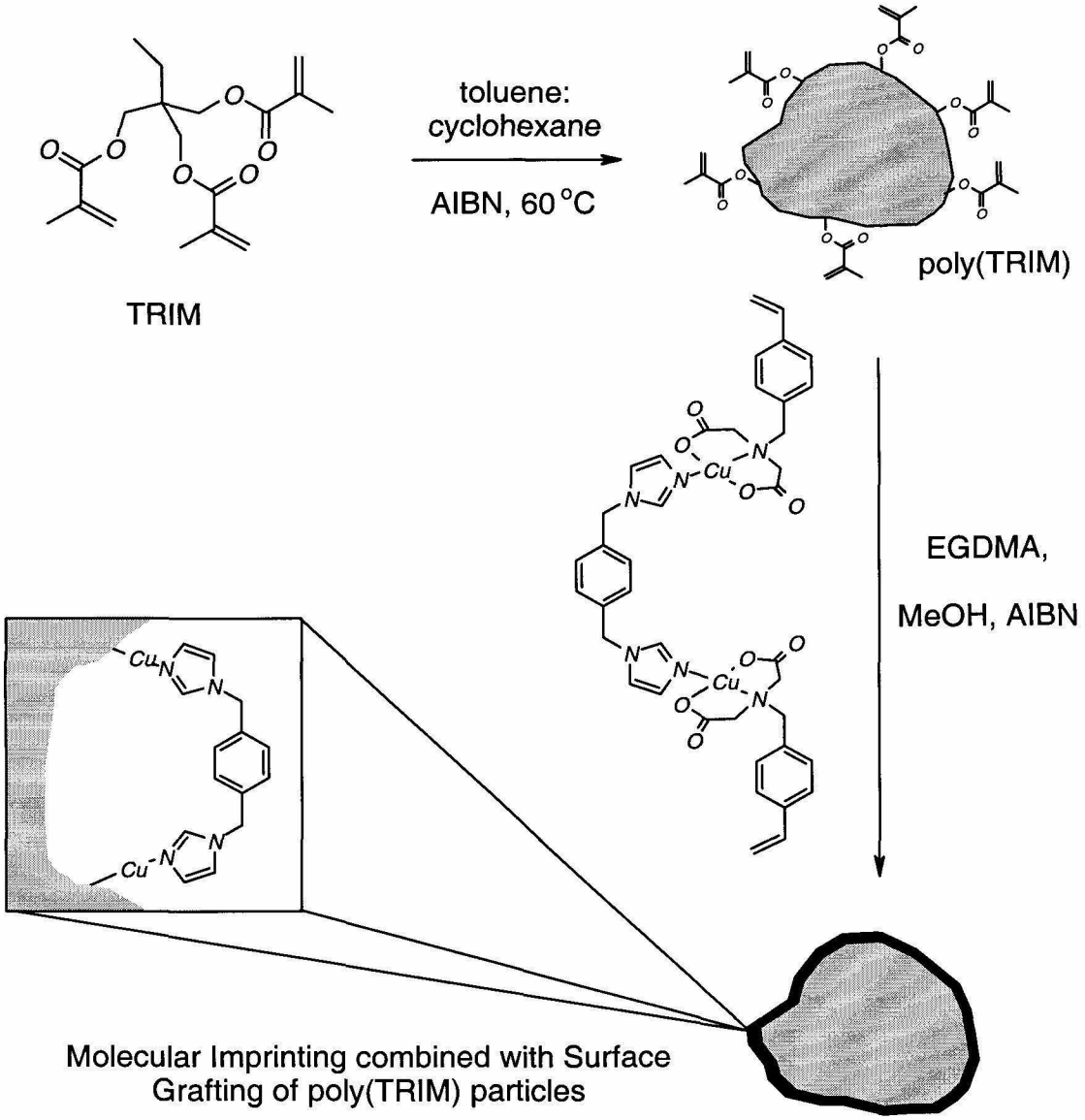

Figure 2. 2. Scheme for preparing molecularly imprinted polymers as surface coats on poly(TRIM) particles. A different solvent system can be used for preparing the bulk polymer of TRIM as compared to the surface coating step, in order to design the physical properties and functional characteristics of the composite polymer material. The polymer coat incorporates copper ions in a geometry determined by the imprinting process.

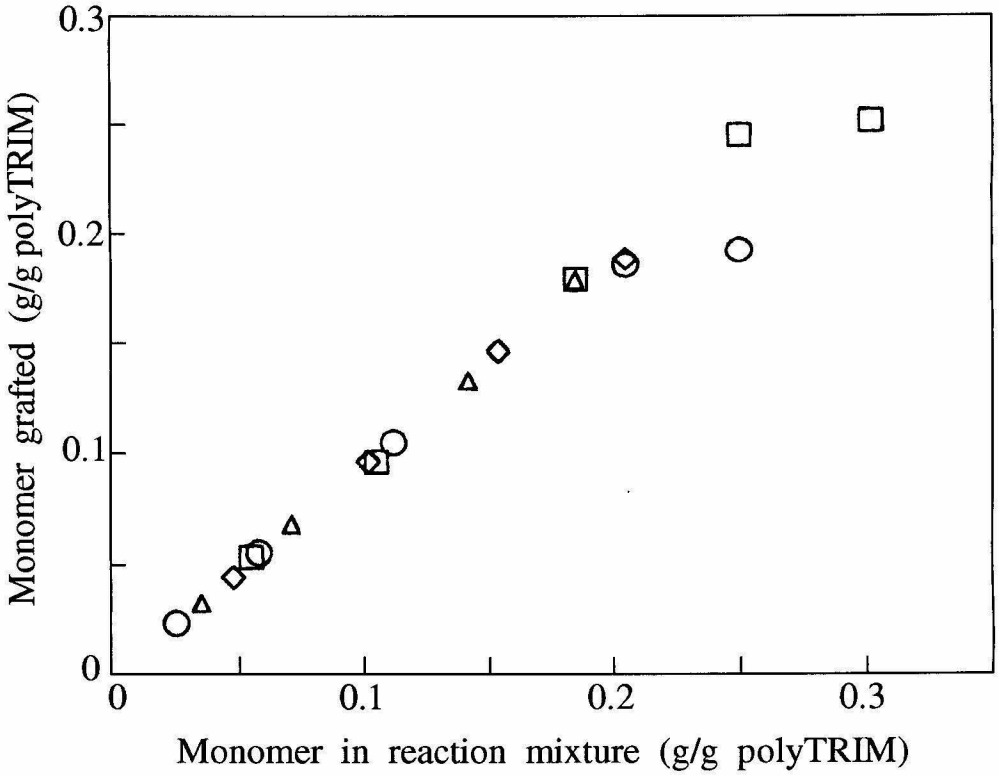

Figure 2. 3. Quantitation of surface grafting of functional monomers on poly(TRIM). Amount of functional monomer grafted onto poly(TRIM) surface as a function of monomer concentration in the polymerization mixture: monomer **2** (•); monomer **3** (•); monomer **4** (Δ) and monomer **5** (•).

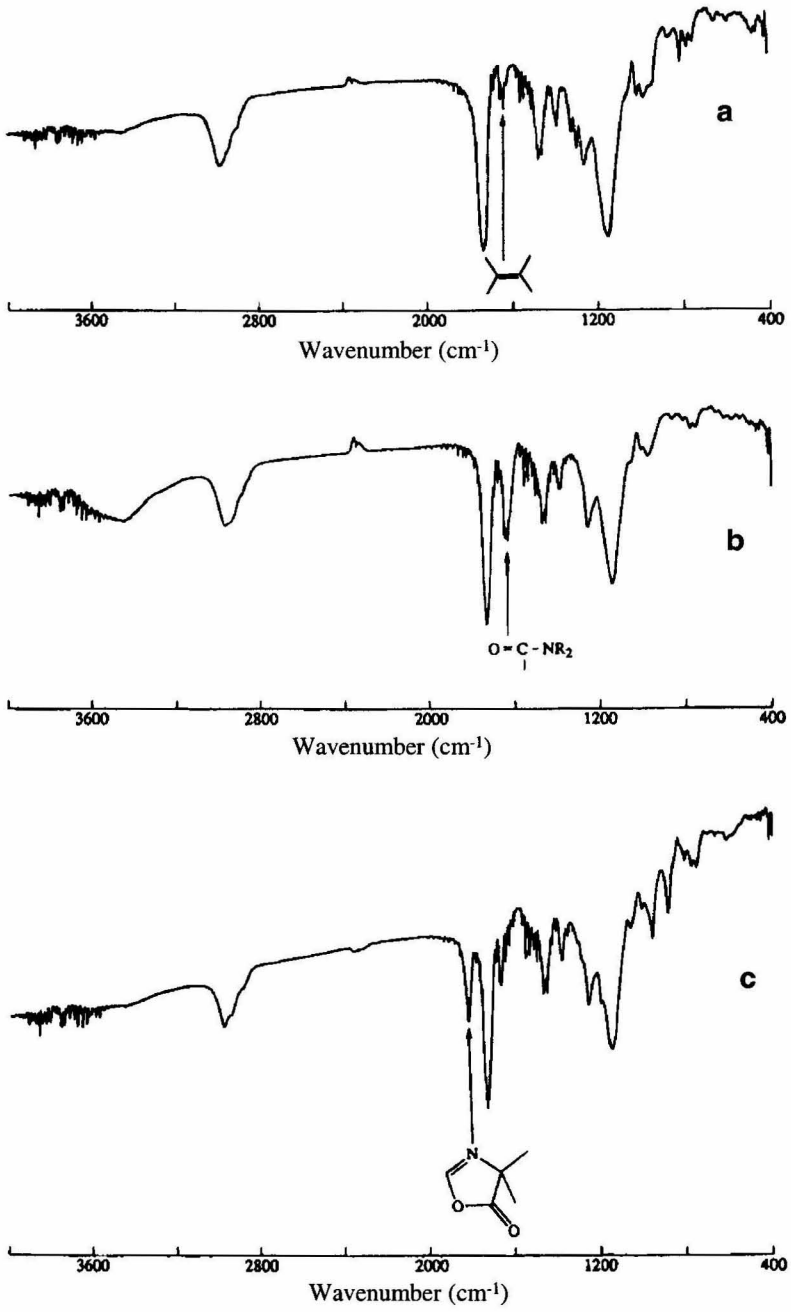

Figure 2. 4. Infrared Spectra of poly(TRIM) and surface grafts. I.

(**a**) bulk polymerized poly(TRIM); (**b**) poly(TRIM) grafted with monomer **3** and (**c**) poly(TRIM) grafted with monomer **4**.

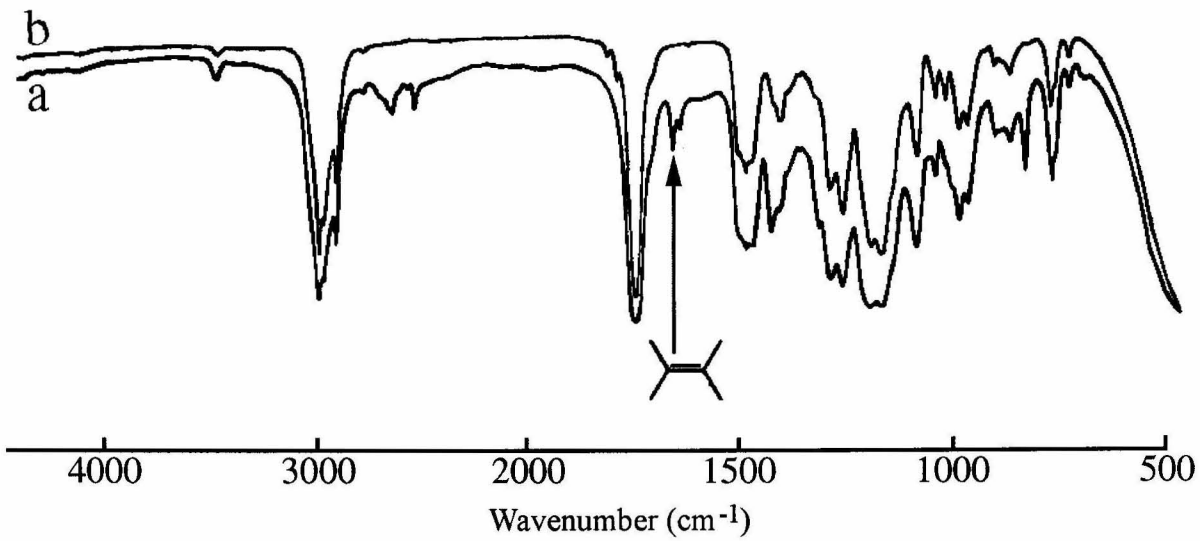

Figure 2. 5. Infrared spectra of poly(TRIM) and surface grafts. II.

(**a**) macroporous poly(TRIM) bearing residual methacrylate groups, and (**b**) the same polymer after annealing at 80 °C for 30 h.

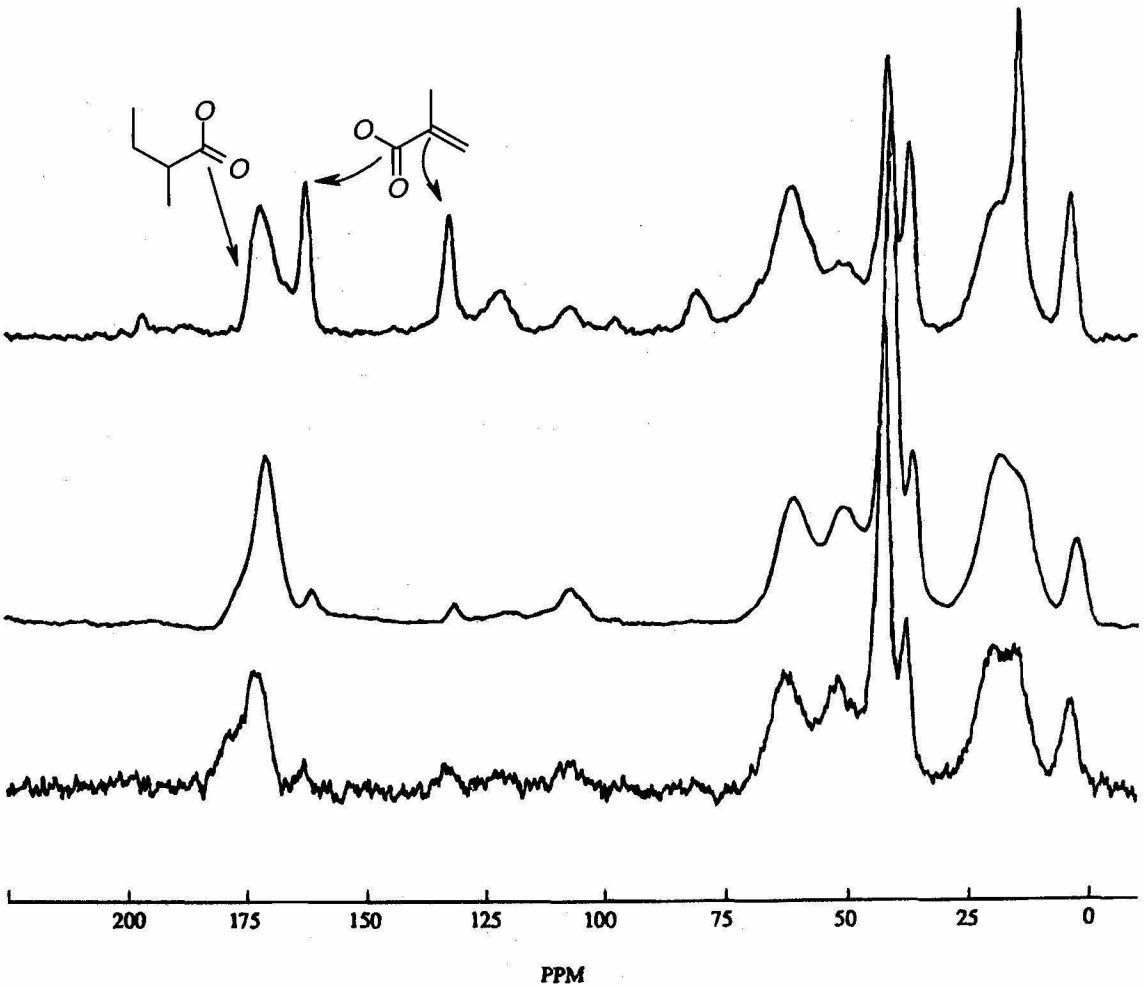

Figure 2. 6. CP-MAS ^{13}C NMR spectra of poly(TRIM) and surface grafts.

(**a**) macroporous poly(TRIM) with residual methacrylate residues, showing carbonyl resonances corresponding to both saturated and unsaturated alpha carbon atoms; (**b**) poly(TRIM) surface grafted with monomer **3**, and (**c**) bulk copolymer of TRIM with monomer **3**. Spectra **b** and **c** show loss of carbonyl resonances corresponding to unsaturated alpha carbon atoms.

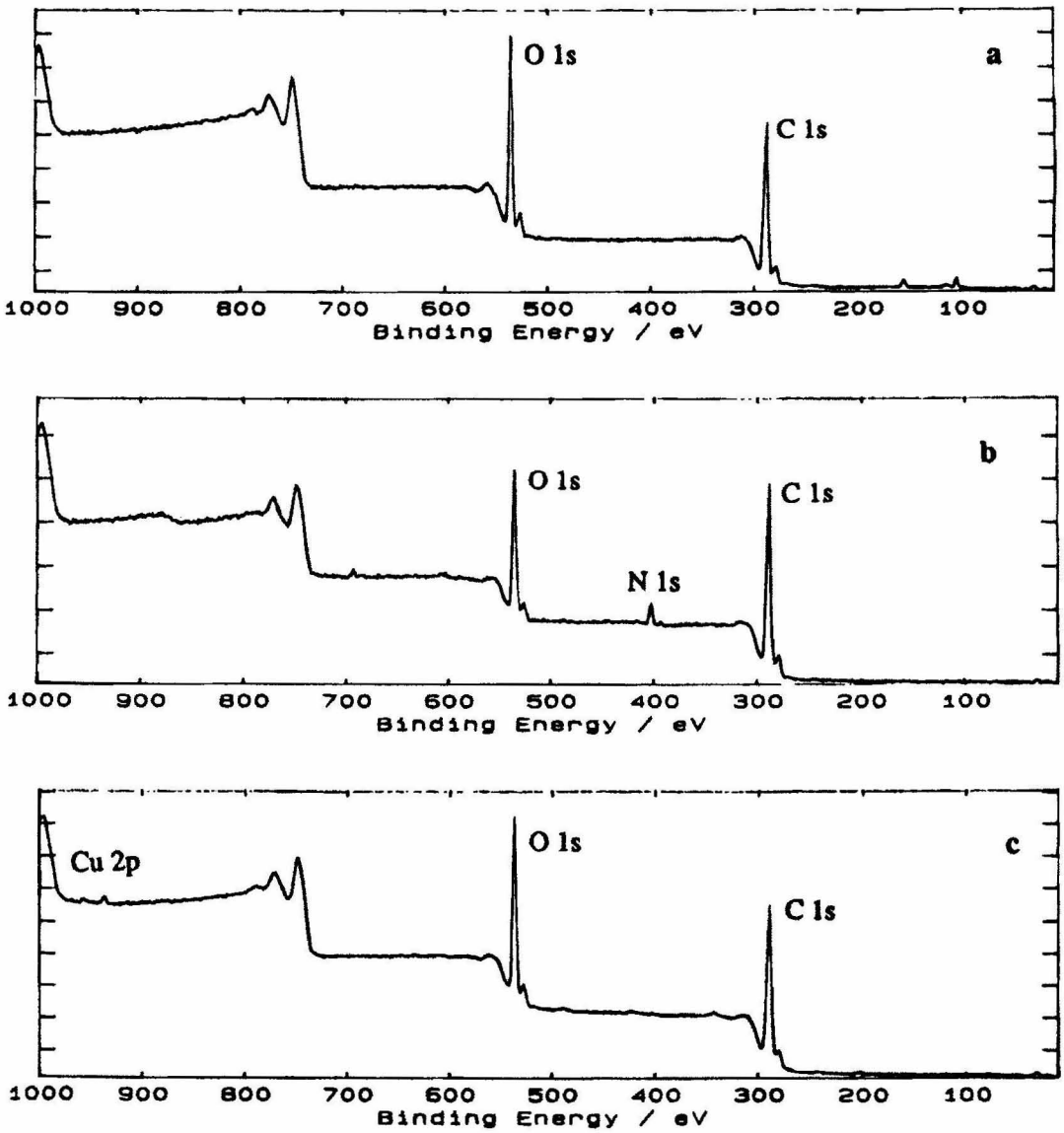

Figure 2. 7. X-ray photoelectron spectra of poly(TRIM) and surface grafts.

(**a**) macroporous poly(TRIM) with residual methacrylate residues; (**b**) poly(TRIM) grafted with monomer **3**; and (**c**) poly(TRIM) grafted with **5**.

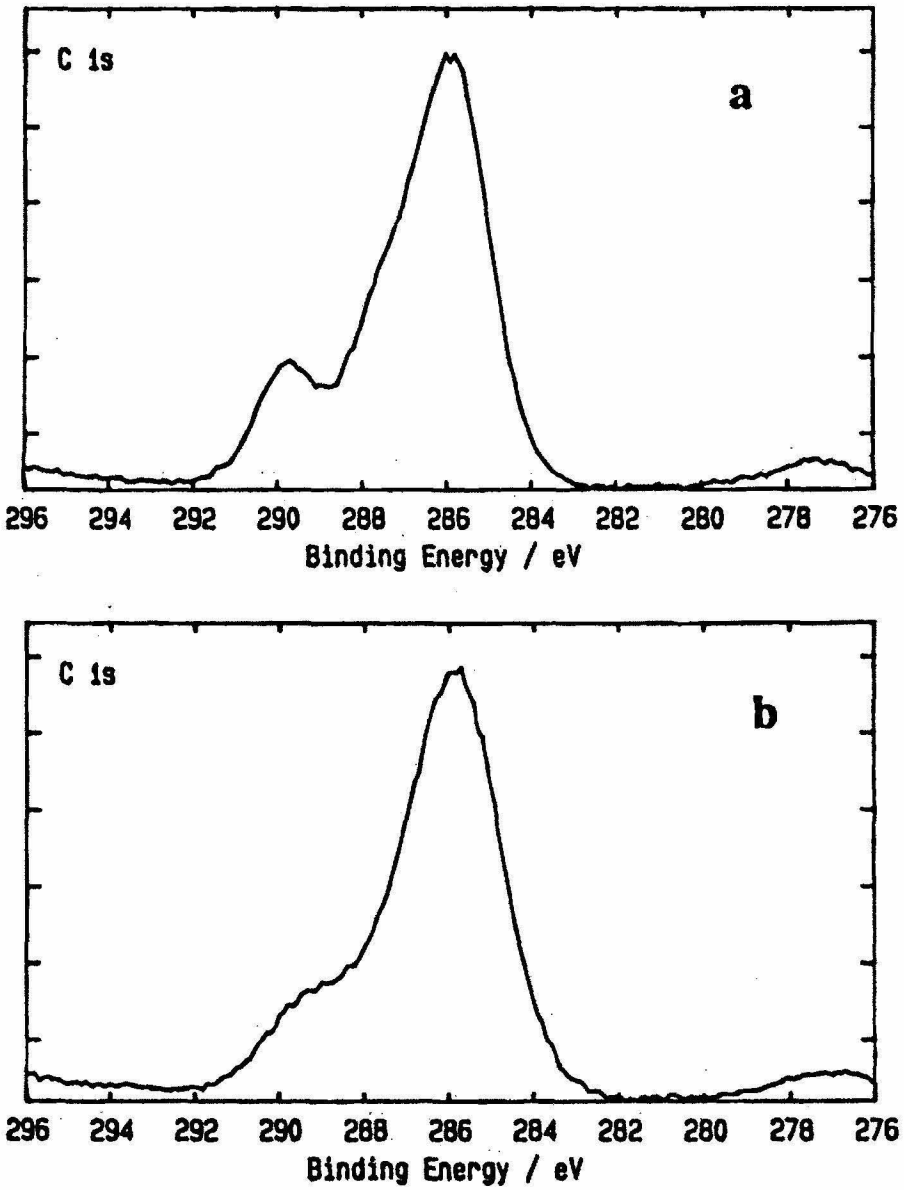

Figure 2. 8. Expanded view of the C(1s) region of X-ray photoelectron spectra.

(**a**) poly(TRIM) with methacrylate residues and (**b**) poly(TRIM) grafted with monomer **3**.

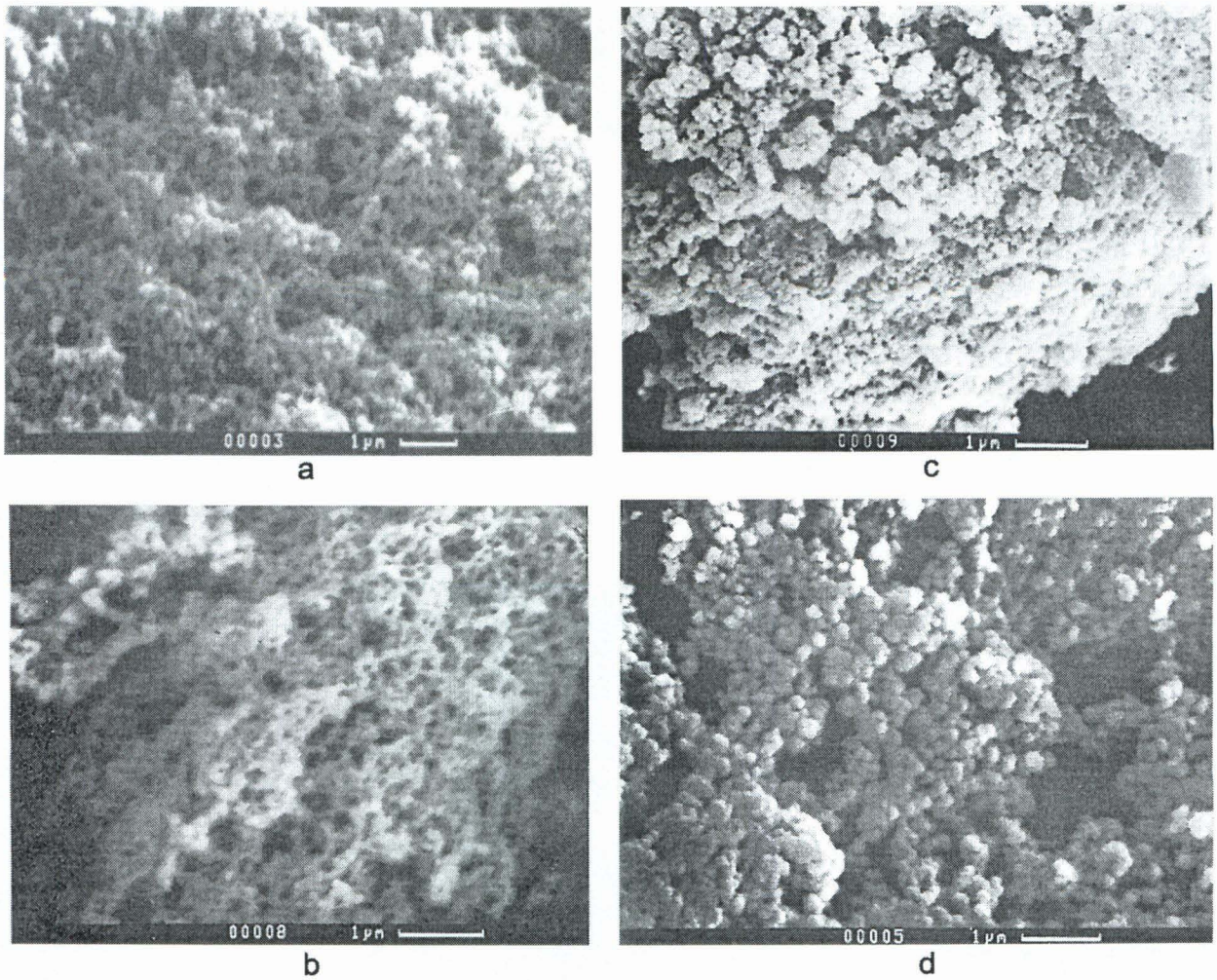

Figure 2. 9. Scanning electron micrographs of poly(TRIM) and surface grafts.

(**a**) poly(TRIM); (**b**) bulk copolymer of TRIM with monomer **3**; (**c**) poly(TRIM) grafted with monomer **2**; and (d) poly(TRIM) grafted with monomer **3**.

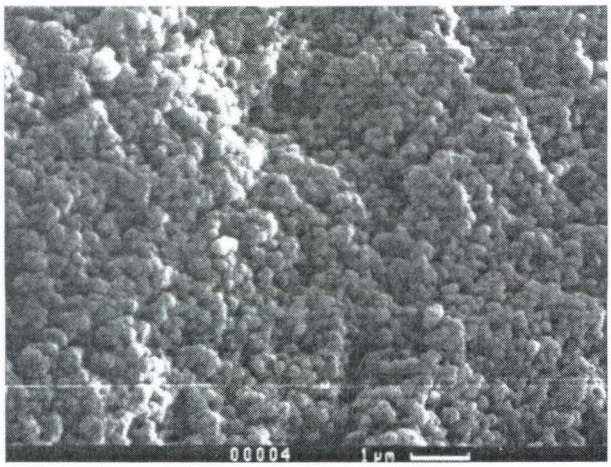

a

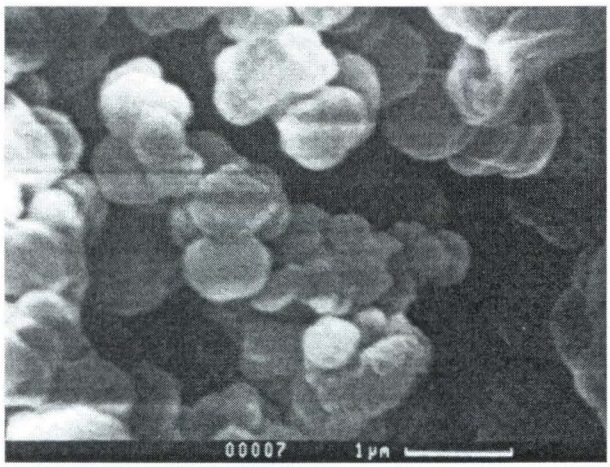

b

Figure 2. 10. Scanning electron micrographs of water-equilibrated samples.

(**a**) poly(TRIM) grafted with monomer **3**; (**b**) bulk copolymer of TRIM with monomer **3**.

Polymer	Comonomer and (mode of incorporation)	Mol % functional monomer in the matrix[a]	Specific surface Area (m^2g^{-1})
P-1	poly(TRIM)	-	285
P-2	**2** (graft)	5.3	215
P-3	**2** (graft)	9.6	212
P-4	**2** (bulk)	5.5	275
P-5	**2** (bulk)	10.2	272
P-6	**3** (graft)	5.5	202
P-7	**3** (graft)	18.5	192
P-8	**3** (graft)[b]	4.3	195
P-9	**3** (graft)[b]	12.6	n.d.[c]
P-10	**3** (bulk)	6.2	257
P-11	**3** (bulk)	15.5	260
P-12	**4** (graft)	7.3	205
P-13	**4** (graft)	14.2	n.d.
P-14	**4** (bulk)	4.5	n.d.
P-15	**4** (bulk)	12.5	n.d.
P-16	**5** (graft)	4.4	208
P-17	**5** (graft)	14.6	196
P-18	**5** (bulk)	5.3	265
P-19	**5** (bulk)	10.3	260

Table 2. 1. Physicochemical characteristics of poly(TRIM) and surface-grafts: Synthesis parameters (identity of graft comonomer and mol% incorporated into the matrix) and specific surface areas as measured by N_2 adsorption. [a]Estimated from elemental analysis data. [b]Water used as the polymerization medium. [c]Not determined.

Polymer Code[a]	Cu(II) (mmol/gm) in the copolymer	Recovery of Cu(II) (mmol/gm) from the copolymer[b]
P-16	0.13	0.11
P-17	0.45	0.41
P-18	0.16	0.10
P-19	0.38	0.25

Table 2. 2. Copper removal from TRIM copolymers by EDTA treatment. [a]Polymer code refers to Table 2. 1. [b]Amount of copper released from the matrix by one step of EDTA extraction, estimated spectrophotometrically.

Polymer code[a]	% swelling in water
P-2	15
P-3	20
P-5	45
P-6	20
P-7	35
P-11	75

Table 2. 3. Swelling of surface-grafted and bulk-copolymerized TRIM-copolymers in water. [a]Polymer code refers to Table 2. 1.

References

Akelah, A. and Most, A. 1990. *Functionalized Polymers and Their Applications,* Chapman and Hall, London, UK.

Albright, R.L. 1972. U.S. Patent 3,663,467.

Albright, R.L. 1986. *React. Polym.* **4:** 155-174.

Allcock, H.R., Fitzpatrick, R.J., and Visscher, K. 1992. *Chem. Mater.* **4:** 775-780.

Arshady, R. 1991. *Adv. Mater.* **3:** 182-190.

Bayer, E. 1991. *Angew. Chem. Int. Ed. Engl.* **30:** 113-129.

Boven, G., Oosterling, M.L.C.M., Challa, G., Schouten, A.J. 1990. *Polymer.* **31:** 2377-2383.

Briggs, D., Seah M.P. 1983. eds. *Practical Surface Analysis by Auger and X-ray Photoelectron Spectroscopy.* John Wiley and Sons, New York, NY.

Dhal, P.K. and Arnold, F.H. 1991. *J. Am. Chem. Soc.* **113:** 7417-7418.

Dhal, P.K. and Arnold, F.H. 1992. *Macromolecules.* **25:** 7051-7059.

Dickey, F.H. 1949. *Proc. Natl. Acad. Sci. U.S.A.* **35:** 227-229.

Dickey, F.H. 1955. *J. Phys. Chem.* **59:** 695-699.

Ekberg, B. and Mosbach, K. 1989. *Trends Biotechnol.* **7:** 92-96.

Fazio, R.C., Grasshoff, J.M., and Taylor, L.D. 1992. *J. Polym. Sci. A.* **40:** 329-331.

Ford, W.T. 1986. ed. *Polymeric Reagents and Catalysts.* ACS Symposium Series 308, American Chemical Society, Washington, DC.

Frechet, J.M.J., Darling, G.D., Itsuno, S., Lu, P.-Z., Meftahi, M.V., and Rolls, W.A. 1988. *Pure Appl. Chem.* **60:** 353-364.

Greenley, R.Z. 1989. In *Polymer Handbook* (eds. Brandrup, J. and Immergut, E.H.), p II/153. John Wiley and Sons, New York.

Hargitai, T., Reinholdsson, P., Tornell, B., and Isaksson, R. 1991. *J. Chromatogr.* **540:** 141-155.

Haupt K. and Mosbach, K. 1998. *Tibtech.* **16:** 468-475.

Hjertberg, T., Hargitai, T., and Reinholdsson, P. 1990. *Macromolcules* **23:** 3080-3087.

Kennedy, J.F., Melo, E.H.M., and Jumel, K. 1990. *Chem. Eng. Prog.* **86:** 81-89.

Kempe, M. and Mosbach, K. 1995. *Tetrahedron Lett.* **36:** 3563-3566.

Lee, K.-W.; McCarthy, T. J. *Macromolecules* 1988, 21, 309-313.

Leydon, D. and Collins, W. 1980. *Silylated Surfaces.* Gordon & Breach: New York, NY.

Mallik, S., Plunkett, S.D., Dhal, P.K., Johnson, R.D., Pack, D., Shnek, D., and Arnold, F.H. 1994. *New J. Chem.* **18:** 299-304.

Merrifield, R.B. 1985. *Angew. Chem., Int. Ed. Engl.* **24:** 799-810.

Morris, L.R., Mock, R.A., Marshall, C.A., and Howe, J.H. 1959. *J. Am. Chem. Soc.* **81:** 377-382.

Nörrlow, O., Glad, M., and Mosbach, K. 1984. *J. Chromatogr.* **299:** 29-41.

Pauling, L. 1940. *J. Am. Chem. Soc.* **62:** 2643.

Plunkett, S.D. and Arnold, F.H. 1995. *J. Chromatogr. A.* **708:** 19-29.

Pouchet, C.J. 1978. ed. *The Aldrich Library of Infrared Spectra,* 2nd ed. p 335F. Aldrich Chemical Co., Milwaukee.

Ramström, O. and Mosbach. K. 1999. *Curr. Opin. Chem. Biol.* **3:** 759-764.

Rasmussen, J.K., Heilmann, S.M., and Krepski, L.R. 1988. *Encyl. Polym. Sci. Eng.* **11:** 558-571.

Reinholdsson, P., Hargitai T., Isaksson, R., and Törnell, B. 1991. *Angew. Makromol. Chem.* **192:** 113-132.

Rosenberg, J.E. and Flodin, P. 1987. *Macromolecules* **20:** 1522-1526.

Shea, K.J. and Sasaki. D.Y. 1989. *J. Am. Chem. Soc.* **111:** 3442–3444.

Shea, K.J., Stoddard, G.J., Shavelle, D.M., Wakui, F., and Choate, R.M. 1990. *Macromolecules.* **23:** 4497-4507.

Sherrington, D.C. and Hodge, P. 1988. eds. *Syntheses and Separations Using Functional Polymers.* John Wiley & Sons, New York, NY.

Unger, K.K. 1979. *Porous Silica.* Elsevier Publishing Co., Amsterdam, Netherlands.

Verweij, P.D. and Sherrington, D.C. 1991. *J. Mater. Chem.* **1:** 371-374.

Walenius, M., Flodin, P., and Porath, J. 1992. *J. Chromatogr.* **604:** 5-11.

Wulff, G. and Sarhan, A. 1972. *Angew. Chem. Int. Ed. Engl.* **11:** 341-355.

Wulff, G. 1986. Molecular recognition in polymers prepared by imprinting with templates. In *Polymeric reagents and catalysts, American Chemical Society Symposium Series, vol. 308.* (ed. Ford W.T.), pp. 186–229. American Chemical Society, Washington, DC.

Wulff, G. 1993. *Trends Biotechnol.* **11**: 85-87.

Yici, G., Yaoyu, W., Ying, Z., and Qizhen, S. 1991. *Polyhedron.* **10:** 1893-1895.

Chapter 3

Molecular Imprinting II: Ligand-exchange Adsorbents for Enantioresolution of Underivatized α-amino acids

Preface

The following chapter describes the molecular imprinting of enantioselective ligand-exchange polymeric adsorbents for amino acid separations. A large part of this chapter is reproduced with permission from the following publication: Sundaresan, V., Ru, M., and Arnold, F.H. 1997. Molecularly imprinted ligand-exchange adsorbents for the chiral separation of underivatized amino acids. *J. Chromatogr. A.* **775:** 51-63. Michael Ru, an undergraduate student at Caltech, assisted in the performance of the necessary experiments, following established protocols in the laboratory.

Abstract

Ligand-exchange adsorbents that are enantioselective for underivatized α-amino acids have been synthesized by molecular imprinting using only achiral monomers. Bulk polymers were prepared by allowing the functional monomer, Cu(II)-*N*-(4vinylbenzyl)iminodiacetic acid, to form complexes with the template amino acid in solution, followed by crosslinking with ethylene glycol dimethacrylate. To make supports suitable for chromatography, the imprinted polymer was grafted to derivatized silica particles. Racemic mixtures of various underivatized α-amino acids are resolved on the imprinted adsorbents. Adsorbents prepared from amino acids with larger, aromatic side chains exhibit the highest selectivities (α = 1.65 for the enantioresolution of D,L-phenylalanine). Cross-selectivity for similar amino acids also depends on side chain size: materials templated with L- or D-phenylalanine exhibit good enantioselectivity when challenged with racemic tyrosine ($\alpha \sim 1.4$) and much reduced enantioselectivities towards D,L-tryptophan or aliphatic amino acids. Materials imprinted with alanine show no selectivity. The ability of a material imprinted with an amino acid enantiomer to resolve an analogous chiral amine is also demonstrated. The mechanisms underlying the observed enantioselectivity are discussed in light of the three-point interaction model for conventional chiral ligand-exchange separations.

Introduction

Ligand exchange chromatography (LEC) has been successfully applied to the chiral separation of a large number of amines (Rogozhin and Davankov 1971), carbohydrates (Caruel et al. 1991) and various β-blocker and adrenergic drugs that contain the amino alcohol functionality (Gubitz et al. 1992). One particularly well-studied application of LEC is the chiral separation of amino acids. Chiral stationary phases (CSP) for LEC of amino acids are typically synthesized by covalent attachment of a chiral metal-chelating ligand such as L-proline to a chromatographic support. A polymerizable derivative of L-proline can be used, for example, as a comonomer in a crosslinking polymerization (Lefebvre 1978), or it can be grafted onto the surface of a silica support (Davankov 1989). During chromatography, the mixed ligand complexes that form at the adsorbent surface have two chiral ligands coordinated to the metal ion, the L-proline from the CSP itself and an enantiomer from the sample. The complex is therefore a diastereomeric adduct, the two forms of which are expected to have different stabilities and are therefore resolved in the chromatographic separation. Formation of a diastereomeric adduct, however, is not sufficient to result in a separation. The interaction between the solid support and the mixed ligand complex is important in determining the resolution, and the retention order of enantiomers on such materials is not always predictable. For example, polystyrene-divinylbenzene derivatized with L-proline (Lefebvre 1978) shows a different order of elution as compared to a polyacrylamide-based material (Davankov 1989) for enantioresolution of D,L-phenylalanine. The choice of adsorbent is therefore a matter of trial and error, as is the optimization of the separation protocol.

We have developed a different, easily generalizable approach towards preparing chirally selective ligand-exchange supports, using the technique of molecular imprinting. This technique is attractive for preparing selective adsorbents for chiral and other separations for which conventional adsorbents might be unsuitable (Mosbach 1994; Wulff 1995). Molecularly imprinted chiral adsorbents, capable of separating different kinds of amino acid derivatives, have been prepared by using hydrogen-bonding interactions with methacrylic acid monomers (Andersson et al. 1984; Sellergren et al. 1985, 1988; Kempe and Mosbach 1991). Amino acid derivatives such as L-phenylalanine anilide or *tert*-butyloxycarbonyl-L-phenylalanine were used as the templates, so that the resulting adsorbents could separate only the correspondingly derivatized amino acid enantiomers. Derivatization helps to eliminate repulsive electrostatic interactions between methacrylic acid and the underivatized amino acid, and the bulky side group also assists chiral recognition. The obvious disadvantages with these approaches are that derivatization is cumbersome and additional steps are required to retrieve the free amino acid after separation. Also, reliance on hydrogen bonding for retention imposes a further limitation in that amino acid enantioresolution on such materials is difficult or impossible in aqueous media. Finally, the hydrogen bonding interaction used during the preorganization step is quite weak, and can lead to random incorporation of the functional monomer and consequent loss in enantioselectivity.

The molecularly imprinted materials for bis-imidazole substrates based on the metal coordination interaction that have been developed in our laboratory (Dhal and Arnold 1992) have already been discussed earlier. Metal coordination and chelation interactions offer certain important advantages over other interactions for molecular

imprinting. Metal coordination interactions are strong relative to hydrogen bonding, especially in water, and therefore can significantly reduce the random incorporation of functional monomers. The strength and kinetics of binding can be tuned through the choice of metal ion, which can be substituted easily once the adsorbent has been prepared. For example, a polymer imprinted using Cu^{2+} ions can be reloaded with Zn^{2+} and used in chromatographic separations (Plunkett and Arnold 1995; Arnold et al. 1998). Fuji et. al. (1985) have synthesized molecularly imprinted polymers for *N*-benzylvaline enantiomers, using a substitution-inert Co^{3+} complex of a chiral monomer that incorporates a Schiff base functionality. These materials have been reported to exhibit excellent enantioselectivity for the chirality of the amino acid derivative used as the template. However, the slow kinetics of ligand rebinding in Co^{3+} complexes are quite unfavorable for fast chromatographic separations.

The following study presents the first use of metal ion complexes of underivatized amino acids for the synthesis of enantioselective molecularly imprinted ligand-exchange adsorbents. Several aliphatic and aromatic amino acids have been investigated in order to evaluate the role of the side group in imparting enantioselectivity. By working with an achiral monomer based on the iminodiacetate functionality, we demonstrate the role of molecular imprinting in creating chiral recognition sites in crosslinked polymer networks.

Results and discussion

Choice of functional monomers and metal ions

In designing molecularly imprinted polymers, it is imperative to have a well preorganized complex between functional monomers and templates before

polymerization. When the mechanism of preorganization is metal ion coordination, three different components have to be organized into a ternary complex: the functional metal chelating monomer, the metal ion and the template molecule. Various factors need to be taken into consideration here.

A transition metal ion is used to form the preorganized complex and in the subsequent application of molecularly imprinted materials. The choice of metal ion can be tailored to suit a particular application, and a wide range of binding strengths and kinetics can be achieved. The strength of binding of Cu^{2+} ions with organic ligands containing amine and/or carboxylate functionalities has been exploited to promote the preorganization of templates and functional monomers. The metal ion can be leached out of the resultant polymer by treatment with ethylenediamine tetraacetic acid (EDTA), and reloaded back on to the polymer by washing the polymer with a solution of an appropriate metal salt. Cu^{2+} has been chosen in all the experiments described below, because this ion binds very strongly to ligands containing amine and carboxylate functionalities.

Coordination complexes of transition metal ions exhibit a variety of geometries: octahedral, square pyramidal, tetrahedral, etc. For a given metal ion, based on our knowledge of its coordination chemistry, a functional monomer can be selected. The important factors that decide this choice are the binding strength, the geometry and the coordination number of the resulting complexes. The chelation of the metal ion by the functional monomer should be sufficiently strong so as to form a 1:1 complex at 1:1 stoichiometry. However, the binding should not be so strong that it satisfies most of the electronic requirements of the metal ion, thereby significantly weakening the binding of a

second ligand to the metal center. The geometry of the resulting complex should also be such that vacant coordination sites are available on the metal center for binding to the template molecule. Another important consideration affecting the choice of the functional monomer is the template molecule with which the polymer is being imprinted. The essential criterion is that a 1:1:1 complex be formed with the functional monomer, the metal ion and the template.

For synthesizing imprinted polymers using Cu^{2+} as the metal ion, monomers based on the iminodiacetic acid (IDA) functionality have been most widely utilized in our laboratory. The binding of IDA to Cu^{2+} satisfies most of the considerations listed above. IDA being a tridentate ligand, it leaves two vacant coordination sites on the metal center, so that an additional ligand such as an amino acid can chelate the same metal ion. It also binds sufficiently strongly to Cu^{2+}, so that the binding of an amino acid does not disrupt the complex between IDA and Cu^{2+}. An additional consideration is the ease of synthesis of the IDA based functional monomer *N*-(4-vinylbenzyl)iminodiacetate (VBIDA) (Fig. 3. 1). It should be noted that Cu^{2+}-[*N*-(4-vinylbenzyl)imino]diacetate (Cu(VBIDA)) is achiral and cannot itself distinguish between L- and D- amino acids.

Effect of pH on preorganization of the monomer-template assembly

The preorganization of the monomer-template assembly involves the formation of a mixed ligand complex of metal-complexing monomer and the pure amino acid enantiomer that will serve as the template. As both the metal chelating functional monomer and the amino acid template are subject to deprotonation equilibria in solution, a number of species can exist in equilibrium with one another over a range of pH. The

right conditions that promote the formation of the ternary complex therefore need to be determined. It is important that the ternary complex of the metal with the functional monomer and the template dominate the metal containing species that enter the polymerization reaction. This is necessary to minimize the amount of functional monomer being non-specifically incorporated into the polymer matrix. The ternary complex of Cu^{2+} is prepared in a step-wise fashion, with the complex between the functional monomer and the metal ion being prepared first and subsequently complexed with the desired amino acid template. Fig. 3. 2 shows the species distribution of IDA as a function of pH. To ensure strong binding between the ligand and metal ion, the working pH needs to be such that the deprotonated forms of the ligand dominate the free ligand species. Fig. 3. 3 shows the equilibrium species distribution of a solution containing a 1:1 stoichiometry of the polymerizable IDA and Cu^{2+}, as calculated from the known protonation constants and Cu^{2+} binding constant of *N*-benzyliminodiacetic acid (Martell 1974). It is assumed that the presence of the vinyl group at the *para-* position on the benzene ring does not significantly change these equilibria for the functional monomer. At low pH values (between 0 and 4), there is substantial competition between protons and Cu^{2+} for the iminodiacetate group. At intermediate pH values (between 6 and 8), the 1:1 Cu(VBIDA) complex is the dominant species in solution. At high pH values (> 9), a hydroxide ion replaces a bound water molecule in the Cu(IDA) complex. Although the equilibrium species distributions do not show any evidence of $Cu(OH)_2$ precipitation, in practice, some turbidity is observed around neutral pH. If the pH is not carefully adjusted during the formation of the Cu(VBIDA) complex, $Cu(OH)_2$ precipitates rapidly, and is

difficult to redissolve. This problem is not encountered if the entire complexation reaction is done by controlling the pH at a constant value above 9.

To calculate the equilibrium species in the formation of a ternary complex of Cu^{2+}, functional monomer and amino acid template, one needs to know the formation constant of the desired complex. The equilibrium binding of the amino acid phenylalanine to the complex of Cu^{2+} with the functional monomer was measured at pH 9.5 using isothermal titration calorimetry (ITC). The calorimetric data shown in Fig. 3. 4 were used to calculate the ternary binding constant, which was used to calculate the species distributions over a range of pH. The ITC cell was loaded with a 1 mM Cu(VBIDA) solution at 25 °C (pH = 9.5). 250 μL of a 20 mM solution of the amino acid solution at the same pH was titrated into the ITC cell (injection volume = 10 μL). These conditions were chosen for the ITC experiment such that the pH change upon amino acid binding was negligible. Thus, the heat measured by calorimetry corresponds primarily to the heat of binding, and there are no significant heat effects from deprotonation equilibria. A one-site binding model used to fit the ITC data gave a binding constant of 2.7 (±0.3) x 10^4 M^{-1} for the binding of L-phenylalanine to Cu(VBIDA). The titration behavior of D-phenylalanine is identical to that of the L- enantiomer, as expected for achiral Cu(VBIDA).

Equilibrium species distributions of the ternary complexes were calculated at three different stoichiometries of the amino acid phenylalanine. At 1:1:1 stoichiometry, the maximum amount of ternary complex [Cu(VBIDA)(Phe)] is formed over a relatively narrow pH range centered at pH ~ 10.5, and corresponds to 82% of the total metal concentration (Fig. 3. 5). The remaining metal remains as $Cu(VBIDA)(H_2O)_2$. The

available pH window and the amount of ternary complex both increase upon addition of excess phenylalanine. With a 100% molar excess of the amino acid, greater than 95% of the total metal concentration is present in the mixed ligand species. The pH range over which the ternary complex is formed also increases to between 9 and 12 (Fig. 3. 6). At a stoichiometry where there is 200% excess amino acid, the amount of ternary complex increases to almost 100% of the total metal concentration (Fig. 3. 7).

These calculations indicate that for synthesizing molecularly imprinted polymers using metal ion coordination interactions for the preorganization of template and monomer, the use of excess amounts of template would reduce the formation of nonspecific binding sites in the resulting polymer. This is in contrast with alternative imprinting techniques where excess amounts of monomers are used to promote hydrogen bonding and other non-covalent interactions between template and monomer molecules.

It must be noted that at lower pH values, the protonation equilibria of the monomer and template ligands compete with metal binding equilibria. At higher pH values, hydroxide ions can compete successfully with the template for binding to the metal ion. The optimum pH range lies intermediate to these two competing factors, and can be estimated by taking all possible competing equilibria properly into account.

Effect of template molecule on choice of functional monomer

The chemical nature of the template molecule also affects the choice of functional monomer. For the monodentate (e.g., imidazole) and bidentate (e.g., amino acid) templates that have been studied in this laboratory, the IDA based functional monomer is a good choice. However, this monomer would not be appropriate for a template molecule

that binds to the metal ion more strongly than an amino acid. In other words, if the binding of the template ligand to the metal ion approaches or exceeds that of IDA, there is an increased probability of competition between the template ligand and the functional monomer for the metal ion. This can result in a situation where the template ligand succeeds in stripping the metal ion from the IDA ligand. This is illustrated in a model system where the template molecule is ethylenediamine (en). Figs. 3. 8 and 3. 9 show the species distributions of a system containing IDA:Cu^{2+}:en at different stoichiometric excesses of the en ligand, calculated using ternary binding constants reported in the literature (Martell 1974; Rao et al. 1992).

At a stoichiometry of 1:1:1 of IDA:Cu^{2+}:en, the maximum amount of ternary complex corresponds to 80% of the total metal concentration. As seen in Fig. 3. 8, however, both free IDA and Cu(IDA) species are present under these conditions. The addition of excess amounts of en does not change this situation, there being both the free IDA and the Cu(IDA) species at high pH values (Fig. 3. 9). The presence of free IDA species indicates that the binding of the diamine to the metal ion is strong enough to strip the functional monomer of metal ions. Obviously, this is to be avoided, in order to minimize the incorporation of nonspecific binding sites into the polymer matrix. Thus, one may conclude that the IDA based monomer would not be an appropriate choice for a diamine template, and one has to use a ligand that binds stronger than IDA to the metal ion. In contrast, this is not a significant concern for the formation of a ternary complex of Cu^{2+} with the IDA based monomer and an amino acid ligand.

Enantiomers of phenylalanine, tyrosine, alanine, valine, leucine, and isoleucine were used as templates. The association constants for these amino acids to Cu(IDA) in

aqueous solution lie between 10^3 to 10^4 M^{-1} (Rao et al. 1992). Formation of the ternary metal complex of phenylalanine and Cu(VBIDA) was monitored at pH 9.5 by isothermal titration calorimetry (ITC). The ITC experiments were carried out in the same concentration range used for subsequent polymerization reactions (~ 20 mM for Cu(VBIDA)). The ITC data indicate that the 1:1 binding between Cu(VBIDA) and L-phenylalanine reaches saturation only when more than two equivalents of amino acid are added (figure 4) and the binding constant is 2.7 (±0.3) x 10^4 M^{-1}. The ITC data also confirm that metal is not stripped out into metal-amino acid complexes at these concentrations. The binding of the amino acid is not strong enough to compete with the IDA monomer for metal ions, as the binding constant for Cu^{2+} to IDA is ~ 10^{11} M^{-1} (Martell 1974). In order to minimize the random incorporation of functional monomer into the polymer matrix in preparing the imprinted materials, a greater than two-fold excess of template amino acid was used during polymerization. Under these conditions of excess template, some of the template remains unbound, but essentially all the Cu(VBIDA) monomer is in a 1:1 complex with amino acid.

Polymerization and workup

The strategy for preparing molecularly imprinted ligand-exchange materials is outlined in Fig. 3. 10. The metal-complexing monomer (Cu(VBIDA)) and the amino acid template (e.g., L-phenylalanine) are preorganized in solution to form the monomer-metal-amino acid complex, as described above. Crosslinking polymerization with ethylene glycol dimethacrylate (EGDMA) with thermal initiation using 4,4'-azobis(4-cyanovaleric acid) in 80:20 v/v methanol-water at 40 °C creates a macroporous polymer

matrix. A 5:95 molar ratio of functional monomer to crosslinker was used. In order to make materials suitable for column chromatography, the polymers imprinted using phenylalanine enantiomers were also synthesized as surface coatings on spherical silica particles (LiChroSpher™, 10 μm size, 1000 Å pores) derivatized with 3-(trimethoxysilyl)propyl methacrylate, using procedures described previously (Plunkett and Arnold 1995).

For each amino acid studied, the following bulk polymers were prepared: polymers imprinted against each enantiomer, a control polymer synthesized using the racemic amino acid as the template, which is expected to show no enantioselectivity. A further control polymer was also synthesized in the absence of any template amino acid. Each bulk polymer was washed thoroughly with water, ground and filtered. The washes were combined, the solvent was removed by lyophilization, and the residual solids were carefully weighed. After drying in a vacuum oven at 60 °C, the polymers were weighed again and then treated with ethylenediaminetetraacetic acid (EDTA) to remove the metal ions and template. The amount of Cu^{2+} removed was estimated by UV/vis spectroscopy. The metal removal step was followed by thorough washing, and the materials were dried in a vacuum oven and weighed again. These gravimetric measurements and the UV/vis spectroscopic estimation of Cu allowed us to calculate the amounts of template removed. For all the amino acids studied, the template removal was typically ~ 97% of the total amino acid used in the polymerization scheme. Thus, after a typical polymer workup procedure, the amount of reversibly bound metal (and template) was estimated to be 25 μmol/gm polymer (dry weight), whereas the amount of residual, irreversibly bound template was always less than 0.8 μmol/g. The dried polymers were sieved, and a size

fraction between 10 μm and 50 μm was used for equilibrium rebinding experiments, both in the metal-free form and after reloading with copper ions. Reloading of Cu^{2+} was achieved by equilibration with a 100 mM solution of $CuSO_4.5H_2O$.

Equilibrium rebinding

Competitive equilibrium rebinding studies were carried out to determine the enantioselectivities of binding for different amino acids at pH 9. In a typical rebinding experiment, 2 g of the polymer reloaded with Cu^{2+} (total Cu capacity ~ 50 μmoles) was equilibrated with an aqueous solution containing a two-fold excess of the racemic amino acid (5 mM, pH 9) for 24 hours, after which the supernatant was recovered by filtration. Polarimetry was used to determine the optical activity of the supernatant solution, and enantiomeric excess was calculated by combining this measurement with UV-absorption measurement of the total amino acid concentration. The Cu-free materials failed to retain free amino acids, indicating the absence of nonspecific binding under these conditions.

Table 3. 1 summarizes the results of these experiments. For each amino acid studied, the control materials prepared using racemic template and using no template showed no preference for either enantiomer. In contrast, the materials imprinted with a single enantiomer are selective for that enantiomer. The highest enantioselectivities were seen for the polymers imprinted with tyrosine and phenylalanine (α ~ 1.45). Materials imprinted with L- or D-alanine showed little enantioselectivity for any of the amino acids studied, including alanine. Polymers imprinted using D- and L-valine showed low enantioselectivities for valine (α ~ 1.08) and no selectivity for enantiomers of any of the other amino acids.

Table 3. 1 also shows that the materials templated with L- or D-phenylalanine exhibit good enantioselectivity ($\alpha \sim 1.4$) when challenged with racemic tyrosine and much reduced enantioselectivities when equilibrated with D,L-tryptophan ($\alpha \sim 1.1$). Little or no selectivity was seen for alanine, valine, leucine or isoleucine. Similarly, materials imprinted with L- or D-tyrosine can distinguish the enantiomers of phenylalanine and tryptophan (not shown in Table 3. 1), but not the aliphatic amino acids. Materials imprinted with a leucine or an isoleucine enantiomer exhibit cross-enantioselectivity for the other amino acid and reduced ability to resolve phenylalanine, while no selectivity was seen for alanine or valine enantiomers.

A consistent trend to higher enantioselectivity with increasing size of the side group is evident, indicating that the size of the amino acid side chain is an important factor in determining enantioselectivity in these molecularly imprinted ligand-exchange polymers. The imprinted polymers also show interesting cross-selectivity patterns. Tyrosine with its phenolic side chain differs only slightly from phenylalanine in molecular size, and polymers imprinted with these templates show comparable enantioselectivities in rebinding the other amino acid. Similarly, leucine and isoleucine are quite similar in size, and the corresponding imprinted polymers show significant cross-selectivity. For amino acids with smaller or more flexible side chains as compared to the template, there is little enantioselectivity. When the side chain is larger than that of the template amino acid, the enantioselectivity also decreases (cf. tryptophan binding to phenylalanine-imprinted polymers and phenylalanine binding to leucine-imprinted polymers).

Another possible explanation for the observed trends in enantioselectivity could be the contribution of inter-ligand •-• interactions to the overall binding. Although the VBIDA monomer is achiral, the resultant molecularly imprinted polymer could preferentially stabilize inter-ligand interactions between the styrene group of the monomer and the amino acid side group upon rebinding. Although this postulate remains unverified, if this effect is significant, it would explain the observation that polymers imprinted for phenylalanine and tyrosine enantiomers show the largest enantioselectivities.

Column chromatography

Enantioresolution of racemic phenylalanine was studied by column chromatography. For this purpose, 10 μm diameter macroporous silica beads (pore size ~ 1000 Å) were coated with polymeric material imprinted for phenylalanine and slurry-packed in an HPLC column (4.6 mm id x 50 mm), following procedures described previously.[15] The material was packed in the metal-ion free form, and copper ions were reloaded under flow. It was not possible to achieve efficient resolution using an acetate buffer as a competitor in the eluent; the phenylalanine was strongly bound due to metal chelation and was retained for more than 10 column volumes. When acetate was replaced by 1.5 mM glycine in the eluent, the retention volumes were reduced and more efficient separations were obtained. Figure 11a shows the separation of D,L-phenylalanine on the adsorbent imprinted with D-phenylalanine. The separation factor is 1.65. The template enantiomer is more strongly retained, eluting as a broad band between 5 and 8 column volumes, while the opposite enantiomer eluted between 3 and 4

column volumes. Similar results were obtained for the support prepared using L-phenylalanine as the template. The control material prepared in the absence of any template was similarly tested in the Cu^{2+} reloaded form. On this column, D,L-phenylalanine eluted as a single peak between 3 and 4 column volumes, comparable to L-phenylalanine on a material imprinted with D-phenylalanine and *vice versa*.

The phenylalanine-imprinted supports were also able to resolve D,L-tyrosine into its enantiomers, with a separation factor similar to that observed for D,L-phenylalanine (α = 1.54) (Figure 11b). Racemic tryptophan eluted as a broad band between 2 and 5 column volumes, but was not resolved on this column under these conditions (data not shown). These columns were also unable to resolve racemic mixtures of alanine, valine, leucine or isoleucine. Finally, samples containing equimolar amounts of phenylalanine and tyrosine enantiomers of like chirality also eluted as single peaks on the colums imprinted with pure enantiomers of phenylalanine. While the molecularly imprinted materials can select for the chirality of the template, they are unable to recognize the small size difference between phenylalanine and tyrosine. The inability of these imprinted materials to recognize small variations of the amino acid side chain is also consistent with the equilibrium rebinding observation that polymers imprinted with alanine showed no measurable enantioselectivity.

These results are consistent with the hypothesis that the size of the template amino acid plays an important role in imparting chiral selectivity. Material obtained by imprinting with a phenylalanine enantiomer is specific only for phenylalanine and the closely related tyrosine. Alanine and valine have smaller side groups compared to phenylalanine, and both enantiomers of these amino acids presumably can fit into binding

sites that will distinguish phenylalanine enantiomers. Thus they are retained, but not enantioselectively. The lack of enantioselectivity for leucine and isoleucine exhibited by the phenylalanine-imprinted materials is probably due to the flexibility of the aliphatic side groups. The retention of tryptophan is slightly greater than for the other amino acids, on the control material prepared in the absence of template amino acid as well as on the imprinted materials, possibly due to additional interactions of the indole side chain with the immobilized copper ions. The larger size of the indole side group could mean that both enantiomers of tryptophan face comparable steric hindrance to binding in a polymer imprinted for a phenylalanine enantiomer. Therefore we see reduced enantioselectivity for tryptophan in the equilibrium rebinding experiment and no enantioresolution in the chromatographic mode.

Mechanisms of enantioselectivity

Possible sources of enantioselectivity observed in the molecularly imprinted ligand exchange polymers are here discussed in the light of the three-point interaction model for conventional chiral stationary phases (CSP) used in LEC. This model requires at least three points of interaction between the chiral selector and the targeted enantiomer for chiral recognition and separation (Davankov and Kurganov 1983; Davankov 1989). In LEC of amino acids on an L-proline bonded phase or with an L-proline metal complex in the mobile phase, at least one point of interaction must be between the mixed metal-ligand complex and the solid support. In conventional LEC supports, at least two points of interaction are available for both enantiomers: simultaneous coordination of the amine and carboxylate groups to the metal ion. The good selector that discriminates between

the two enantiomers should therefore stabilize the third interaction with one of the enantiomers to the maximum possible extent. Chiral selectivity can also be achieved if the third interaction is destabilized for one of the enantiomers relative to the other. The nature of the interaction of the mixed ligand complex with the support matrix thus plays a crucial role in chiral recognition, and this interaction can vary significantly, even for closely related materials.

It is not immediately clear where the origins of chiral selectivity lie for the molecularly imprinted ligand exchange materials. Because we have used an achiral crosslinker and an achiral metal complex attached to the support, the interaction that decides the enantioselectivity must arise either from the residual incorporation of the chiral template amino acid or from the formation of enantioselective binding sites in the polymers imprinted with chiral template. We do not believe that residual incorporation of chiral template can explain our results. This conclusion is based on the small amount of template remaining in the polymers after washing, the nature of the coordination/chelation interaction, and the fact that the enantioselectivities obtained by molecular imprinting increase with the size of the amino acid side chain. The polymers contain less than 0.8 μmol/g residual template, as compared to ~25 μmol/g for the amount of template and metal ions that can be reversibly bound. The metal ions and template that could not be removed by washing with EDTA are probably inaccessible to both EDTA and any more amino acid. In any case, the residual template cannot account for the selectivities measured, even if those few sites were exclusively specific for rebinding a substrate of like chirality, with the remaining sites having zero selectivity. For example, the equilibrium rebinding experiments utilized a two-fold excess of racemic

substrate. The maximum enantioselectivities that could be obtained by this route are only ~ 13/12 = 1.08, considerably less than those observed for the larger amino acids. In addition, the specific directional nature of the metal coordination/chelation bonds would make it difficult for a second amino acid to bind to a metal ion already bound to iminodiacetate and a template molecule. Finally, although the levels of residual amino acid incorporated in the imprinted polymers are similar, the enantioselectivities of these materials are markedly different.

The only explanation possible is that molecular imprinting has achieved chiral recognition through the formation of chirally selective binding sites. In light of the three-point interaction model, this implies that formation of the polymer network around the monomer-template complex stabilizes the binding of the template enantiomer and/or destabilizes (sterically hinders) binding of the opposite enantiomer. As shown in Fig. 3. 12 for a polymer templated with D-phenylalanine, rebinding of the D-enantiomer proceeds through chelation of the metal ion, in addition to which the aromatic side chain fits into a cavity that selects for both the size and shape of this group. In contrast, metal chelation by the L-enantiomer would be sterically hindered. Alternatively, if the side group of the L-amino acid fits into the cavity, only monodentate binding to the metal would be possible. Either one would destabilize the metal chelation interaction. If this were the only mechanism for enantioselectivity, the magnitude of this destabilization could be estimated from the magnitude of the selectivity. The maximum separation factor seen on any of these imprinted materials is 1.65 in the case of phenylalanine, which corresponds to a free energy difference of only ~300 cal/mole. The steric destabilization imposed by

the cavity therefore appears to be weak as compared to the energetics of the metal chelation interaction.

The above explanation is based upon an idealized view of the nature of the binding cavities obtained by molecular imprinting. The maximum separation factor obtained for phenylalanine enantiomers is comparable to that shown by the conventional ligand-exchange CSP-s (Davankov 1989). However, baseline separations have been obtained on the conventional CSP-s, whereas there is a large degree of peak overlap in the chromatograms from molecularly imprinted materials. The poor resolution is accompanied by greater broadening of the peak corresponding to the more strongly retained enantiomer. These features, which have been observed in separations on other molecularly imprinted materials, have been generally attributed to heterogeneity in the binding sites (Andersson et al. 1984; Kempe and Mosbach 1991; Plunkett and Arnold 1995). Molecular imprinting seems to result in the formation of binding sites with a distribution of binding strengths. Fig. 3. 12 thus probably illustrates only the most selective sites, whereas an average over all binding sites is measured during separation.

The above explanation of the origin of enantioselectivity in these imprinted materials is applicable to amino acids, which chelate the metal ion. However, for chiral molecules that bind to metal ions in a monodentate fashion, the metal coordination interaction will provide only one of the three necessary for enantioselectivity. Thus, in order to successfully resolve molecules such as chiral amines or carboxylic acids, molecular imprinting has to contribute the equivalent of at least two other points of interaction between the polymer matrix and the substrate. To further probe the nature of the enantioselectivity of the molecularly imprinted adsorbent, we tested the imprinted

polymer-coated silica column synthesized for phenylalanine for its ability to separate two racemates which are analogous to phenylalanine and which coordinate to the metal ion only in a monodentate fashion, α-methylphenethylamine and α-methylhydrocinnamic acid (Fig. 3. 13). Glycine binds more tightly to the metal ion than α-methylphenethylamine and α-methylhydrocinnamic acid, causing both to elute at close to one column volume without enantioresolution. Thus the chromatography was carried out using 1.5 mM acetate at pH 8, instead of glycine in the elution buffer. The column imprinted with D-phenylalanine was able to resolve the chiral amine, as shown in Fig. 3. 14. However, the chiral carboxylic acid still eluted early without being resolved. Further attempts to resolve the chiral carboxylic acid by reducing the pH were unsuccessful.

Although the chiral amine cannot chelate metal ions, the polymer imprinted with a phenylalanine enantiomer was able to resolve its chiral amine analog. The chiral amine binds more strongly than acetate to the metal complex. Therefore in the presence of competition from acetate, the amine is retained; it is also resolved into its enantiomers. However, binding of the carboxylic acid analog is not strong enough to result in significant retention in the presence of competition from acetate. Seen in the light of the three-point interaction model, the ability of the material imprinted with a phenylalanine enantiomer to resolve an analogous chiral amine indicates that the steric interaction between the side group and the binding cavity involves more than one point of contact. Alternatively, if the •-• interaction between the styrene group of the functional monomer and the amino-acid side group is significantly strong, that would contribute an additional point of interaction. Thus, there is sufficient evidence here to conclude that molecular imprinting with a chiral template has created chirally selective binding cavities. This

selectivity must result from a microstructure of the binding cavity that is complementary to the side group of the template amino acid.

Conclusions

This is the first report of the preparation of molecularly imprinted polymers for the chiral separation of *underivatized* amino acids. The same polymers can be used to resolve related chiral amines. The amino acid template forms the stronger complex, which is advantageous for the fidelity of molecular imprinting. The size, shape and nature of the amino acid side group contribute to the chiral resolution. The use of achiral reactants has highlighted the role of molecular imprinting in creating the enantioselective adsorbents. It may be possible to improve the enantioselectivities of these materials further by choosing appropriate chiral functional monomers. Alternatively, the use of comonomers or crosslinkers that provide additional interactions with the side groups of the amino acid templates could contribute to improved resolution, provided the stabilization is preferential for the targeted enantiomer.

Experimental Procedures

Instrumentation and Analytical Techniques

Elemental analyses were carried out at Galbraith laboratories, Knoxville, TN. Electronic absorption spectroscopic measurements were carried out with a Milton Roy 3000 spectrophotometer. Isothermal titration calorimetry was carried out on a Microcal calorimeter and the data analyzed using software supplied by Microcal, Northamptom, MA. Optical activity measurements were carried out using a Perkin-Elmer 300

polarimeter equipped with a sodium lamp. Chromatography experiments were carried out in a 4.6 mm id x 50 mm column using a Hitachi HPLC system with a L-6200 pump and UV-detection at 270 nm using a Kratos Spectroflow 783 detector.

Isothermal Titration Calorimetry : The preorganization of the Cu(VBIDA) monomer with phenylalanine was followed by isothermal titration calorimetry. In this experiment, a 1 mM solution of Cu(VBIDA) was prepared at a pH of 9.5, and 1 mL of this solution was loaded into the calorimetry sample cell, which is equilibrated at 25 °C. 250 μL of a 20 mM solution of the phenylalanine solution at the same pH was titrated into the sample cell, the volume of each addition being 10 μL. The reference cell was loaded with distilled water that had been brought to a pH of 9.5 by addition of NaOH. The binding of phenylalanine to the Cu(VBIDA) to form the mixed ligand complex is exothermic, and the power required to maintain the sample cell at the same temperature as the reference cell was measured. The data were fit to a one-site model using software supplied by Microcal to calculate the binding constant of phenylalanine to Cu(VBIDA).

Materials and Methods

α-Methylphenethylamine sulfate was purchased from Chem Service, Westchester, PA. All other materials were obtained from Aldrich and purified, if necessary, using standard literature procedures.

Preparation of Monomer-Metal-Amino Acid Complex : Preparation of the complex involved two steps - isolation of Cu[*N*-(4-vinylbenzyl)imino]diacetate (Cu(VBIDA)) followed by the addition of amino acid. Here we describe the preparation of the ternary complex with phenylalanine. Mixed-ligand complexes incorporating the

amino acids tyrosine, leucine, isoleucine, valine and alanine were obtained using similar procedures.

VBIDA was synthesized as reported previously (Dhal and Arnold 1992). However, the Cu^{2+} complex of VBIDA was prepared using a modification of the previously reported procedure. 5.00 g of VBIDA was dissolved in 150 mL distilled water. The pH was adjusted to 9.5 using 6 M NaOH. 5.00 g of $CuSO_4.5H_2O$, dissolved in 150 ml distilled water, was added dropwise to the VBIDA solution, adjusting the pH with 1 M NaOH to maintain its value at 9.5. This high dilution was necessary to keep all species in solution as the $CuSO_4$ solution was titrated into the VBIDA solution. The high pH helped to keep the IDA ligand deprotonated for chelation to the Cu^{2+} ion as it was titrated in. In order to avoid irreversible precipitation of Cu^{2+} as a hydroxide species, the $CuSO_4$ solution was added dropwise. The chelation of Cu^{2+} by VBIDA could be seen by the shift in the color of the solution to a dark blue, and the binding reaction was also followed by UV/vis spectroscopy (λ = 700 nm).

The resulting dark blue solution was vacuum filtered and diluted to 500 mL with distilled water. The solution was frozen at –70 •C and lyophilized. The lyophilized powder was dissolved in 100 mL of 100% methanol and stirred for 1 hour. The methanol solution was vacuum filtered and the solvent removed by rotary evaporation. The solid obtained was then redissolved in 50 mL 100% methanol and stirred for 1 hour. The solution was filtered and the solvent removed by rotary evaporation of the filtrate, after which the desired complex was obtained as a dark blue solid. Yield: 62%. At high pH, the Cu^{2+} complex of VBIDA was isolated as the Na salt of $Cu(VBIDA)(OH)(H_2O)$.

Anal. Calculated for $C_{13}H_{16}O_6NCuNa$: C, 42.34; N, 3.8; H, 4.37; Cu, 17.23. Found C, 42.55; N, 3.77; H, 4.42; Cu, 17.20.

The Cu(VBIDA)(Phe) complex was formed by titrating the amino acid solution into a solution of the Cu(VBIDA) complex. 2 g of the purified Cu(VBIDA) was dissolved in distilled water to make a 20 mM solution. 1.4 g (2 molar equivalents, as suggested by the ITC experiments) of phenylalanine was dissolved in 30 mL of distilled water and added dropwise to the Cu(VBIDA) solution, maintaining the pH between 9 and 9.5 using 1 M NaOH. The solution was stirred for 1 hour and subsequently cooled to –70 °C and lyophilized (yield = 84%). The ternary metal complex incorporating the amino acid was also isolated as the sodium salt as the reaction was done at high pH. Anal. Calculated for $C_{22}H_{23}O_6NCuNa$: C, 58.61; H, 5.14; N, 6.21; Cu, 14.09. Found: C, 58.59; H, 5.09; N, 6.19; Cu, 14.03. Complexes using racemic Phe, D-phenylalanine and L-phenylalanine were prepared by the above method, to obtain Cu(VBIDA)(*rac*-Phe), Cu(VBIDA)(D-Phe) and Cu(VBIDA)(L-Phe) respectively. Mixed ligand complexes incorporating the enantiomers of the amino acids alanine, valine, leucine, isoleucine and tyrosine were prepared using identical procedures.

Polymerization and Workup : In a typical polymerization reaction, 0.5 g of the MMA complex was dissolved in 5 mL of water, and the solution is stirred for 6 h under nitrogen atmosphere. An excess of ethylene glycol dimethacrylate (~95 mol %) and 4,4'-azobis(4-cyanovaleric acid) (1 wt % with respect to total monomers), dissolved in 15 mL of methanol, were added to this solution. The polymerization mixture was cooled to liquid nitrogen temperature, evacuated, thawed, and then purged with nitrogen. This procedure was repeated thrice to remove oxygen, and polymerization was carried out at

40 °C for 48 h under nitrogen. The solid polymer thus obtained was cooled, ground, and extracted thoroughly with methanol to remove unreacted monomers and crosslinkers. The resulting blue polymers were then dried to constant weight at 50 °C under vacuum and sieved to an appropriate particle size. Particles between 10 μm and 50 μm in size were used for the equilibrium rebinding experiments.

Derivatization of Silica Particles : In order to prepare imprinted materials suitable for chromatographic separations, the polymers were also synthesized as surface coats on silica particles, following procedures developed earlier in this laboratory.[15] Silica (LiChroSpher 1000, 10 μm particles, 1000 Å pores, supplied by E. Merck, Darmstadt, Germany) was washed with distilled water and boiled in 5% HNO_3. The particles were filtered on a fine-fritted filter, washed extensively with distilled water, and dried at 150• C for 24 h. A 1 μm vacuum was applied to the oven-dried silica in a three-neck flask for 30 min, after which the vessel was sealed. Toluene, dried over sodium and distilled, was added to the silica under vacuum. 3-(trimethoxysilyl)propyl methacrylate (50% w/w silica) and a trace of triethylamine were added to complete the reaction mixture. This mixture was refluxed for 15 h under nitrogen. The silica was isolated by filtration over a fine-fritted filter and freed of any residue by successive washing with toluene, acetone, and ether. The derivatized silica was dried to constant weight under vacuum for 24 h.

Polymer Coating Process : A typical procedure for preparing templated polymers using Cu(VBIDA)(D-Phe) is outlined below. Identical procedures were used for synthesis of materials with L-amino acid and *rac*-amino acid as templates. 4 g of propylmethacrylate-derivatized silica were placed in a 50 mL three-necked round-bottom flask and a 1 μm vacuum applied. 80% aqueous methanol was added under vacuum to

cover the surface (about 10 mL). 0.76 g ethylene glycol dimethacrylate (EGDMA) and 0.08 g Cu(VBIDA)(D-Phe) were then added to the silica particles under vacuum. After mixing for 1 hr, this mixture was sonicated for 20 min to allow penetration of solvent into the pore spaces of the silica particles. 10 mg of the initiator, 4,4'-azobis(4-cyanovaleric acid) was dissolved in 5μL of methanol and added under vacuum, after which the vessel was sealed. The reaction mixture was then placed in a constant temperature shaker bath at 40 °C for 48 h with gentle agitation. The coated silica was then washed thoroughly with methanol to extract out the unreacted monomers, following which it was dried to constant weight at 50 °C under vacuum.

Template and Cu^{2+} Removal and Reloading : Removal of both the amino acid template and Cu^{2+} was achieved by equilibrating the imprinted polymers with 1 M ethylenediaminetetraacetic acid (EDTA) at pH 8 for 48 h. The amount of Cu^{2+} removed was studied by UV/vis spectroscopy. The polymers were subsequently washed three times with 50 mL portions of distilled water in order to remove residual EDTA and template molecules. Then enough water was added to immerse the polymer particles and a few drops of 1 M NaOH were added until the pH stabilized to reach a final value of 8. The mixture was then centrifuged down and the polymer was filtered off. To reload the polymers with Cu^{2+}, 20 mL of a 0.5 M solution of $CuSO_4$ was added. After equilibration overnight, the polymer was washed thrice with 50 mL portions of distilled water (until solution was no longer blue), saving the supernatants. The amount of Cu^{2+} in the supernatant liquid was determined as $[Cu(EDTA)]^{2-}$ by UV/vis spectroscopy and the reloading capacity calculated. Reloading was nearly quantitative with at least 98% of

Cu^{2+} reloaded, based on the amount of Cu^{2+} removed earlier from the material. Similar procedures were followed for the workup of the polymer coated silica materials.

Polarimetric Analysis: Equilibrium Rebinding : In a typical equilibrium rebinding experiment, 50 mg of amino acid, e.g., D,L-Phe, were dissolved in 10 mL of distilled water. The amino acid solution was equilibrated to a pH of 9 with a few drops of 1M NaOH and added to 1 g of the imprinted polymer to equilibrate for 24 hours, following which the supernatant was decanted out after centrifugation. The silica was then washed thoroughly with 25 mL of distilled water, followed by another centrifugation and the supernatant was decanted. The total phenylalanine concentration in the supernatant solution was determined using UV/vis spectroscopy. The combined supernatant was then freeze-dried to a smaller volume of 10 mL for polarimetry analysis. Optical rotation was observed at 25 °C using a sodium lamp emitting at 589 nm. The observed optical purity of the supernatant, combined with a mass balance, was used to calculate equilibrium rebinding selectivity.

Chromatography : The Cu-free polymer-coated silica was packed into a chromatography column (4.6 mm id x 50 mm) following procedures developed previously (Plunkett and Arnold 1995). Cu^{2+} was reloaded onto the column by washing with 20 mM $CuSO_4$ solution at a flow rate of 1 mL/min, followed by washing with water until a steady baseline was reached. 100 μL of a 1 mM solution of racemic amino acid was used as the sample loading in a typical experiment. Chromatographic separations were at 50 °C, with 1.5 mM glycine in the eluent for the elution of amino acid enantiomers. The elution of α-methylphenethylamine and α-methylhydroxycinnamic acid was carried out using isocratic elution with 1.5 mM acetate at pH 8, 50 °C.

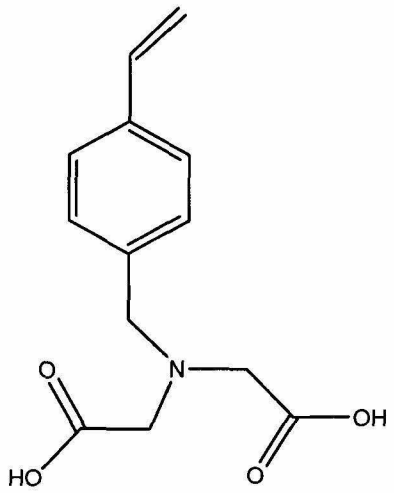

1

[N-(4-vinylbenzyl)]iminodiacetic acid

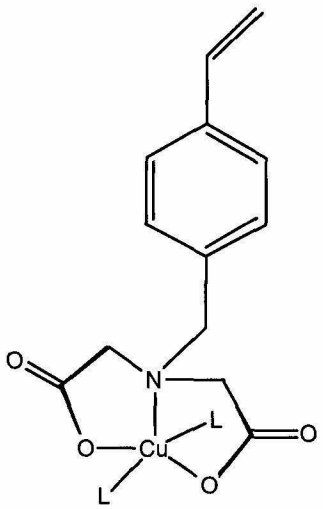

mer-Cu(II)[N-(4-vinylbenzyl)iminodiacetate]

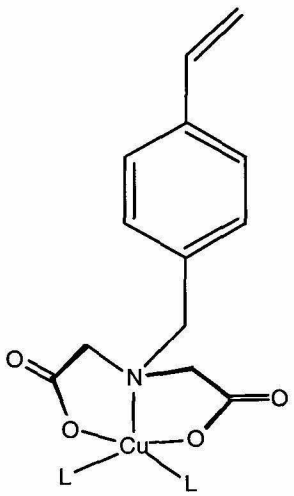

fac-Cu(II)[N-(4-vinylbenzyl)iminodiacetate]

Figure 3. 1. An achiral functional monomer based on iminodiacetic acid. The Cu^{2+} complex of [*N*-(4-vinylbenzyl)]iminodiacetate (Cu(VBIDA)) can have facial or meridional geometries.

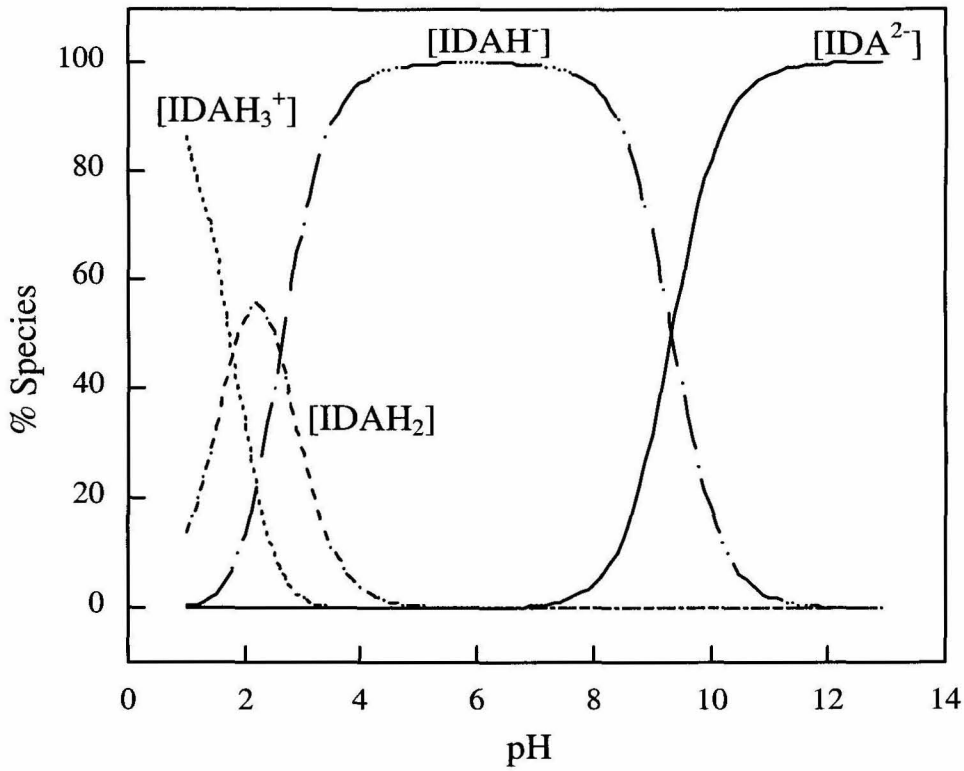

Figure 3. 2. Equilibrium species distribution of iminodiacetic acid as a function of pH. The equilibrium species of *N*-benzyliminodiacetic acid depend similarly upon pH, as the protonation constants are very similar.

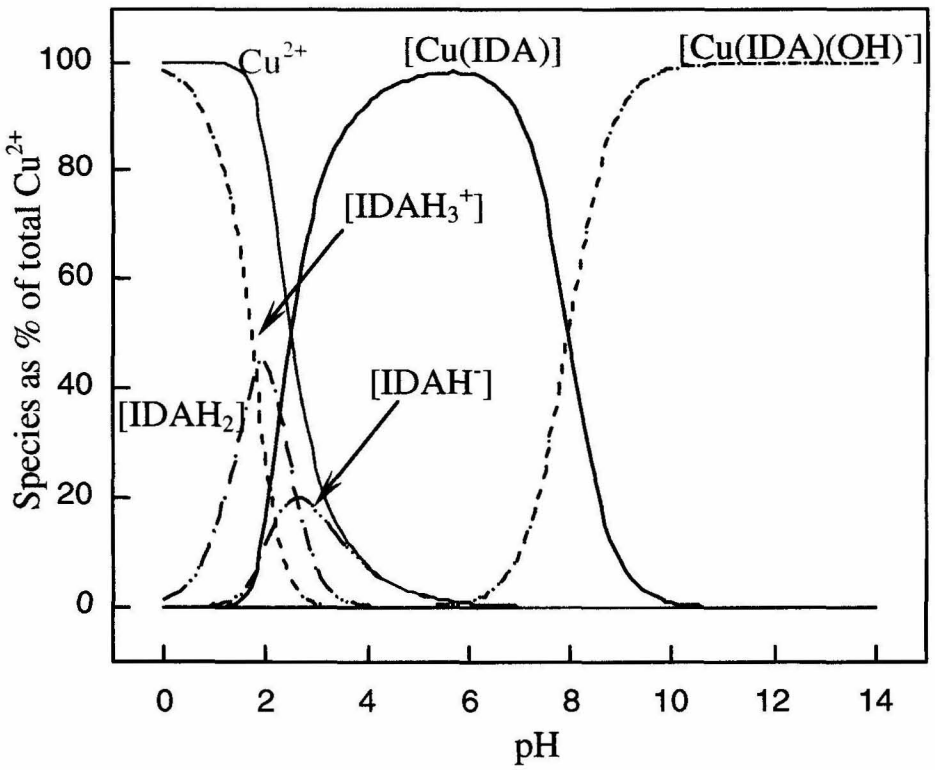

Figure 3. 3. Equilibrium species distribution of a 1:1 system of Cu^{2+} and *N*-benzyliminodiacetic acid as a function of pH, at a total Cu^{2+} concentration of 10 mM. All species are expressed as a percentage of total metal concentration.

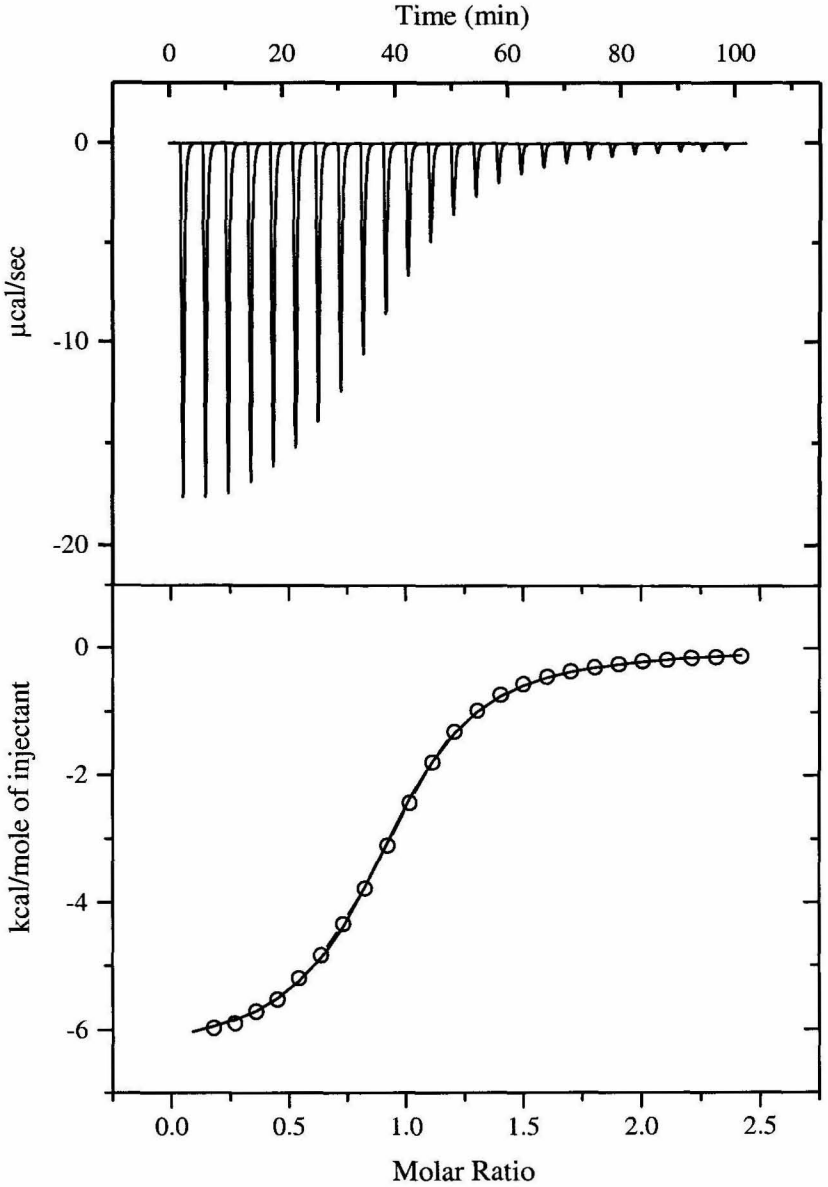

Figure 3. 4. ITC data for binding of phenylalanine to Cu(VBIDA). The ITC cell was loaded with a 1 mM Cu(VBIDA) solution at 25 °C (pH = 9.5). 250 µL of a 20 mM solution of the amino acid solution at the same pH was titrated into the ITC cell (addition volume = 10 µL). The one-site binding model used to fit the data gave a binding constant of 2.7 (±0.3) x 10^4 M^{-1} for the binding of phenylalanine to Cu(VBIDA).

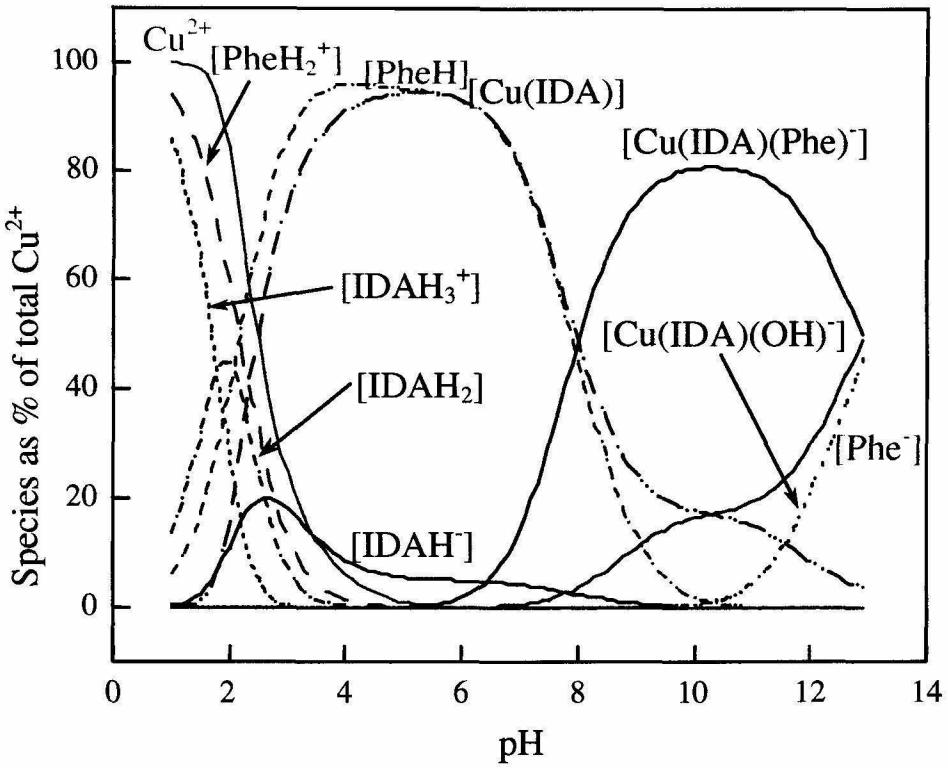

Figure 3. 5. Equilibrium species distribution of a 1:1:1 system containing Cu^{2+}, VBIDA and a phenylalanine enantiomer as a function of pH. All species are expressed as a function of total metal concentration. $[IDA^{2-}]$ and $[Cu(Phe)^+]$ remain at less than 1% through the entire pH range.

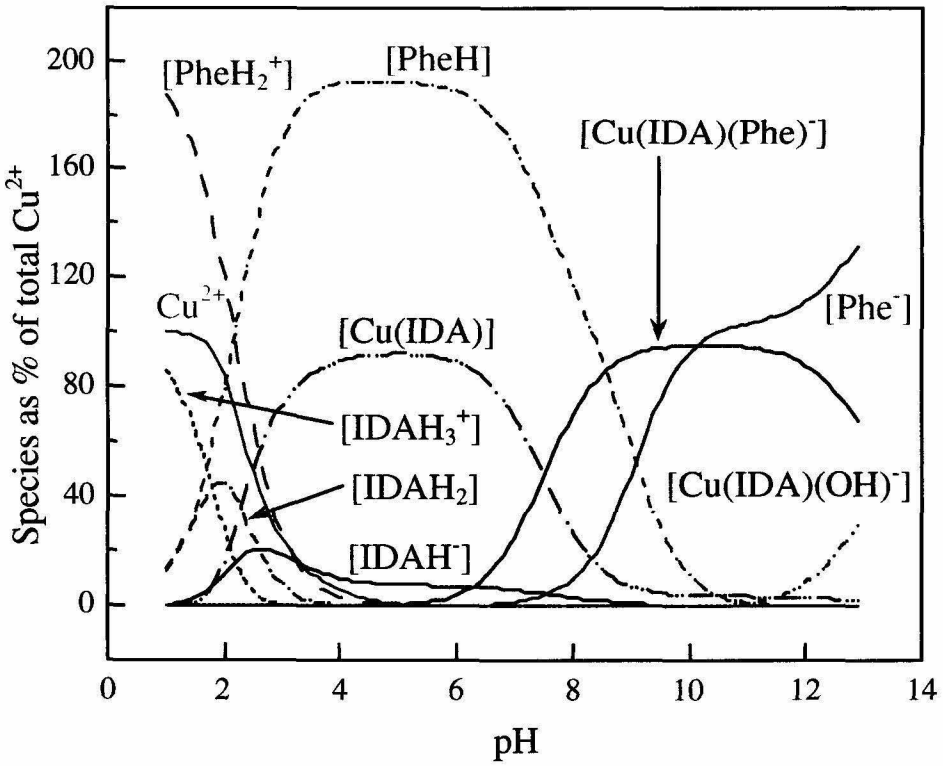

Figure 3. 6. Equilibrium species distribution of a 1:1:2 system containing Cu^{2+}, VBIDA and a phenylalanine enantiomer as a function of pH. All species are expressed as a function of total metal concentration. $[IDA^{2-}]$ and $[Cu(Phe)^{+}]$ remain at less than 1% through the entire pH range.

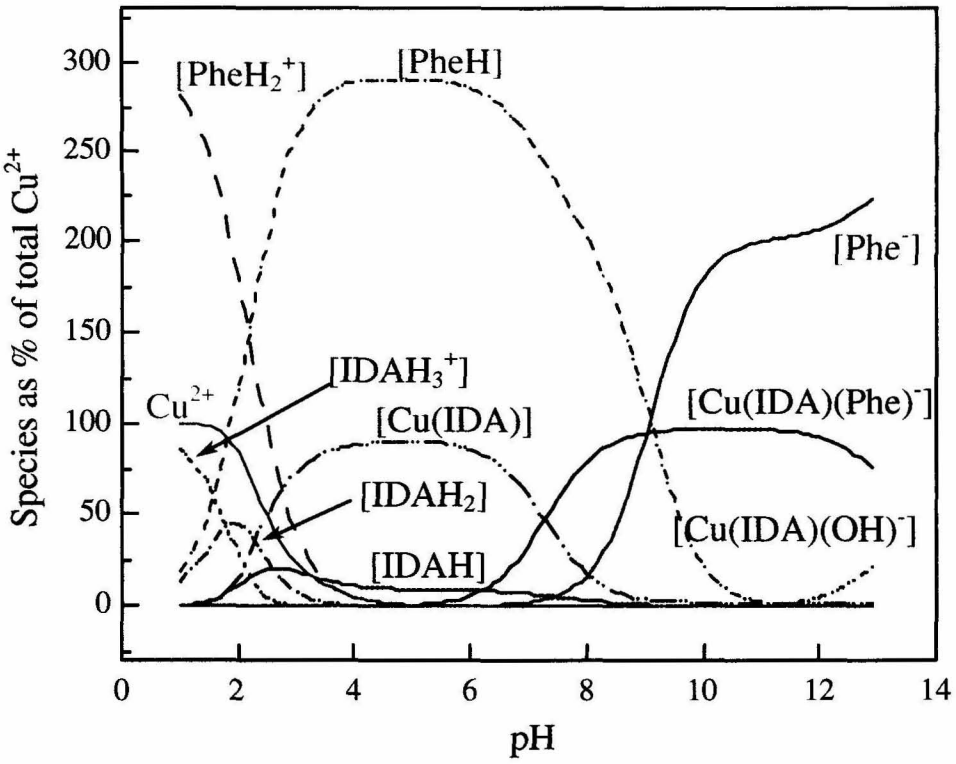

Figure 3. 7. Equilibrium species distribution of a 1:1:3 system containing Cu^{2+}, VBIDA and a phenylalanine enantiomer as a function of pH. All species are expressed as a function of total metal concentration. [IDA^{2-}] and [$Cu(Phe)^+$] remain at less than 1% through the entire pH range.

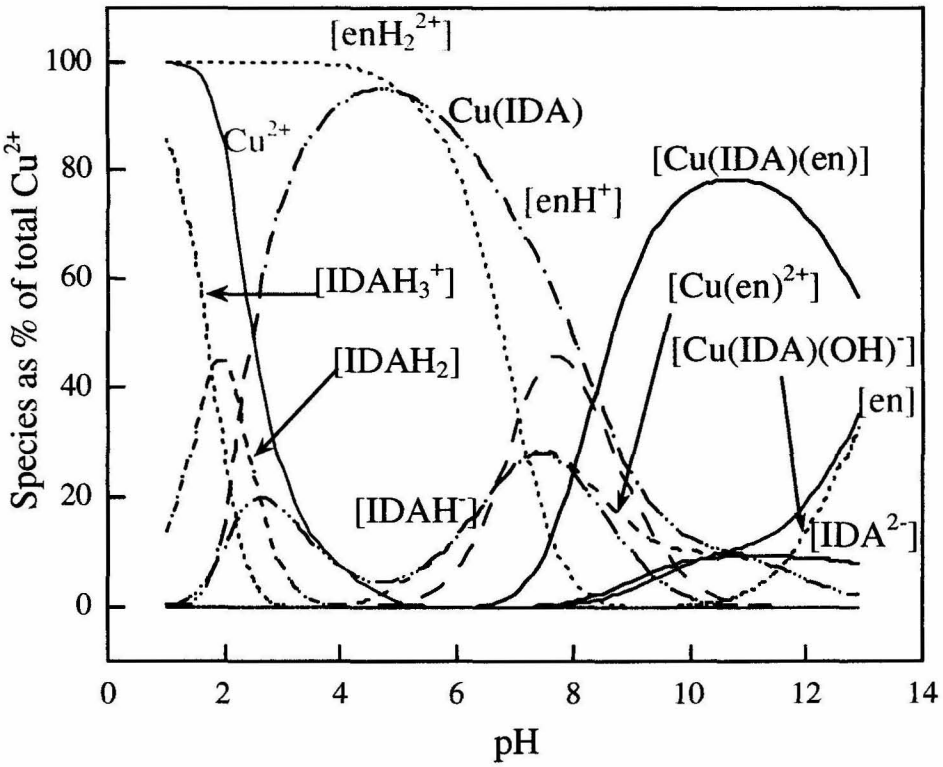

Figure 3. 8. Equilibrium species distribution of a 1:1:1 system containing Cu^{2+}, VBIDA and ethylenediamine (en) as a function of pH. All species are expressed as a function of total metal concentration.

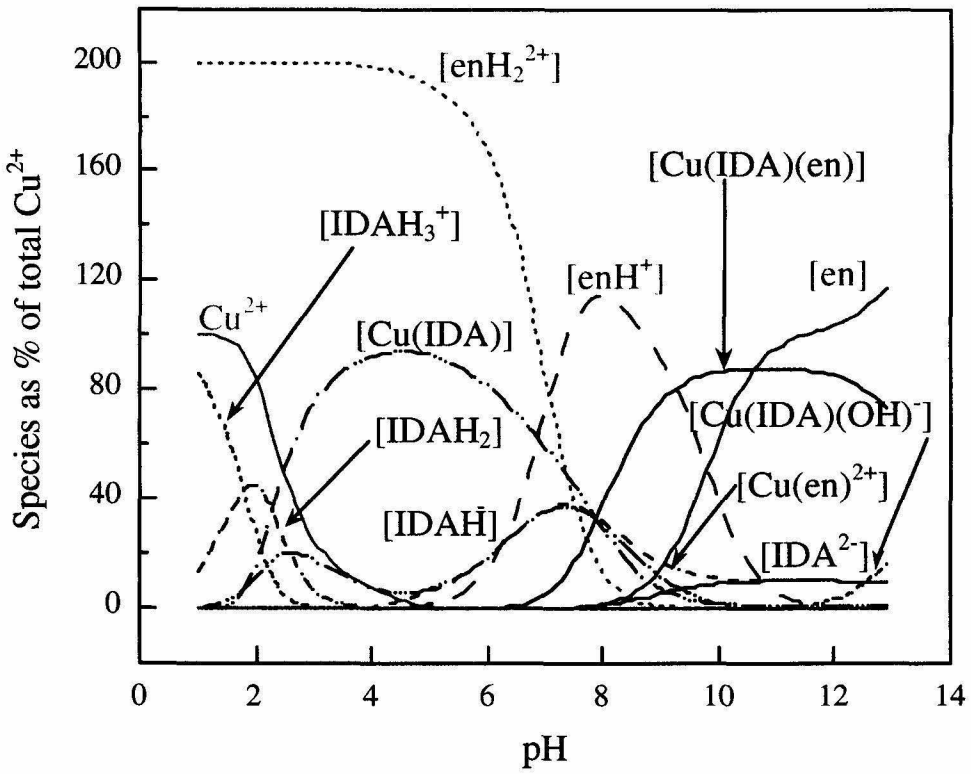

Figure 3. 9. *Equilibrium species distribution of a 1:1:2 system containing* Cu^{2+}, VBIDA and ethylenediamine (en) as a function of pH. All species are expressed as a function of total metal concentration.

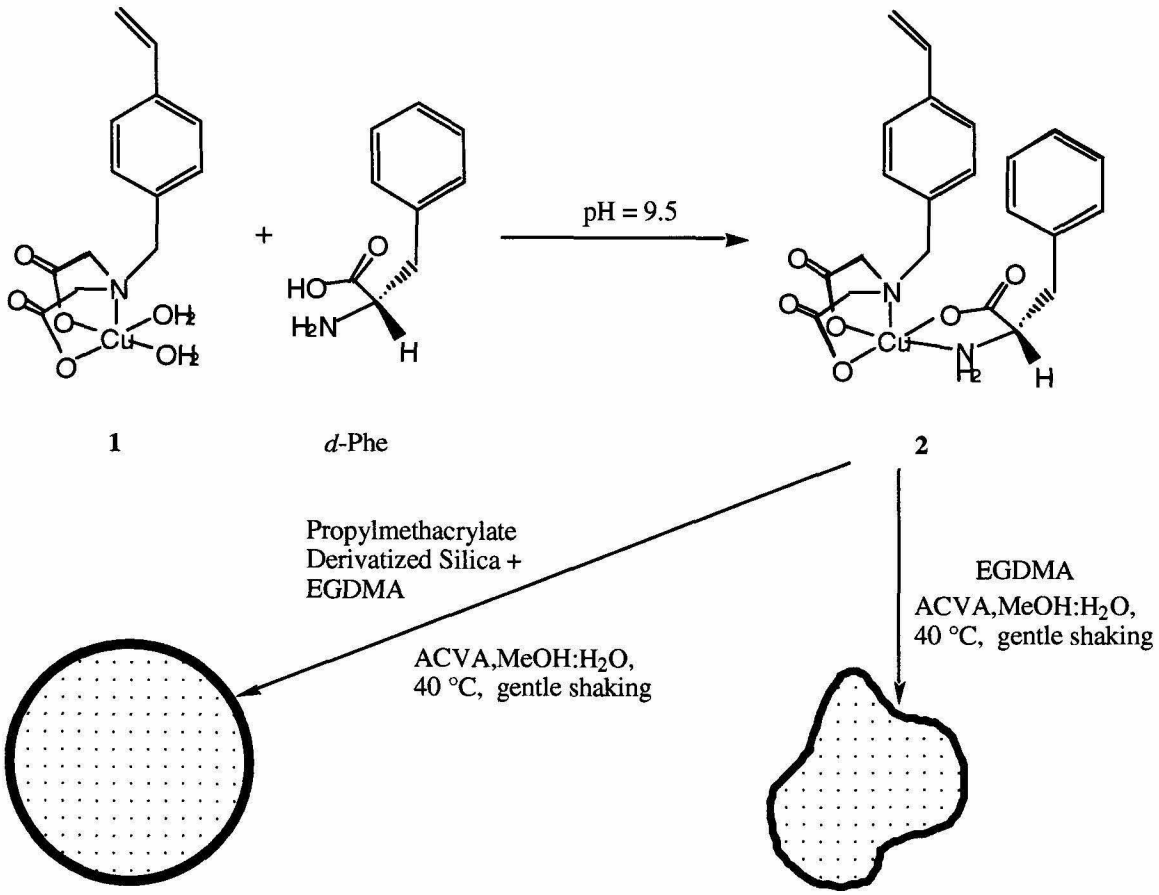

Figure 3. 10. Molecular imprinting of amino acid enantiomers. Phenylalanine is shown here as a test case. The imprinted material is prepared either as **(a)** a polymer coating on the surface of silica particles or **(b)** a bulk polymer.

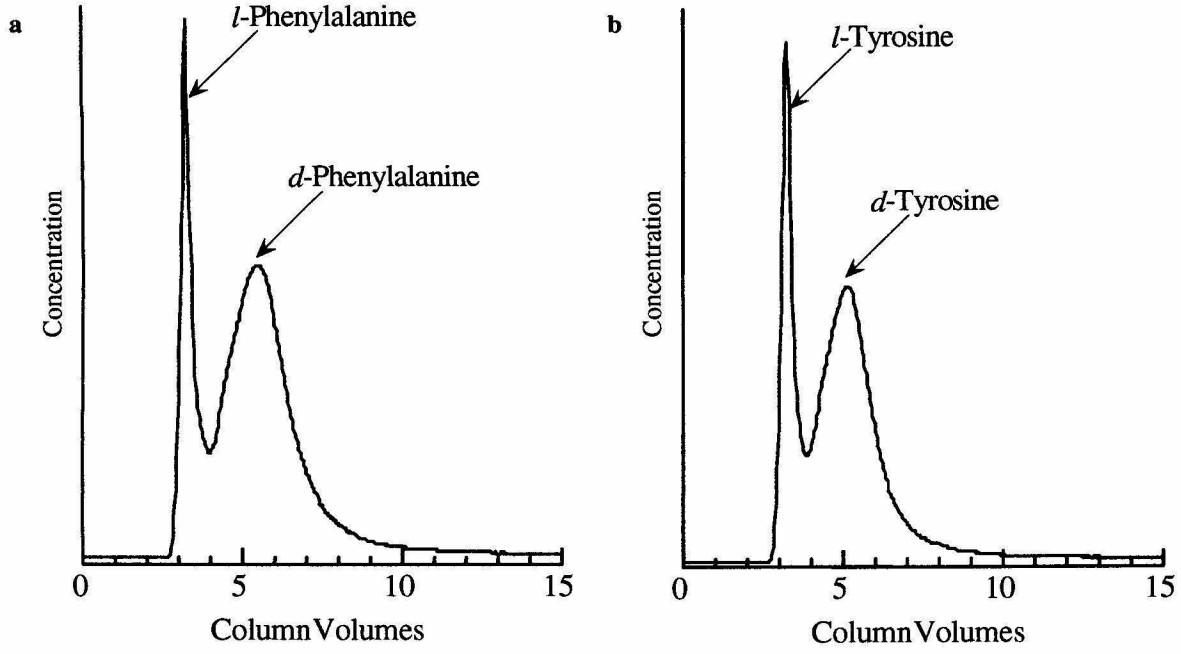

Figure 3. 11. Chromatographic resolutions of amino acids on imprinted adsorbents. **(a)** D,L-phenylalanine and **(b)** D,L-tyrosine on D-phenylalanine-imprinted polymer-coated silica (4.6 mm id x 50 mm column). Peak identification was confirmed by comparison with the retention times of the pure enantiomers. Sample size: 100 μL of 1 mM solution. Running conditions: 1 mL/min, 50 °C, 1.5 mM glycine. Chromatographic separation factors are **(a)** 1.65 for D,L-phenylalanine and **(b)** 1.54 for D,L-tyrosine.

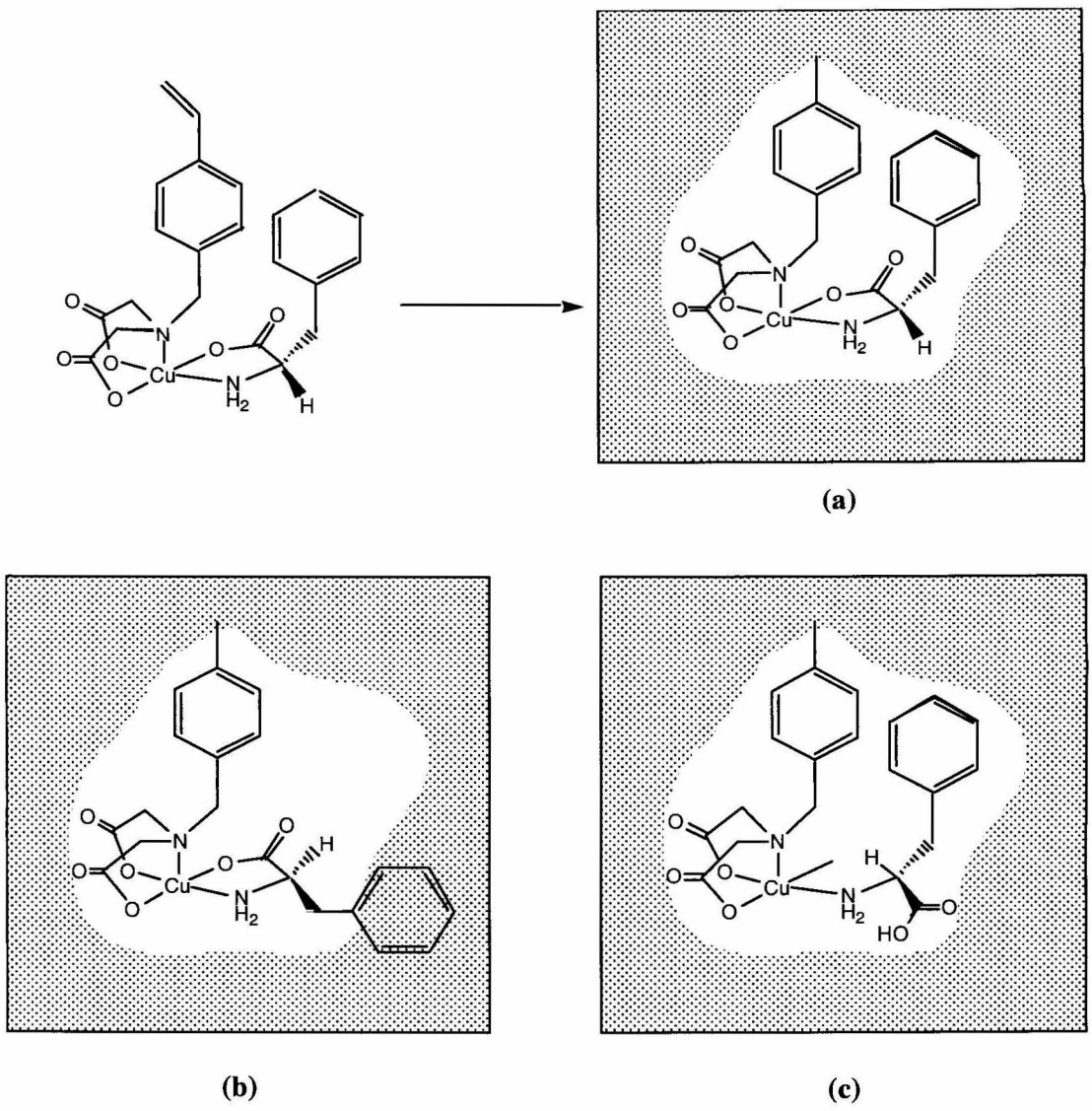

Figure 3. 12. Proposed mechanism of enantioselectivity in imprinted ligand-exchange materials. Molecular imprinting with L-Phe gives a cavity that is selective for L-Phe. **(a)** The L-isomer can simultaneously chelate to metal ion and fit into the shape-selective cavity. **(b)** Rebinding of the D-isomer is hindered because chelation of the metal ion by the D-isomer is sterically unfavorable. **(c)** Alternately, if the molecule fits into the cavity, it cannot chelate Cu^{2+}. This idealized picture of the origin of enantioselectivity is probably true only for a small fraction of the binding sites.

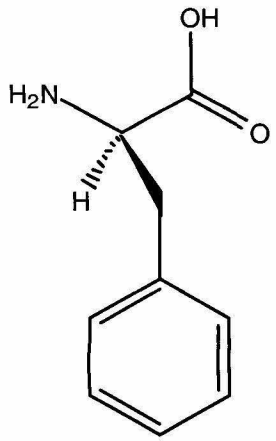

Phenylalanine

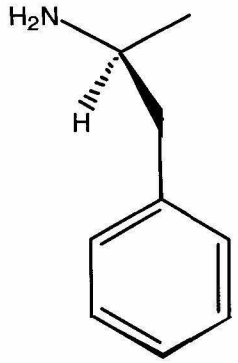

α-methylphenethylamine

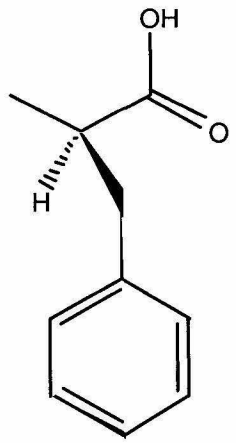

α-methylhydrocinnamic acid

Figure 3. 13. Phenylalanine, *α*-methylphenethylamine and *α*-methylhydrocinnamic acid. The last two molecules are analogous to phenylalanine, in the sense that each one has one of the amine or the carboxylate groups in the amino acid replaced by a methyl group.

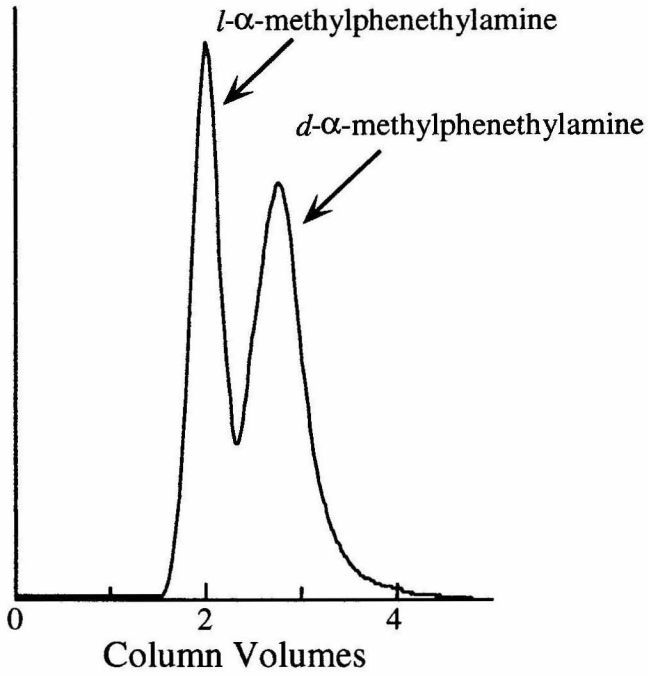

Figure 3. 14. Chromatographic resolution of α-methylphenethylamine. This separation was observed in a column packed with phenylalanine-imprinted polymer-coated silica (4.6 mm id x 50 mm). Sample size: 100 μL of 1 mM solution. Running conditions: 1 mL/min, 50 °C, 1.5 mM acetate, pH 8. Chromatographic separation factor is 1.32.

Polymers	**Enantioselectivity for Amino Acid Substrates**					
	D,L Ala	D,L-Val	D,L-Leu	D,L-Ile	D,L-Phe	D,L-Tyr
L-imprint			$\alpha_{L/D}$			
P-L-A	1.02 (0.01)	1.01 (0.01)	1.01 (0.01)	0.98 (0.03)	0.99 (0.03)	1.00 (0.02)
P-L-V	1.00 (0.01)	**1.08** (0.01)	1.01 (0.02)	1.00 (0.01)	1.01 (0.01)	1.02 (0.01)
P-L-L	0.99 (0.01)	1.03 (0.01)	**1.19** (0.01)	**1.14** (0.01)	1.07 (0.01)	1.06 (0.03)
P-L-I	0.99 (0.03)	1.02 (0.02)	**1.18** (0.01)	**1.23** (0.01)	1.08 (0.03)	1.07 (0.02)
P-L-F	0.98 (0.01)	1.01 (0.01)	1.04 (0.02)	1.07 (0.02)	**1.45** (0.01)	**1.38** (0.01)
P-L-Y	1.01 (0.03)	1.00 (0.01)	1.05 (0.02)	1.08 (0.02)	**1.36** (0.01)	**1.42** (0.01)
D-imprint			$\alpha_{D/L}$			
P-D-A	1.01 (0.01)	0.99 (0.01)	0.99 (0.01)	1.00 (0.03)	0.98 (0.02)	1.00 (0.02)
P-D-V	1.01 (0.01)	**1.09** (0.01)	1.00 (0.02)	0.99 (0.01)	1.00 (0.02)	1.02 (0.01)
P-D-L	1.00 (0.01)	1.01 (0.01)	**1.15** (0.01)	**1.12** (0.01)	1.08 (0.01)	1.07 (0.01)
P-D-I	1.01 (0.03)	1.03 (0.02)	**1.16** (0.01)	**1.24** (0.04)	1.08 (0.03)	1.06 (0.02)
P-D-F	0.99 (0.01)	1.00 (0.01)	1.05 (0.02)	1.07 (0.03)	**1.47** (0.01)	**1.39** (0.01)
P-D-Y	1.00 (0.02)	0.99 (0.01)	1.04 (0.01)	1.08 (0.01)	**1.36** (0.01)	**1.43** (0.01)
Controls			$\alpha_{L/D}$			
P-D,L-A	1.01 (0.01)	1.00 (0.03)	1.00 (0.01)	1.00 (0.03)	0.99 (0.03)	1.00 (0.02)
P-D,L-V	0.99 (0.03)	1.01 (0.01)	1.00 (0.01)	1.01 (0.01)	1.00 (0.01)	1.01 (0.01)
P-D,L-L	1.00 (0.01)	0.99 (0.02)	1.01 (0.01)	0.98 (0.02)	1.01 (0.01)	1.00 (0.01)
P-D,L-I	1.01 (0.01)	1.00 (0.02)	1.00 (0.01)	0.99 (0.01)	0.98 (0.02)	0.99 (0.02)
P-D,L-F	0.98 (0.03)	1.01 (0.01)	0.99 (0.01)	1.01 (0.01)	1.01 (0.01)	1.00 (0.02)
P-D,L-Y	0.99 (0.02)	1.01 (0.02)	1.00 (0.02)	0.99 (0.01)	1.00 (0.01)	1.01 (0.01)
P-0	1.01 (0.01)	1.00 (0.03)	1.01 (0.01)	0.99 (0.01)	1.01 (0.02)	1.01 (0.03)

Table 3. 1. Enantioselectivities of molecularly imprinted polymers in equilibrium rebinding experiments. The polymers are coded according to the chirality of the template and the one letter code of the amino acid. P-0 is the control polymer synthesized in the absence of any template. The selectivities that are ~ 1.1 or higher are indicated in bold.

References

Andersson, L., Sellergren, B., and Mosbach, K. 1984. *Tetrahedron Lett.* **25:** 5211-5214.

Arnold, F.H., Plunkett, S.D., and Vidyasankar, S. 1994. *Polymer Preprints.* **35:** 996-997.

Caruel, H., Rigal, L., and Gaset, A. 1991. *J. Chromatogr.* **558:** 89-104.

Davankov, V.A. and Kurganov A. A. 1983. *Chromatographia* **17:** 686-690.

Davankov, V.A. 1989. Ligand-exchange phases. In *Chiral Separations by HPLC: Application to Pharmaceutical Compounds.* (ed. A.M. Krstulovich), pp. 446-475. Ellis Horwood, Chichester.

Dhal, P. K. and Arnold, F. H. 1992. *Macromolecules.* **25:** 7051-7059.

Fuji I.Y., Matutani, K., and Kikuchi, K. 1985. *J. Chem. Soc. Chem. Comm.* 415-417.

Gubitz, G., Pierer, B., and Wendelin, W. 1992. *Chirality* **1:** 333-337.

Kempe, M. and Mosbach, K. 1991. *Anal. Lett.* **24:** 1137-1145.

Lefebvre, B., Audebert, R., and Quivoron, C. 1978. *J. Liq. Chromatogr.* **1:** 761-770.

Martell, A.E. and Smith, R.M. 1974. *Critical Stability Constants.* Plenum Press, New York.

Mosbach, K. 1994. *Trends Biochem Sci.* **19:** 9-14.

Plunkett, S.D. and Arnold, F.H. 1995. *J. Chromatogr.* **708:** 19-29.

Rao, A.K., Kumar, G.N., Mohan, M.S., and Kumari, Y. 1992. *Ind. J. Chem.* **31:** 256-259.

Rogozhin, S.V. and Davankov, V.A. 1971. *J. Chem. Soc.* 490.

Sellergren, B., Ekberg, G., and Mosbach. K. 1985. *J. Chromatogr.* **347:** 1-10.

Sellergren, B., Lepisto, M., and Mosbach, K. 1988. *J. Am. Chem. Soc.* **110:** 5853-5860.

Sundaresan, V. and Arnold, F.H. 1995. *Curr. Opin. Biotechnol.* **6:** 218-224.

Wulff, G. 1995. *Angew. Chem.* **34:** 1812-1832.

Chapter 4

Molecular Imprinting III: Conclusions

Summary: Molecularly imprinted ligand-exchange materials

In the preceding chapters, the term "ligand-exchange" has been used specifically in the sense used in the literature on chromatographic separations, i.e., the reference is to the reversible coordination of electron-donating groups to transition metal ions. Ligand-exchange chromatography (LEC) is most often used for the difficult problem of enantioresolution, which is increasingly becoming critical for a large number of molecules. LEC is intrinsically restricted to those substrates that offer electrons to be donated to metal ions, but a substantial number of molecules of biological and pharmaceutical interest incorporate heteroatoms like N and O, which can indeed coordinate to metal ions. Therefore, LEC can potentially be used to resolve closely related structural isomers of a wide variety of interesting molecules.

Correspondingly, the metal ion coordination interaction can be used in the molecular imprinting technique, to preorganize monomers and templates in complementary binding geometries. This approach offers certain advantages over both conventional ligand-exchange adsorbents and imprinted polymers prepared using other molecular interactions such as hydrogen bonds and covalent bonds. Unlike in the synthesis of conventional ligand-exchange adsorbents, the scientist can incorporate predetermined patterns of selectivity into ligand-exchange materials, using molecular imprinting. In comparison with other kinds of imprinted polymers, the ligand-exchange materials described in this thesis differ in certain key features. Metal coordination interactions are characterized by higher strengths of binding as compared to hydrogen bond formation, in combination with rapidly reversible kinetics as compared to covalent bond formation. Therefore, for a given template molecule, a judicious choice of

functional monomers and metal ions, in conjunction with carefully designed synthesis procedures, can offer good control over the physical and chemical properties of the resultant materials. The functional monomer can be chosen so as to bind more strongly to the metal ion than the template molecule. Therefore, unlike the common method used when hydrogen bond formation is used for molecular imprinting, there is no need to introduce a large excess of metal-chelating functional monomers to promote monomer-template binding. Thus, the random incorporation of binding functionalities in the resultant polymer can be minimized or even eliminated, leading to narrower distributions of heterogeneous binding sites as compared to other molecularly imprinted materials.

Future directions

Our experiments with molecular imprinting for small molecule templates show that it is possible to impart substrate selectivity and enantioselectivity to polymeric adsorbents. The imprinting procedure appears to be sensitive to small changes in molecular size and shape, as demonstrated by the selectivities seen for bis-imidazole substrates and α-amino acids. Non-specific binding, arising from binding site heterogeneity, does not seem to be a significant problem for these materials. However, in common with other molecularly imprinted polymers, the ligand-exchange adsorbents have certain inherent problems that remain to be addressed. The imprinting process calls for a large excess of crosslinking monomer to be used during the polymerization, in order to create a rigid network with well-defined positioning of binding functionalities. This implies that the loading capacity in these materials is inherently limited. Typically, a few micromoles of substrate are adsorbed per gram of imprinted polymer. Synthetic

strategies need to be developed to address the problem of how to improve upon this parameter. Another issue is that the mechanistic models of selectivity that have been proposed by various researchers are not based on direct evidence of binding of substrates to imprinted polymers. Direct characterization of the binding event remains to be addressed for many imprinted polymeric systems. This remains a tough problem to solve, because of the amorphous nature of the crosslinked polymer network.

In particular, the template removal step needs better quantitative analysis. There is always some amount of residual template that is inextricable from the polymer. Especially in the area of enantioresolutions, this raises a question of what role imprinting plays in imparting selectivity to polymeric adsorbents. It is usually assumed that multiple interactions exist between each monomer molecule and template molecule and that the binding sites remain isolated from one another in the imprinted polymer. However, it has recently been shown (Katz and Davis 1999) that in the case of molecular imprinting using methacrylate monomers for anilide derivatives of amino acids, these assumptions are no longer valid. This raises serious questions of whether molecular imprinting always succeeds in imparting shape and size selectivity to a polymer or whether the observed separations are all due to the influence of the residual template in the polymer. These issues need to be investigated for the molecularly imprinted ligand-exchange adsorbents also. The lack of substrate binding in the absence of metal ions indicates that the mechanisms involved in rebinding enantioselectivity could be quite complex.

Most of the research in molecular imprinting has hitherto been focused on synthesizing materials that are capable of selective separations. Krebs and Borovik (1995) and Sharma and Borovik (2000) have demonstrated the ability of molecularly

imprinted ligand-exchange polymers to act as selective carriers of O_2, CO and other gases. Other obvious directions in which metal coordination interactions in combination with molecular imprinting methodology hold great promise are the development of novel heterogeneous catalysts and sensors. Molecularly imprinted materials for selectively recognizing heavy metal ions can be synthesized, for use as diagnostic tools and also for application in the clean up of toxic wastes. In the context of catalysis, the major hurdle to be crossed seems to be the design of appropriate transition state analogs for use as templates during the imprinting process. Some research has already been initiated recently, towards developing molecularly imprinted polymers incorporating Pt^{2+} ions (Brunkan and Gagne 2000) and Ru^{3+} ions (Polborn and Severin 2000), for use in asymmetric catalysis. While most catalysts prepared using the imprinting methodology exhibit only modest rate enhancements for targeted reactions, there is enormous scope for improvement in this area.

References

Brunkan, N.M. and Gagne, M.R. 2000. *J. Am. Chem. Soc.* **122:** 6217-6225.

Katz, A. and Davis, M.E. 1999. *Macromolecules.* **32:** 4113-4121.

Krebs J.F. and Borovik, A.S. 1995. *J. Chem. Soc. Chem. Comm.* 553-554.

Polborn, K. and Severin, K. 2000. *Chem. Eur. J.* **6:** 4604-4611.

Sharma, A.C. and Borovik, A.S. 2000. *J. Am. Chem. Soc.* **122:** 8946-8955.

Chapter 5

A General Model for Stereoselectivity in Ligand-Receptor Interactions

Abstract

Receptor-substrate interactions in enzymatic, neurological and immunological systems are typically characterized by a high degree of stereoselectivity towards complex substrates. We propose a novel stereocenter-recognition (SR) model for stereoselectivity of proteins towards substrates that have multiple stereocenters, based on the topology of substrate stereocenters. The model provides the minimum number of substrate *locations* that need to enter into any of binding, shape-selective, shape-inductive, or steric interactions with receptor *sites*, for stereoselectivity to occur. A substrate *location* may interact with multiple receptor *sites*, or multiple substrate *locations* may interact with a single receptor *site*. However, a stereoselective receptor has to offer, in the correct geometry, at least as many interactions as the required minimum number of substrate *locations*. The SR model predicts that stereoselectivity towards an acyclic substrate with N stereocenters distributed along a single chain requires interactions involving a minimum of $N + 2$ substrate *locations*, distributed over all stereocenters, such that three "effective" *locations* exist per stereocenter. Thus, enantioselective recognition of molecules with one chiral center requires a protein to interact with a minimum of three substrate *locations*, while stereoselectivity towards substrates with two stereocenters requires a minimum of four *locations*, and substrates with three stereocenters call for a minimum of five *locations*. We demonstrate the general applicability of this model to protein-substrate interactions, by interpreting previous experimental observations.

Introduction

In the previous chapters, the mechanisms of enantioselectivity in molecularly imprinted polymers have been discussed in terms of three-point interaction, which is derived from a model of biological molecular recognition. Ligand-receptor binding is the first event in catalytic, signaling and other biologically important pathways, and is usually characterized by a high degree of selectivity. One of the most interesting selectivity properties of proteins is their ability to distinguish between different stereoisomers of the same molecule. In general, stereoselectivity can be defined as a receptor's ability to preferentially recognize one out of all possible stereoisomers of a ligand. A special case of stereoselectivity is enantioselectivity, where two enantiomers of a molecule are to be distinguished. Fischer's "lock-and-key" analogy (1894) for explaining the substrate selectivity of enzymes was extended by Ehrlich, in the year 1900, to cover toxin receptors and drug receptors (Parascandola and Jasensky 1974). However, these early geometric models were not entirely satisfactory explanations of the ability of biological receptors to selectively bind to and to carry out biological functions on particular stereoisomers of their ligands. Cushny (1926) proposed that drug receptors are optically active, forming different complexes with each enantiomer of an optically active molecule, so that the resultant drug-receptor adducts are no longer mirror images of each other. Although this postulate erroneously held optical activity to be responsible for pharmacological activity, it nevertheless highlighted an essential condition for chiral recognition. For enantioselectivity to occur, the interactions of a receptor with two enantiomers should differ energetically. It follows that a receptor that distinguishes between enantiomers of a chiral ligand would itself need to be chiral. The resultant

ligand-receptor complexes would then be diastereomers, with differing energies of formation. While this is a fundamental thermodynamic requirement, various geometric and structural models have also been proposed to explain the origins of selectivity in molecular interactions.

The three-point attachment (TPA) model

The currently accepted and most widely cited explanation of enantioselectivity originates in the three-point attachment (TPA) model. Easson and Stedman (1933) pointed out that contrary to Cushny's assumption, both optical activity and enantiospecificity in drug action are functions of a more fundamental property of a molecule, namely its structure. Their observations of the preferential drug action of L-adrenaline at adrenergic receptors led to the first proposal of the TPA model. According to this model, if one enantiomer of a chiral molecule binds to a protein simultaneously at three sites (Fig. 5. 1a), the opposite enantiomer can bind at most to two of the same three sites (Fig. 5. 1b). Although terms such as prochirality and enantiotopes had not yet been coined, Easson and Stedman effectively pointed out that in this picture of ligand-receptor interactions, the two enantiotopic groups in a prochiral ligand could also be distinguished by such a receptor. Ogston (1948) independently proposed a similar model, which calls for three attachment sites in an enzyme that catalyzes the preferential conversion of a prochiral substrate to one enantiomer of a reaction product (Fig. 5. 1c-e). If a prochiral substrate binds to an enzyme at least at three points, and if the two chemically identical groups on the substrate bind to catalytically distinct sites, then the reaction can proceed through an enantiospecific pathway. A similar idea underlies the polyaffinity model of

Bergmann et al. (1936), which was proposed to explain the enantiospecific proteolytic activity of aminopeptidases. In this model, an enzyme must contain at least three different atoms or functional groups, forming a hypothetical binding plane. Similarly, three active groups in the peptide (amide, free amine group and α-carbon) form the hypothetical binding plane of the substrate. The two planes approach each other in such a manner as to allow the proteolysis of only those peptides that incorporate the correct enantiomer of the N-terminal amino acid. As three points determine a plane in three-dimensional Euclidean space, the polyaffinity model is conceptually similar, and geometrically equivalent, to the models of three-point attachment.

The three-point interaction (TPI) model

Several prominent stereochemists (Mislow 1962; Bentley 1978) have held that although three-point attachment is conceptually simple and attractive, it is not a fundamental prerequisite for stereoselective differentiation. For example, when a chiral cation and a chiral anion form diastereomeric ion pairs in solution, the energies of formation are measurably different (Arnett and Zingg 1981). It does not seem necessary to invoke three-point attachment in order to explain this phenomenon. Bentley (1983) lists examples of enzyme-substrate binding where the TPA model seems to be violated, and holds that as both substrates and enzymes are chiral molecules, the fundamental factor behind chiral discrimination is the difference in the thermodynamic stabilities of diastereomeric adducts. The idea that three-point attachment results in enantioselectivity has also been questioned by Booth et al. (1997), with respect to the resolution of benoxaprofen enantiomers on amylose-based chromatographic adsorbents. Both

enantiomers of this molecule seem to bind to the adsorbent at the same three points, but the binding of one enantiomer occurs in a strained conformation (Booth and Wainer 1996). A conformationally driven process of enantioresolution has therefore been postulated for these materials.

It is important to note that the term "point of attachment" presumes a one-to-one binding interaction between a functional group in one molecule and a corresponding one in the other. However, it is not necessary that the interactions between two molecules should all be binding in nature. The importance of factors like steric hindrance has long been recognized (Bergmann and Fruton 1937; Popjak and Cornforth 1966). While binding interactions would result in thermodynamic stabilization, steric hindrance would contribute to enantioselectivity by the relative destabilization of one enantiomer. In the absence of similar steric factors, the opposite enantiomer would be able to bind relatively more strongly, thereby resulting in receptor enantioselectivity (Fig. 5. 2). It has also been recognized from the earliest times that ligand-receptor interactions may involve the contour of a large part of the receptor surface, rather than individual points in the two molecules (Easson and Stedman 1933; Bentley 1983). The stereochemical principles underlying the three-point attachment (TPA) model have therefore been extended to a three-point interaction (TPI) model, where other kinds of interactions are also taken into account (Davankov 1997). Thus, the idea of three-point attachment has rarely been applied rigidly. Even in instances where only one or two "points of attachment" can be identified, enantioselectivity has been explained by invoking a total of three interactions, some of which may be non-binding in nature. The cumulative result of the three interactions is either a stabilization of the binding of one enantiomer or a relative

destabilization of the opposite enantiomer. This picture of enantioselectivity does not preclude the fact that significant conformational changes in the receptor can result from the binding of a ligand (Koshland 1958; Koshland et al. 1966).

The idea of three-point interactions is conceptually attractive and continues to be cited as an explanation for many enantioselective systems. Pirkle and Pochapsky (1986) provide intermolecular nuclear Overhauser experimental evidence for chiral recognition in chromatographic systems involving π-donor-acceptor interactions, and hold that a three-point interaction has to be involved in the formation of diastereomeric adducts between ligand and receptor. Such direct evidence is not available for most other systems, but the basic idea of a three-point interaction continues to be well accepted as a significant structural mechanism that underlies enantioselectivity in molecular interactions. Versions of the TPI model continue to be cited for a variety of receptors, including enzymatic systems (Fersht 1999; Copeland 2000), drug-receptor interactions (Silverman 1992), H-2 receptors for histamine (Nederkoorn et al. 1996), ligand binding to chiral porphyrins (Kuroda et al. 1993), taste receptors for sweetness (Shallenberger 1983; Suami and Hough 1993), and inclusion complexes in cyclodextrins (Ahn et al. 2001). Three-point interactions between chiral ions have also been postulated for chiral recognition in solution (Ács 1995; Caira et al. 1997; Reetz et al. 1999) and for chromatographic enantioresolutions (Dalgliesh 1952; Davankov and Kurganov 1983; Pirkle et al. 1983; Nesterenko et al. 1994; Morris et al. 1996; Sundaresan et al. 1997). Pirkle has successfully applied the TPI model to the design of different chiral stationary phases and mobile phases for chromatography (Welch 1994). Pirkle (1997) also holds that the TPI model is a necessary consequence of Euclidean geometry, while Davankov

(1997) cites a number of examples from ligand-exchange chromatography (LEC) and reiterates that a three-point interaction is a minimum requirement for enantioselectivity.

The rocking tetrahedron model: two-point attachment in three-point interactions

Both the TPA model (Easson and Stedman 1933; Ogston 1948) and its extension to a TPI model presuppose that a face of an asymmetric tetrahedron has to interact with a receptor surface. These models apply both to enantiomer discrimination in a binding interaction and to the enzymatic conversion of prochiral molecules in an enantiospecific manner. More recently, Sokolov and Zefirov (1991) have proposed an alternative model for enantiospecific conversion of prochiral molecules. This model involves two-points of attachment (Fig. 5. 3), where an edge of a tetrahedron binds to the receptor surface. A prochiral substrate binds to an enzyme at two points, but its direction of approach and the rotational and vibrational degrees of freedom of the molecule are restricted in the bound state. If we assume that the bound molecule has a limited ability to "rock" around the axis formed by the two points of attachment, in a pendular motion, there would be a small region in space that is equally accessible to both enantiotopic groups. However, there would also be other regions that are relatively more accessible to one enantiotopic group than the other, and regions that are accessible solely to one of these two groups. Therefore, depending on the residence time of the substrate in each of these different regions, the spatial location of a catalytic site in the enzyme, and the angle of attack, the conversion of the substrate can take place either in a completely enantiospecific manner, or with varying degrees of enantioselectivity. Thus, this model requires only two points of attachment, but nevertheless invokes a third interaction, involving one of the

enantiotopic groups in a prochiral molecule. If the reactive transfer of electrons between two molecules were also counted as one kind of interaction, the "rocking tetrahedron" model is ultimately a TPI model. Its extension to non-enzymatic receptors that distinguish between two enantiomers of a molecule is straightforward. Its strength lies in the fact that it replaces a static view of three-point interaction with a more dynamic picture of ligand-receptor interactions.

The four location (FL) model

The TPI model has recently been rejected in a study of the binding of isocitrate stereoisomers to bacterial isocitrate dehydrogenase. This enzyme catalyzes the conversion of D-isocitrate to oxalosuccinate and then to α-ketoglutarate, in the presence of the coenzyme, NADP (nicotinamide adenosine dinucleotide phosphate), and Mg^{2+} ions. Crystal structures showed that in the presence of Mg^{2+}, D-isocitrate is found in the active site of the enzyme, but in the absence of Mg^{2+}, only L-isocitrate preferentially binds to the enzyme (Mesecar and Koshland 2000a). In each case, four different functional groups in isocitrate have been observed to bind to distinct sites in the enzyme. The –OH group of D-isocitrate binds to the metal ion when it is present, while the –OH group of L-isocitrate binds to an arginine residue in the absence of metal ions. The three carboxylate groups in isocitrate interact with the same groups of enzyme residues in both cases. Mesecar and Koshland (2000b) therefore reject the TPI model, and explain this phenomenon by means of a four location (FL) model of protein stereoselectivity. The FL model holds that chiral discrimination requires a minimum of four designated locations, either as four attachment sites or as three attachment sites and a direction (Fig. 5. 4).

Theoretical analyses of chiral interactions: Necessity of specifying four points

In the context of this alternative model, it is necessary to briefly review theoretical analyses of chiral molecular recognition. Salem et al. (1987) have calculated the differential forces and interaction energies between two chiral tetrahedral molecules in the free relative molecular rotation limit, by modeling the chiral selector and the chiral selectand as simple asymmetric tetrahedra. Chiral recognition does not seem possible if the interactions between two asymmetric tetrahedra were purely vertex-to-vertex (Fig 5. 5a,b) or edge-to-edge (Fig. 5. 5c,d) in nature, and requires a face-to-face (three-point) interaction (Figs. 5. 5e,f). This study would seem to support the geometric models originally proposed by Easson and Stedman (1933) and Ogston (1948), and defended by Davankov (1997) and Pirkle (1997). However, Topiol and Sabio (1989) have pointed out that the analysis of Salem et al. (1987) implicitly rules out other kinds of interactions between two asymmetric tetrahedra, in particular the ones involving a vertex-to-face contact (Fig. 5. 5g,h). Formal distance-matrix analysis (Topiol and Sabio 1996) shows that it is necessary to account for the distances of all four vertices of a tetrahedral chiral selectand from those of the chiral selector. This holds true, irrespective of the number of points of binding between a chiral selector and a chiral selectand. Monte Carlo simulations of the mutual interactions of alanine enantiomers (Andelman and Orland 1993) also show that enantioselectivity is a function of distance between two chiral molecules, involving all four vertices of the asymmetric tetrahedra.

These analyses are all based on geometric perspectives of interactions between two simple asymmetric tetrahedra, and would not be directly applicable to more complex

molecules. Many biologically significant ligands are small molecules, but biological and biomimetic receptors are usually macromolecules, with defined structures, so that their function as chiral selectors cannot be modeled as simple tetrahedra. Nevertheless, from the perspective of the ligand, the conclusions reached in these theoretical discussions are important. It is necessary to identify the relative positions all four substituents on a chiral carbon atom in order to provide unambiguous nomenclature for such molecules. The requirements for molecular recognition in the context of a ligand-receptor interaction would be similar. For any tetrahedron, three vertices determine a plane, but it is necessary to also specify where the fourth vertex (or equivalently, the chiral carbon atom) lies with respect to this plane. Therefore, either the relative spatial coordinates of a fourth point need to be specified, or a directional constraint needs to be provided.

Implicit assumptions in the TPI and FL models

It is important to note that there is indeed a directional constraint implicit in all three-point interaction (TPI) models. Mesecar and Koshland (2000b) hold that the TPI model would be valid only if a ligand molecule approaches a flat receptor surface from a particular direction. However, the TPA model, as originally proposed by Easson and Stedman (1933) and Ogston (1948), assumes only that a ligand binds to one side of a receptor surface (Wilcox et al. 1950), and imposes no particular restrictions upon the curvature of the receptor surface. This assumption would be valid in most cases, as binding sites are typically located on the solvent-accessible surfaces of macromolecular receptors. The three-dimensional interior structure of the receptor would prevent the approach of a ligand to the "opposite side" of the binding surface. Therefore, when

extending the TPA model to the TPI model, it is assumed that in ligand-receptor binding, the ligand is largely restricted to a particular side of the receptor surface.

A second assumption is made in the TPI model, regarding the bound orientation of the ligand. The model assumes not only that the approach of a ligand is restricted to one side of a receptor surface, but also that this occurs in such a manner as to orient a face of a tetrahedron towards the receptor surface (Fig. 5. 6a). This implicitly rules out the possibility of vertex-to-surface orientation (Fig. 5. 6b). One of the most common reasons for this would be steric hindrance faced by a bulky group that would project into a receptor surface. This was explicitly pointed out in the early polyaffinity model for enzymes (Bergmann and Fruton 1937), which viewed the binding event in terms of the approach of a binding plane of the enzyme towards that of the substrate. Bergmann et al. (1936) had already pointed out that if large groups were positioned such that they occupy the space between the two binding planes, then the close approach of these planes towards each other would be prevented by steric hindrance. It is important to note that if two ligand enantiomers bind in opposite orientations to the same receptor, it might appear as if one enantiomer has approached the receptor surface from the "opposite side," although this would be physically impossible. As will be shown below, the FL model (Mesecar and Koshland 2000b) fails to distinguish between the directionality of approach of a ligand molecule towards the receptor and its relative orientation when bound to the receptor. These may be constrained independently, and one factor should not be confused for the other.

A general statement of the TPI model may thus be defined. If both enantiomers of a ligand approach a receptor surface from the same side and bind in similar

orientations, the receptor needs to provide a minimum of three interactions, in order to preferentially recognize one over the other. This is consistent with the theoretical analysis of chiral interactions as provided by Topiol and Sabio (1996). The constraints of directionality of approach and bound orientation of ligand together serve to uniquely specify a fourth point in an asymmetric tetrahedron, with respect to the plane determined by the three points of interaction.

There is a third important assumption in the TPA model, which seems to have been completely overlooked. The model of Easson and Stedman (1933) was originally proposed to explain the differential recognition of a pair of enantiomers of a drug molecule with a single chiral center. Similarly, Ogston's TPA model (1948) was meant to explain how an enzymatic reaction could convert a prochiral carbon to a chiral product in an enantiospecific manner. The extension of the TPA model to a TPI model also carries over an assumption that only a single stereocenter is of interest in chiral molecules. The classical picture of three-point interactions can therefore be applied only to molecules that have a single chiral center or to enantiospecific enzymatic reactions at a prochiral center in a substrate. An important consequence of this is that the TPI model would fail to fully explain ligand-receptor interactions where the stereochemistry at multiple stereocenters in the ligand molecule plays an important role. There is no reason to believe that the simple binding geometry assumed by the TPI model would hold true for all ligand-receptor interactions, irrespective of the number of stereocenters in the ligand. This point has been largely overlooked in discussions of stereoselectivity where the picture of three-point interactions has been either unsatisfactorily invoked or summarily rejected with respect to ligands that have multiple stereocenters.

The recently proposed FL model of Mesecar and Koshland (2000a, 2000b) is partly an explicit statement of the implicit constraint in the TPI model, regarding the direction of approach of the ligand to the receptor surface. It also provides an alternative requirement of a minimum of four attachment points. As shown in Fig. 5. 4, the FL model also assumes that a chiral ligand has only one center of asymmetry. However, it must be noted that isocitrate is a molecule that has two stereocenters, and that the FL model is an attempt to explain the metal-dependent reversal of stereoselectivity of isocitrate dehydrogenase. This model's requirement of four attachment sites does not adequately explain the fact that the four points of interaction between isocitrate and isocitrate dehydrogenase are distributed on two stereocenters in isocitrate. Similarly, in the binding of α_2-adrenergic receptors to (1R,2S)-α-methylnoradrenaline (Triggle 1976; Ruffolo 1983) and analogous molecules, the functional groups involved in interactions with the receptor are distributed on two stereocenters in the drug.

Need for a general model of stereoselectivity

Neither the TPI model nor the FL model can adequately account for the stereoselectivities observed in these systems. Bentley (1983) finds the idea of three-point interactions to have outlived its usefulness, and cites instances where there is clear evidence for interactions at more than three points. Among these examples, the one that involves phenylalanine, a ligand with a single chiral center, will be discussed in greater detail below. The other examples cited by Bentley are of L-arabinose binding protein, which binds to L-arabinose, and the proteolysis of *N*-acetyl tryptophan and *N*-acetyl phenylalanine by chymotrypsin, where the L- enantiomers are substrates, but the D-

enantiomers are inhibitors (DeTar 1981). It should be noted that arabinose contains four stereocenters in a heterocyclic ring. The crystal structures of sugar-binding receptors, bound to molecules like arabinose, glucose and galactose, have been solved (Quiocho and Vyas 1984; Vyas et al. 1988). In each case, the hydroxyl groups in the bound sugar molecule, distributed over more than three stereocenters, interact with multiple enzyme residues and water molecules, through a network of hydrogen bonds (Fig. 5. 7). Thus, there are not just three or four, but a large number of interactions involved, distributed over all stereocenters in the sugar and over a large surface area in the corresponding receptor. The TPI model of enantioselectivity is simply inapplicable to such cases, as each of these sugar molecules has multiple stereocenters. As for chymotrypsin, the reaction mechanism proceeds through an intermediate in which the carbonyl carbon of the substrate is converted to an asymmetric tetrahedral carbon. This results in the introduction of a second stereocenter adjacent to the chiral α carbon of the amino acid. The mechanism of chymotrypsin inhibition by D- enantiomers of amino acid esters would therefore be more complex than what is indicated by models developed for molecules with a single chiral center.

In general, a molecule with N stereocenters has a maximum of 2^N stereoisomers. Many biologically important molecules have multiple stereocenters. In addition to naturally occurring peptides and sugars, significant examples include the anti-inflammatory ephedrines (two stereocenters), the artificial sweetener aspartame (two centers), the toxic and carcinogenic epoxides (typically two centers, e.g., stilbene oxide), the antibiotic penicillin (three centers), the insecticide deltamethrin (three centers), riboflavin or vitamin B2 (three centers), the antimalarial drug quinine (four centers), the

beta-blocker nebivolol (four centers), the cytochrome complex inhibitor stigmatellin A (four centers), and the angiotensin converting enzyme inhibitor perindopril (five centers). Stereoselective recognition of such molecules necessarily implies an unambiguous specification of the geometric structure at each stereocenter. The rigorous system of nomenclature for such molecules follows the rules originally proposed by Cahn, Ingold and Prelog (1966), which separately specify the configuration at each stereocenter. Similar rules also apply to stereogenic axes and planes, but the lack of a rigorous theoretical understanding of molecules that have many such complex stereoelements often leads to inconsistent nomenclature (Nickolau et al. 2001). A deeper lacuna in theoretical understanding seems to affect many discussions of stereoselective interactions of receptors with ligands that have multiple stereocenters. None of the models discussed earlier adequately takes into account the complex stereochemical requirements involved in receptor binding to ligands with multiple stereocenters.

It is to be expected that rather than a minimum of three or four interactions, the number of geometric requirements for a receptor to uniquely recognize one out of 2^N stereoisomers would be a function of both the number (N) and the topological distribution of stereocenters in the molecule. However, the TPI and FL models cannot be directly extended to such molecules, by merely requiring a stereoselective receptor to provide a minimum of $3N$ or $4N$ interactions. The following discussion provides a new model for ligand-receptor stereoselectivity for the general case of molecules that have multiple stereocenters. As the molecular structure and the distribution of these stereocenters in the structure may also be expected to be important, molecules that have one, two or three stereocenters in acyclic structures are examined in detail. A general model is presented

for molecules with *N* stereocenters in linear and branched structures, and preliminarily extended to the case of molecules with multiple stereocenters in cyclic structures.

The stereocenter-recognition (SR) model

Definitions

A stereocenter-recognition (SR) model is proposed here, to rigorously account for the minimum number of *locations* on each stereocenter in a ligand that need to interact with receptor *sites*, for a chiral recognition to occur. This means that a receptor that is stereoselective has to interact with at least as many ligand *locations* as the minimum required by the model. It does not preclude the possibility that in specific instances, structural and/or energetic considerations may require receptor interactions with more than the minimum number of ligand *locations*. This model assumes that it is physically impossible for a ligand to approach the "opposite side" of the binding surface of a receptor (Wilcox et al. 1950). However, it allows for the possibility that different ligand stereoisomers may bind to the same side of a receptor surface, but in different orientations. We define a ligand *location* as a functional group or groups attached to a stereocenter in the ligand, which can interact, either favorably (e.g., due to binding) or unfavorably (e.g., due to steric hindrance) with one or more receptor *sites*. A receptor *site* may comprise either specific functional group(s) in the receptor or the contour of a large part of the receptor surface (Easson and Stedman 1933; Bentley 1983), interacting with one or more ligand *locations*. These definitions are applied to the ligand-receptor complex, and not to the structures of the free receptor and ligand. They allow for a broad range of stereochemical and thermodynamic factors in ligand-receptor interactions, and

also adequately address the issue of how to count the number of interactions involved. Interactions between ligand *locations* and receptor *sites* are rarely one-to-one. For example, a carboxylic acid group attached to a chiral carbon can possibly enter into multiple hydrogen bonds with different receptor *sites*, but only one ligand *location* is constrained by all these interactions put together. Similarly, a hydroxyl group attached to a stereocenter can function both as an electron donor through the oxygen atom and as an electron acceptor through the hydrogen atom. Multiple hydrogen bonds with receptor *sites* are possible in this case too, but the hydroxyl group would count only as one ligand *location*. A single ligand *location* may even consist of many functional groups capable of binding to multiple functional groups in a receptor. Conversely, multiple ligand *locations* may enter into binding interactions with the same *site* in a receptor. The possibility of repulsion between ligand *locations* in some stereoisomers and receptor *sites* bearing like charges should also be taken into account. A bulky group attached to a stereocenter can potentially result in steric hindrance to the binding of one stereoisomer and should be counted as a ligand *location*. Non-binding interactions are known to contribute significantly to the stereospecific proteolytic action of aminopeptidase (Bergmann and Fruton 1937) and chymotrypsin (Fersht 1999). They have also been postulated to play an important role in the differential retention of amino-acid enantiomers on cellulose in thin-layer chromatography (Dalgliesh 1952) and to enantioselective adsorbents used in ligand-exchange chromatography (Davankov and Kurganov 1983; Sundaresan et al. 1997). Thus, the minimum number of ligand *locations*, with which a receptor needs to interact in order to be stereoselective, can be

distinguished from the total number of "attachment points" that can be identified for the binding of a preferred stereoisomer of a ligand to its receptor.

Ligands with one stereocenter

When a ligand has only one chiral center, a receptor needs to distinguish only between two enantiomers. As carbon is tetravalent, a maximum of four ligand *locations* can possibly interact with receptor *sites*. A receptor that interacts with all four ligand *locations* will necessarily be enantioselective, while interactions with only one or two ligand *locations* will not result in enantioselectivity. The three-point interaction (TPI) model would hold true in most cases, so long as its constraints of directionality of approach and binding orientation are satisfied. All three *locations* could be involved in binding interactions, as in the TPA model (Fig. 5. 1). Alternatively, two *locations* in the preferred enantiomer could bind to the receptor. Although the same two *locations* in the opposite enantiomer would also bind to the same two receptor *sites*, thermodynamic and/or kinetic enantioselectivity would result from other conditions preventing the binding of the two enantiomers from being exactly identical. This might be due to either steric hindrance at a third ligand *location* (Fig. 5. 2), or the dynamic factors (Sokolov and Zefirov 1991) involved in the rocking tetrahedron model (Fig. 5. 3).

It may be seen from the following examples that the number of ligand *locations* and the number of receptor *sites* that interact with one another need not be identical. The binding of glycyl-L-tyrosine to the enzyme carboxypeptidase A has been cited as an example that apparently violates the TPA model (Bentley 1983). On the other hand, once the above definition of a ligand *location* is taken into account, it is obvious that the

multiple interactions between carboxypeptidase A and glycyl-L-tyrosine (Mackenzie et al. 1985) can be counted in terms of three ligand *locations*. Thus, both the amide group linking L-tyrosine to glycine and the free amine group of glycine together constitute a single ligand *location* attached to the chiral carbon of tyrosine (Fig. 5. 8a). The converse case of a single receptor *site* interacting with more than one ligand *location* can be seen in the chelation of transition metal ions (Fig. 5. 8b) by the amine and carboxylate groups of chiral amino acids (Davankov and Kurganov 1983; Sundaresan et al. 1997). Thus, the total number of functional groups in the receptor interacting with a chiral ligand may be more (or less) than the number of ligand *locations*, but a receptor needs to interact with a minimum of three *locations* in a ligand with a single chiral center, in order to be enantioselective.

The concept of three-point interactions has been questioned in the case of benoxaprofen binding to amylose based chiral stationary phases, and a "conformationally driven" process of enantioselectivity has been postulated. Both the S and R enantiomers of this drug molecule apparently bind to the amylose based adsorbent through hydrogen bonds involving the same chemical moieties (Booth and Wainer 1996). The S enantiomer presents the small hydrogen atom towards the surface of the adsorbent, and consequently is able to bind in a stable conformation, but the R enantiomer binds in a strained conformation (Fig. 5. 9), because of steric hindrance between the adsorbent surface and the methyl group attached to the chiral carbon in this enantiomer. Counting this steric hindrance as an interaction, it is clear that the proposed conformationally driven mechanism also involves interactions of the receptor with three ligand *locations*. Indeed, in cases where one ligand *location* faces steric hindrance to binding, it may be

expected that the other two *locations* in both ligand enantiomers would enter into similar binding interactions with receptor *sites*. However, the hindered binding of one enantiomer would be energetically less favorable than that of the opposite enantiomer, resulting in thermodynamic enantioselectivity.

In principle, for a ligand with a single chiral center, enantioselectivity could result from a combination of two non-binding interactions and a single binding interaction, resulting in a single-point attachment. Such cases would probably be rare in biological systems, because of the decrease in total binding energy resulting from two unfavorable interactions. However, irrespective of the number of "points of attachment," interactions with at least three ligand *locations* are necessary for enantioselectivity.

Conformational Flexibility and Rotamer Stabilization

The case where enantiomers bind in opposite orientations to the same receptor surface is more complicated. Schematic figures that depict the four different groups attached to a chiral carbon atom as *A*, *B*, etc., are idealized and highly simplified pictures of ligand-receptor interactions. The exact spatial coordinates of an electronic interaction between a receptor *site* and a ligand *location* may often be farther away from the chiral center, and not exactly at the vertex of a tetrahedron. For example, a carboxylate group attached to a chiral center interacts through its oxygen atoms, which are once removed from the chiral center, in terms of molecular connectivity. Similarly, in many of the natural amino acids, the R group is a flexible chain, with a chemical functionality at the end of the chain. In such cases, the maximum possible distance between the chiral center and the actual spatial position of the interaction with the receptor would increase with

chain length. As an increase in chain length also results in an increase in flexibility, the space potentially probed by such a *location* on one enantiomer would overlap significantly with that probed by an identical *location* on the opposite enantiomer. Therefore, the probability increases for the event that the same set of *locations* in both enantiomers interacts with the same set of receptor *sites*, but in different orientations. If the resultant binding strengths were comparable for both enantiomers of such a ligand, a reduction in enantioselectivity would ensue.

One highly significant example that illustrates the above point is found in the case of phenylalanine ammonia-lyase. This enzyme is involved in the phenylpropionic acid pathway in plants, taking L-phenylalanine as the natural substrate, and converting it to *trans*-cinnamate through a concerted *anti*-elimination mechanism (Havir and Hanson 1968). D-phenylalanine is a strong inhibitor, with an inhibition constant (K_I) that is comparable to the Michaelis-Menten constant (K_M) of the enzyme for L-phenylalanine. The difference in ΔG for the binding of the two enantiomers has been estimated to be just about 0.5 kcal/mole (Hanson 1981). Both enantiomers of 2-aminooxy-3-phenylpropionic acid are superinhibitors of this enzyme (Amrhein et al. 1976). Hanson (1981) has explained these observations by a mirror image packing model, in which the flexibility allowed by the benzylic methylene group of phenylalanine plays an important role. Both L- and D-phenylalanine bind to the enzyme active site using the same three *locations* (amine, carboxylate and phenyl groups), but in orientations that are mirror images of each other. A hypothetical plane may be drawn as shown in Fig. 5. 10, intersecting the phenyl ring and passing through the amine nitrogen and the carboxyl carbon atoms. In L-phenylalanine, the chiral carbon (C_α) and the methylene carbon (C_β) atoms would lie to

the right and left of this plane respectively (Fig. 5. 10a). D-phenylalanine would bind in a mirror image conformation, with the C_α and C_β atoms lying respectively to the left and right of this plane (Fig. 5. 10b). If both enantiomers were imagined to occupy the enzyme active site simultaneously, the amine nitrogen and the carboxyl carbon would be in the same positions, while the phenyl rings would overlap substantially (Fig. 5. 10c).

Bentley (1983) argues that this binding model of phenylalanine enantiomers to phenylalanine ammonia-lyase invalidates the TPI model. However, it should be noted that while phenylalanine is a chiral substrate, the product, *trans*-cinnamic acid, is achiral. It should also be noted that along with the removal of the amine group from the chiral center, the enzymatic reaction results in the removal of one of the enantiotopic hydrogen atoms at the benzylic methylene carbon, which is prochiral. In the enzyme-substrate complex, the relative orientations of the functional groups attached to the prochiral carbon would be as important for the reaction mechanism as those of the groups attached to the chiral center. The proposed mirror image packing model for D- and L-phenylalanine successfully explains the observations that K_I for D-phenylalanine is comparable to K_M for L-phenylalanine, and that both enantiomers of 2-aminooxy-3-phenylpropionic acid are transition state analogs for the enzymatic reaction. The mirror image orientations of the two enantiomers in the enzyme active site are achieved merely by explicitly accounting for the flexibility afforded by the benzylic methylene group. Crystal structures of this system do not seem to be available, but the binding enantioselectivity observed is fairly small even though the enzymatic reaction is highly enantiospecific. The fact that the chiral carbon and the methylene carbon in D-phenylalanine lie in mirror image spatial positions as compared to L-phenylalanine seems

to be sufficient to prevent the deamination reaction from proceeding on the D- enantiomer (Hanson 1981). Therefore, this example does not invalidate the stereochemical requirement that enantioselectivity results from interactions of the enzyme with a minimum of three substrate *locations*. The enantiospecificity of the enzymatic reaction, the comparable strengths of binding of D- and L- phenylalanine and enzyme inhibition by both enantiomers of 2-aminooxy-3-phenylpropionic acid may all be explained by considering only three interactions between enzyme *sites* and substrate *locations*.

It may be concluded that for ligands with a single chiral center, a requirement of at least three points of interaction is a necessary but not a sufficient condition for binding enantioselectivity. Thus, if a receptor is enantioselective, then it must interact with such a ligand at least at three *locations*, but interactions with just three ligand *locations* do not always ensure binding enantioselectivity. It is theoretically possible for both enantiomers of a chiral ligand to approach and bind to the same *sites* in a receptor, with comparable binding strengths, but in orientations that are mirror images of each other. A mirror plane would relate the two enantiomers in their bound conformations, and the chiral carbon atom may lie on opposite sides of this plane (Fig. 5. 11a) or on the mirror plane itself (Figs. 5. 11b). As even a single methylene group in a ligand *location* can give rise to the conformational flexibility needed for this to occur, such binding situations cannot be ruled out *a priori*. The assumption implicit in the TPI model, that the approach of the ligand is restricted in its directionality, is not violated by an observation that both enantiomers of a ligand can bind to the same set of receptor *sites*, but in opposite orientations. The possibility raised in the FL model (Fig. 5. 4), that a protein may have binding sites that allow ligand enantiomers to bind to two "opposite sides" of a binding

surface, seems to be erroneous. However, the second assumption implicit in the TPI model, regarding the bound orientation of ligand enantiomers on the receptor (Fig. 5. 6), would not always be satisfied. The presence of flexible groups within a ligand *location*, the size of an atomic group that may jut out towards the receptor surface and the angle at which it is positioned with respect to the binding surface would all influence the enantioselectivity characteristics of the receptor.

Racemase enzymes present a different instance, where binding enantioselectivity is less important than the ability of the enzyme to bind to both enantiomers of a substrate. It may also be expected that such enzymes have to provide a different reaction pathway for converting each enantiomer of the substrate to the opposite one. There is significant evidence to show that in the enzymes mandelate racemase (Gerlt et al. 1992), alanine racemase (Sun and Toney 1999) and glutamate racemase (Glavas and Tanner 1999), each enantiomer of the respective substrates interacts with different sets of enzyme residues. This results in distinct thermodynamic and kinetic characteristics for the binding of substrate enantiomers and the racemization reaction. Thus, each set of sites, considered separately, provides selectivity towards the two enantiomers of the substrate, but taken as a whole, the enzyme binds to both enantiomers and converts each to the other.

Finally, it should be noted that the proposed mirror image packing of phenylalanine enantiomers in the active site of phenylalanine ammonia-lyase (Fig. 5. 10) is possible only in some rotamer conformations of the amino acid. Kinetic observations of the enzymatic reaction (Hanson 1981) suggest a concerted *anti*-elimination mechanism, in which the plane of the phenyl ring is aligned with that of the carboxylate group, and both planes are then collapsed together in the product, *trans*-cinnamic acid.

This reaction mechanism requires the phenyl ring to lie *trans* to the carboxylate group (Fig. 5. 12a), which rules out all eclipsed rotamer conformations of the amino acid. However, even in the conformation where the phenyl ring lies *trans* to the amine group and *gauche* to the carboxylate group (Fig. 5. 12b), a similar mirror image packing, with C_α and C_β lying on opposite sides of the mirror plane, would be theoretically possible. The hindered conformation, with the phenyl ring lying *gauche* to both the amine and the carboxylate groups (Fig. 5. 12c), would position both C_α and C_β on the same side of the amine, carboxylate and phenyl groups. The proposed mirror image packing of phenylalanine enantiomers, where the C_α and C_β atoms are on opposite sides of the hypothetical mirror plane, would not be possible for this rotamer. This may be contrasted with the case of metal-ion chelation by chiral amino acids, where the hindered conformation of the amino acid seems to be stabilized (Vestues and Martin 1980), so that the C_α and C_β atoms would both lie on the same side of the mirror plane. Such detailed considerations of rotamer conformations of the bound ligand would be necessary in all cases where conformational flexibility plays an important role. The ligand rotamer that is stabilized by binding to the receptor may not always be the same as the conformation that is most stable in solution. This has significant implications for a model of stereoselectivity towards ligands that have multiple stereocenters, because each such center serves as a point that introduces flexibility of conformation with respect to the other stereocenters. Moreover, in a molecule with multiple stereocenters, if stereocenters are not adjacent to each other, each intervening carbon atom adds to the number of possible rotamer conformations. As the SR model accounts for the minimum number of

interactions needed for stereoselectivity, it is necessary to first examine the case of molecules with adjacent stereocenters here.

Ligands with two stereocenters

For ligands with two stereocenters (C_I and C_{II}), stereoselectivity refers to a receptor's preferential recognition of one out of four possible stereoisomers. Fig. 5. 13 shows a receptor's possible interactions with three *locations* on an acyclic ligand with two stereocenters. The case where these are adjacent to each other is shown, but the conclusions reached below may be readily extended to the case where they are located farther apart in the molecule. If these *locations* are distributed in a (3-0) configuration in one ligand stereoisomer (all three *locations* directly attached to C_I and none directly attached to C_{II}; Fig. 5. 13a), its enantiomer can have at most two *locations* at C_I interacting with the receptor (Fig. 5. 13b). If this difference results in sufficient $\Delta\Delta G$ for the two sets of interactions, thermodynamic enantioselectivity will be possible. An identical conclusion may be stated for a receptor interacting with a (0-3) configuration of ligand *locations*. This would hold true in all cases where the geometry at only one stereocenter in a ligand is important, even though the molecule has multiple stereocenters. As in the case of single chiral center molecules, interactions of receptor *sites* with a minimum of three *locations* on the stereocenter of interest would be necessary for enantioselectivity. However, if the relative stereochemistry of both stereocenters in a ligand with two stereocenters is important, interactions at only three ligand *locations*, in a (3-0) or a (0-3) configuration, will not generally result in stereoselectivity. For the (3-0) configuration, the receptor does not interact directly with

any *locations* on C_{II}. This would result in a diminished ability of the receptor to distinguish between diastereomers possessing opposite stereochemistry at C_{II} (Figs. 5. 13a,c). Similarly, if a receptor interacts with a (0-3) configuration of ligand *locations* (not shown in Fig. 5. 13), diastereomers that have opposite stereochemistry at C_I would interact in similar ways, again resulting in diminished stereoselectivity. In these cases, any thermodynamic preference for one member of a diastereomeric pair would probably be attributable more to the intrinsic energetic differences between diastereomers and to the corresponding rotamer conformations in the bound state.

If three ligand *locations* interacting with the receptor are distributed in a (2-1) configuration (two *locations* directly attached to C_I and one to C_{II}), the receptor would again have difficulty discriminating between the two diastereomers with opposite stereochemistry at C_{II}, although it may possibly distinguish between enantiomers (Figs. 5. 14a-c). However, each stereocenter offers possibilities for different orientations for the interactions of the *locations* on the other stereocenter. Thus, an enantiomeric pair can bind in mirror image orientations (Figs. 5. 14d,e), with the mirror plane intersecting the ligand molecule itself. As in the case of phenylalanine ammonia-lyase discussed above, the resultant binding strengths would be comparable, and enantioselectivity would get significantly reduced. It follows that the (1-2) configuration of ligand *locations* would likewise be problematic, with respect to both an enantiomeric pair and a diastereomeric pair with opposite stereochemistry at C_I. Clearly, a receptor needs to interact with more than three *locations* on a ligand with two stereocenters, in order to ensure stereoselectivity.

Fig. 5. 15 takes into consideration four ligand *locations* interacting with the receptor. If these *locations* are distributed in a (3-1) configuration (Figs. 5. 15a,b), the receptor still fails to distinguish between the two diastereomers that have opposite stereochemistry at C_{II}. Likewise, the (1-3) distribution of *locations* (not shown in Fig. 5. 14) would fail to recognize the stereochemistry at C_I. However, distributing these four *locations* in a (2-2) configuration on one ligand stereoisomer (two *locations* directly attached to C_I and two attached to C_{II}; Fig. 5. 15c) results in a unique recognition of that stereoisomer, and both the enantiomer (Fig. 5. 15d) and the diastereomers (Figs. 5. 15e,f) may be distinguished. Therefore, the SR model concludes that selectivity towards one out of four possible stereoisomers of a ligand with two stereocenters requires a receptor to interact with a minimum of four ligand *locations*, distributed in a (2-2) configuration on the two stereocenters.

An important caveat regarding the bound orientation of the ligand needs to be added. The geometry of saturated carbon atoms can result in four or more points in a molecule coming to lie on the same plane. This is due to the possibility of rotation about carbon-carbon bonds, with a particular rotamer conformation being energetically preferred over others. If all four *locations* in the (2-2) configuration on the two stereocenters can be brought into a coplanar arrangement, a theoretical possibility exists for mirror image packing of a pair of enantiomers. A loss or reduction of stereoselectivity may therefore be expected. This may be possible both with a staggered conformation of the ligand, with the two stereocenters lying on opposite sides of the plane determined by these four *locations* (Fig. 5. 16a), or in an eclipsed conformation, with the two stereocenters lying on the same side of this plane (Fig. 5. 16b). Therefore,

given a (2-2) configuration of ligand *locations*, a stereoselective receptor has to impose structural conditions preventing the binding of one of the possible mirror image orientations, and/or stabilize a ligand rotamer conformation in which the four *locations* involved are in a *non-coplanar* arrangement. If neither condition can be satisfied in a particular ligand-receptor system, additional interactions involving a fifth or sixth ligand *location* may be necessary for stereoselectivity. Similarly, when the two stereocenters are not adjacent to each other, the possibility of bond rotations resulting in conformational flexibility would mean that interactions with more than four ligand *locations* might be necessary to determine receptor stereoselectivity.

The requirement of distributing four ligand *locations* in a (2-2) configuration on two stereocenters (Fig. 5. 17a) may be explained as a logical extension of the minimum requirement of three *locations* for a ligand with a single chiral center. The (2-2) configuration of *locations* on a ligand that has two stereocenters means that each stereocenter has two *locations* directly attached to it. In addition, all *locations* on C_{II} effectively act together as the third *location* on C_I (Fig. 5. 17b) as they are attached indirectly to C_I *via* C_{II}. Similarly, all *locations* on C_I effectively act together as the third *location* on C_{II} (Fig. 5. 17c). Thus, a stereoselective receptor has to effectively interact with at least three *locations* on each stereocenter in the ligand. This is not possible with four ligand *locations* distributed in the (3-1) or the (1-3) configurations. A higher number of ligand *locations*, distributed in the (2-3) or (3-2) or (3-3) configurations will also lead effectively to at least three *locations* on each stereocenter, and thus result in stereoselectivity. How this model coherently explains previously reported experimental findings from three different systems is demonstrated below.

Example 1: Metal-dependent stereoselectivity of isocitrate dehydrogenase

The NADP-dependent enzyme isocitrate dehydrogenase (IDH) from *E. coli* selectively catalyzes the conversion of (2R,3S)-isocitrate (the D-isomer) to α-ketoglutarate, in the presence of Mg^{2+}. Mesecar and Koshland (2000a) report that in the absence of Mg^{2+}, only (2S,3R)-isocitrate (the L-isomer) binds to the enzyme active site but catalytic activity is lost. These researchers propose the four location (FL) model (2000b), based on their interpretation that three groups attached to the C2 atom of D- and L-isocitrate bind to the same enzyme residues in IDH, but the fourth group on the C2 carbon (–OH) binds differently in the two cases.

Fig. 5. 18 shows stereoviews of the crystal structures of D- and L-isocitrate bound in the active site of IDH, in the presence and absence of Mg^{2+} respectively, superposed on each other (Mesecar and Koshland 2000b). The four groups attached to the C2 carbon of isocitrate are –H, the C3 carbon atom, $–COO^-$ and –OH. In the absence of metal ions, the $–COO^-$ group binds to the same Arg129 residue as in the presence of metal ions, but it should be noted that this is possible only because of the flexibility of the side chain of arginine. The –OH group binds to the metal ion in its presence and to an arginine residue in its absence. The substituents at the C3 carbon interact with the same enzyme residues in both cases. There are no direct interactions of enzyme residues or water molecules with the –H atom. During catalysis, it is abstracted by NADP, which is not present in the crystal structures of the metal-free enzyme bound to L-isocitrate and the metal-containing enzyme bound to D-isocitrate. A comparison of the enzyme-substrate complexes in the presence and absence of Mg^{2+} shows that the –H atom on the C2 carbon occupies a very similar position with respect to that of NADP modeled onto the crystal structure.

However, the use of the D/L nomenclature is misleading for a molecule like isocitrate, which has two stereocenters. The FL model proposed by Mesecar and Koshland (2000b) is based on mirror image binding geometries of a molecule that has a single chiral center (Fig. 5. 4), and fails to explain the metal-ion dependent stereoselectivity characteristics of IDH. The observed reversal of stereoselectivity is better explained through the SR model for ligands with two stereocenters. The interactions at the C2 and C3 stereocenters of isocitrate involve four *locations*, in a (2-2) configuration (Fig. 5. 19a). These are the –OH and the $-C_{\alpha}OO^{-}$ groups attached to the C2 carbon and the $-C_{\beta}OO^{-}$ and $-CH_2C_{\gamma}OO^{-}$ groups attached to the C3 carbon. In both the stereoisomers of isocitrate that have been studied [(2R,3S) and (2S,3R)], the C2 carbon has effectively three *locations* interacting with the receptor. In addition to the two *locations* directly attached to the C2 carbon, the two *locations* attached to the C3 carbon in isocitrate together act as an effective third *location*. These enter into interactions with specific enzyme residues in such a manner that the –H group on the C2 carbon and the C3 carbon both occupy almost identical spatial positions in both cases. No direct interactions of the –H atom have been observed with enzyme residues, while the position of NADP has only been modeled onto the crystal structures. The bond between the C2 carbon and the –H group is oriented in mirror image conformations in the two enantiomers, which may explain the lack of catalytic activity on L-isocitrate. In an idealized view, the plane determined by the –H atom, the carbon atom of the $-C_{\alpha}OO^{-}$ group and the C3 carbon atom therefore act as a mirror plane relating the two bound stereoisomers, with the C2 carbon atom lying on opposite sides (Fig. 5. 19b).

It should be noted that the (2R,3S) and (2S,3R) stereoisomers bind in orientations that ensure a non-coplanar arrangement of the four *locations* in isocitrate. Three of these *locations* bind to the same sets of residues in both metal-free and metal-containing enzymes. These are the two *locations* on the C3 carbon (the $-C_{\beta}OO^{-}$ and $-CH_2C_{\gamma}OO^{-}$ groups) and one *location* on the C2 carbon (the $-C_{\alpha}OO^{-}$ group). Only the binding of the –OH group on the C2 carbon takes place in a metal-ion dependent manner (Figs. 5. 19c,d). In the presence of Mg^{2+}, the –OH group of (2R,3S)-isocitrate binds strongly to the metal ion. The –OH group of the (2S,3R) isomer of isocitrate would be in an orientation that only allows binding to the Arg119 residue. This isomer is therefore not seen in the IDH binding site in the presence of Mg^{2+}. In the metal-free enzyme, the –OH group of (2S,3R)-isocitrate binds to Arg119, but in this case, there is no receptor group to bind to the –OH group of the (2R,3S) stereoisomer. Thus, the metal-containing enzyme binds exclusively to (2R,3S)-isocitrate, and the metal-free enzyme to (2S,3R)-isocitrate. In both cases, interactions with four *locations*, in a (2,2) configuration and a non-coplanar geometry, determine the observed patterns of binding stereoselectivity.

It is interesting to note that the two isocitrate stereoisomers bind to IDH in opposite orientations at the C2 carbon, while interacting identically at the C3 carbon. To elaborate, both the R and S configurations of the C3 carbon result in the same binding patterns for both *locations* on that stereocenter. However, with respect to the C2 carbon, the presence or absence of the metal ion results in the enzyme selecting for the R or S configuration respectively. This is a consequence of the conformational flexibility possible in the isocitrate molecule. The idealized picture of the binding interactions shown in Fig. 5. 19b may therefore be substituted by the following one. A hypothetical

plane may be drawn through (a) the carbon atom of the $-C_{\alpha}OO^{-}$ group, (b) the –H group on the C2 carbon, (c) the carbon atom of the $-C_{\beta}OO^{-}$ group, and (d) the methylene carbon atom of the $-CH_2C_{\gamma}OO^{-}$ group. If both (2R,3S)- and (2S,3R)-isocitrate were theoretically docked into the enzyme binding cavity simultaneously, this plane would be a mirror plane that relates the two stereoisomers. In the (2R,3S) stereoisomer, the C3 carbon and its –H group lie to the left of this mirror plane, but the C2 carbon and the –OH group on it lie to the right, facilitating binding to the metal ion. On the other hand, in the (2S,3R) isomer, the C3 carbon and its –H group lie to the right of the mirror plane, but the C2 carbon and the –OH group on it lie to the left, which allows binding to the Arg119 residue (Fig. 5. 20). The groups on the plane remain in the same positions, which allows the $-C_{\alpha}OO^{-}$ and $-C_{\beta}OO^{-}$ groups to bind to the same enzyme residues in both cases. However, the additional flexibility provided by the $-CH_2-$ group allows the $-C_{\gamma}OO^{-}$ group to lie on the same side of the mirror plane in both cases, thereby facilitating its binding to the same enzyme residues. It is important to note that of the four *locations* that interact with the receptor, the –OH group does not lie on this mirror plane. The –H group on the C2 carbon lies on the mirror plane, but makes no direct interactions with protein residues. Thus, the metal-containing enzyme possesses one set of receptor *sites*, which make it stereoselective for the (2R,3S) stereoisomer, while the metal-free enzyme has a different set of *sites*, and is stereoselective for the (2S,3R) stereoisomer.

Only the binding of the naturally occurring (2R,3S) stereoisomer of isocitrate and its (2S,3R) enantiomer have been hitherto studied, and in the absence of NADP, the coenzyme required for catalysis. IDH catalyzes a dehydrogenation reaction at the C2 carbon, to convert isocitrate to oxalosuccinate, and a second decarboxylation reaction at

the C3 carbon, which converts oxalosuccinate to α-ketoglutarate. Each step converts one chiral carbon center to an achiral one. It is therefore necessary to investigate whether the (2S,3R) stereoisomer that binds to the enzyme in the absence of metal ions undergoes catalytic conversion to oxalosuccinate when NADP is present. In the presence of Mg^{2+}, this stereoisomer is not seen in the enzyme active site, but the binding characteristics of the other two isocitrate stereoisomers remain unknown. It is also necessary to study the binding and catalytic behavior of IDH towards all four stereoisomers of isocitrate, in the presence and absence of metal ions, and in the presence and absence of NADP. A more complete picture and better insight into the interactions involved in this system would perhaps be obtained from these studies. Clearly, if the metal ion binds to both *locations* at the C2 carbon of the (2R,3R) stereoisomer of isocitrate, the interaction at one *location* at the C3 carbon would have to be sacrificed. On the other hand, the *locations* at the C3 carbon are chemically similar, involving carboxylate groups ($-C_\beta OO^-$ and $-CH_2C_\gamma OO^-$), and the methylene group provides additional flexibility. This might result in a measurable binding of the (2R,3R) stereoisomer, but in a different rotamer conformation as compared to the (2R,3S) stereoisomer. It may then be postulated that dehydrogenase activity should be observed for the (2R,3R) stereoisomer also. On the other hand, as the presence of metal ions results in selecting for the R configuration at the C2 carbon, there will probably be no measurable binding of the (2S,3S) stereoisomer at the enzyme's active site. However, in the absence of metal ions, the (2S,3S) isomer of isocitrate might effectively compete with the (2S,3R) isomer, in terms of binding to the enzyme, although catalytic activity may not be observed. Crystal structures and kinetic experiments with these two stereoisomers would be necessary to elucidate these issues.

It would also be interesting to study the interactions of all four stereoisomers of isocitrate, in the presence and absence of metal ions and/or NADP, with a bacterial IDH mutant that has the Arg119 residue suitably changed by site directed mutagenesis. This is the group that primarily interacts with the –OH group of (2S,3R)-isocitrate, in the absence of metal ions. The metal-free bacterial mutant would be unable to bind to the hydroxyl group in any of the isocitrate stereoisomers, but the carboxylate groups in isocitrate (distributed in a (1-2) configuration) would still interact with other enzyme residues in the active site. The SR model predicts that such a binding configuration resulting from this mutation would result in loss of binding stereoselectivity, with respect to the C2 carbon of isocitrate. In the presence of Mg^{2+}, binding stereoselectivity towards (2R,3S)-isocitrate would still be retained. However, it is more difficult to predict the effect of replacing Arg119 on the catalytic activity of bacterial IDH. It has been shown that mutating homologous arginine residues in rat IDH (Jennings et al. 1997) and porcine IDH (Soundar et al. 2000) results in appreciable loss of catalytic activity.

Example 2: Drug action of (1R,2S)-α-methylnoradrenaline

The (1R,2S) stereoisomer of α-methylnoradrenaline binds selectively to α_2-adrenergic receptors, and has greater drug potency than (1R)-noradrenaline. However, for α_1-adrenergic receptors, (1R,2S)-α-methylnoradrenaline is equipotent with (1R)-noradrenaline. This difference in the drug response of these receptors has been explained in terms of four interactions of (1R,2S)-α-methylnoradrenaline with α_2-adrenergic receptors, as opposed to three interactions with α_1-receptors. Rufollo (1983) postulates

that the α-methyl group in the preferred stereoisomer binds to a hydrophobic site in the α_2-receptor. Triggle (1976) however postulates only that the presence of the α-methyl group sterically alters the binding of the α_2-receptor to the three polar groups in the drug molecule (amine, catechol and β-hydroxyl groups). In either case, the binding of (1R,2S)-α-methylnoradrenaline to α_2-receptors involves four ligand *locations* in a (2-2) configuration. These are the amine and α-methyl groups attached to one stereocenter in the molecule, and the β-hydroxyl and catechol groups on the second stereocenter (Fig. 5. 21a). However, α_1-receptors do not seem to offer any interaction with the α-methyl group of the ligand, binding only to the other three ligand *locations*, in a (2-1) configuration (Fig. 5. 21b). Therefore, for α_1-receptors, the potency of (1R,2S)-α-methylnoradrenaline, a drug molecule with two stereocenters, is comparable to that of (1R)-noradrenaline, a molecule with a single stereocenter. Many other drug molecules have structures analogous to noradrenaline, and their differential action at various types of adrenergic receptors may be explained similarly.

Example 3: Inactivation of carboxypeptidase A by 2-benzyl-3,4-epoxybutanoic acid

The (2S,3R) and (2R,3S) stereoisomers of 2-benzyl-3,4-epoxybutanoic acid (Fig. 5. 22) are highly efficient and fast acting inactivators of carboxypeptidase A, while the (2S,3S) and (2R,3R) stereoisomers do not exhibit any irreversible inhibitory activity (Lee et al. 1995). Crystal structures indicate that both the (2S,3R) and (2R,3S) stereoisomers of this molecule inactivate the enzyme through the formation of a covalent complex. An ester bond is formed between the C4 carbon and a carboxylate oxygen in the Glu270

residue of carboxypeptidase A (Yun et al. 1992; Ryu et al. 1997). The epoxy oxygen atom gets converted to a –OH group on the C3 carbon, and is in a position to coordinate to the Zn^{2+} ion in the enzyme. In carboxypeptidase A, both Glu270 and Zn^{2+} are involved in substrate binding (Fig. 5. 8a), so that the covalent bond formation with 2-benzyl-3,4-epoxybutanoic acid inactivates the enzyme irreversibly. In this case too, crystal structures reveal that the (2R,3S) and (2S,3R) stereoisomers of this molecule bind in mirror image orientations (Fig. 5. 22a-c). The C2 and C3 carbon atoms lie on opposite sides of a plane determined by the C4 carbon, the oxygen atom attached to C3, the carbon of the $–COO^-$ group and the benzylic methylene carbon. Thus, in both cases, the –OH group generated on the C3 atom can coordinate Zn^{2+}, and an ester bond can be formed between the carboxylate of Glu270 and the C4 carbon. The $–COO^-$ group on the C2 carbon atom is stabilized by Arg145 and the phenyl ring fits into a binding pocket formed by hydrophobic residues in the enzyme. In this example, it is important to note that the four *locations* on the inactivating molecule that bind to enzyme sites lie on the same plane, in a staggered rotamer conformation. The two chiral carbon atoms lie on opposite sides, so that this plane would be a mirror plane relating the (2R,3S) and the (2S,3R) stereoisomers, if they are docked into the enzyme binding cavity simultaneously. Therefore, both stereoisomers are able to covalently modify the active site and thereby inactivate the enzyme. For the (2R,3R) and (2S,3S) stereoisomers of 2-benzyl-3,4-epoxybutanoic acid (Fig. 5. 22d), a coplanar arrangement of these four *locations* would only be possible in an unfavorable eclipsed conformation, with the *locations* on the C3 carbon positioned farther away from those on the C2 carbon. As these isomers do not

inactivate carboxypeptidase A, it may be concluded that in these two cases, simultaneous interactions of all four *locations* with corresponding *sites* in the enzyme are disfavored.

It is important to note that although the (2S,3R) and (2R,3S) stereoisomers bind in mirror image orientations and irreversibly inactivate carboxypeptidase A, their kinetics of covalent bond formation with the Glu270 residue in the enzyme are measurably different. The inactivation rate constant for the (2S, 3R) stereoisomer is more than twice as large as the inactivation rate constant for the (2R, 3S) stereoisomer (Ryu et al. 1997). This may be compared with the case of phenylalanine ammonia-lyase (Fig. 5. 10), where the two enantiomers of phenylalanine bind to the enzyme active site in mirror image orientations, but with a small difference in the free energy of binding (Hanson 1981). In general, although structural data might suggest mirror image binding orientations for a pair of enantiomers of a ligand to a receptor, the resultant complexes are diastereomeric in nature. The thermodynamics and kinetics of the binding events are not likely to be completely identical to each other. Therefore, in most cases, there would be measurable binding and/or reactive stereoselectivity even when only the minimum number of ligand *locations* is involved in interactions with the receptor.

Ligands with three stereocenters

For ligands with three stereocenters (C_I, C_{II} and C_{III}), one out of eight possible stereoisomers needs to be preferentially recognized. It is clear that more than four ligand *locations* would have to interact with a receptor, to achieve uniquely stereoselective recognition. It is also clear that to a receptor has to interact with at least one *location* directly attached to each stereocenter in such a ligand, in order to recognize uniquely any

given stereoisomer. Fig. 5. 23 illustrates two of the many ways in which five *locations* can be distributed on three adjacent stereocenters in a linear chain, such that there is at least one *location* directly attached to each stereocenter interacting with the receptor. As in the case of ligands with two stereocenters, the conclusions reached below may be extended to the case where the three stereocenters are not adjacent. The (2-2-1) configuration of ligand *locations* results in the same set of interactions for the two diastereomers involving different stereochemistry at C_{III} (Figs. 5. 23a,b). The (1-2-2) configuration (not shown in Fig. 5. 23) would lead to similar results with respect to the stereochemistry at C_I. However, distributing five ligand *locations* in a (2-1-2) configuration can resolve any pair of stereoisomers of the ligand (Figs. 5. 23c,d). Thus, a minimum of five *locations*, distributed in the (2-1-2) configuration, is necessary for the unique stereoselective recognition of a ligand with three stereocenters. It would probably be more difficult to bring five different *locations* distributed over three stereocenters into a coplanar arrangement, as compared to four *locations* on ligands with two stereocenters. In the general case, the probability of such a binding geometry would depend on the preferred rotamer conformation at each stereocenter in the bound ligand. In cases where a coplanar arrangement is possible, and in cases where the three stereocenters are distributed farther apart in the molecule, giving rise to additional degrees of freedom, interactions with additional ligand *locations* on any of the three stereocenters would be necessary to result in stereoselectivity.

It may be noted that two *locations* have to be directly attached to each of the two terminal stereocenters (C_I and C_{III}), whereas one *location* is needed on the inner stereocenter (C_{II}). This can be explained on the basis of the molecular connectivity of the

ligand (Fig. 5. 24). All *locations* on C_{II} and C_{III}, taken together, effectively act as a single *location* with respect to the stereocenter C_I. Similarly, all *locations* on C_I and C_{II} effectively act together as a single *location* on C_{III}. However, for the inner stereocenter C_{II}, all *locations* on C_I effectively act together as one *location*, while all *locations* on C_{III} effectively form a second *location*. The stereoselectivity requirement of a (2-1-2) configuration for ligands with three stereocenters thus implies that each stereocenter always has effectively three *locations* interacting with the receptor. This is consistent with the requirement of three *locations* in a ligand with a single chiral center.

Generalizations for ligands with multiple stereocenters

The stereocenter-recognition (SR) model can now be generalized for ligands with multiple stereocenters. Molecules with *N* stereocenters distributed in acyclic structures are examined below, by defining terms according to topological theory. An acyclic molecule with multiple stereocenters can be represented as a **tree**, consisting of **nodes**, connected by **edges**. For the first level of approximation, the non-stereogenic primary and secondary carbon atoms and the substituents on the chiral centers can simply be excluded in this tree representation. This would result in ignoring the exact chemical structure of the molecule in between two consecutive stereocenters, which would then get represented as adjacent nodes in the tree. However, this would be justified in an attempt to count the *minimum* number of interactions required for stereoselectivity. In cases where the flexibility of the segment of the molecule between two stereocenters should be an important consideration, additional requirements would be necessary, but each such molecule would be unique and would have to be investigated separately. Unlike the non-

stereogenic primary and secondary carbons, if stereocenters are distributed on different branches in a molecule, the tertiary and quarternary carbon atoms that connect the various branches should be included in this representation, even if they are not themselves stereocenters. This is because such branch points determine the connectivity and distribution of stereocenters in the molecule. Similarly, if a heteroatom links three or more branches, each branch containing stereocenters, such a heteroatom should also be included in the tree representation. Thus, two different kinds of nodes may be distinguished in the tree. The stereocenters in the molecule may be called the **fundamental nodes** in the tree, while the other atoms that have to be included in order to determine the connectivity pattern of the stereocenters represent **auxiliary nodes**. It should be noted that a terminal node in the tree need not correspond to a terminal carbon atom in the molecule and that two adjacent nodes in the tree are not necessarily adjacent in the molecule itself. Correspondingly, an edge that connects two adjacent nodes in the tree does not necessarily correspond to carbon-carbon bonds in the molecular structure. The number of edges connected to a node determines its **degree**. Terminal nodes are connected only to one edge in the tree, and are first-degree nodes. Nodes that connect two edges in the tree are second-degree nodes, while higher degree nodes are connected to more than two edges, and are branch points. First-degree and second-degree nodes are always fundamental nodes, while third and fourth-degree nodes may be either fundamental or auxiliary nodes. The highest possible degree for any node in the tree is four, and the number of nodes of degree i in the tree is given by n_i, where $i = 1-4$. As

only the fundamental nodes are stereocenters, in the general case, the number of stereocenters in the molecule, $N \leq \sum n_i$.

The simplest case is when all stereocenters are distributed along a single linear chain in the molecule, i.e. the tree representation has no nodes of degree three or four. Some representative examples are shown in Fig. 5. 25. In this case, $n_1 = 2$, $n_2 \geq 0$, $n_3 = n_4 = 0$, and $N = n_1 + n_2$. The two first-degree nodes (the two terminal stereocenters) are analogous to the C_I and C_{III} stereocenters in ligands with three stereocenters as discussed above, and all second-degree nodes are analogous to the C_{II} stereocenter. A minimum of N + 2 *locations,* distributed in the (2-1-1-...1-2) configuration, would therefore be necessary for stereoselective recognition. This ensures that each stereocenter has effectively three *locations* interacting with the receptor. It may be noted that this conclusion would hold true not only for all linear molecules but also for any branched molecule, so long as all the stereocenters are distributed along the same linear chain. When stereocenters are distributed in different branches, the terminal stereocenter in each branch requires interactions at two ligand *locations*, while the inner stereocenters in each branch would require one *location* each. All the *locations* on each branch would act effectively together as one *location* with respect to the node that connects the different branches. In the ideal case, if a branch point were a fundamental third-degree node, the minimum requirement of three effective *locations* for the corresponding stereocenter in the molecule would be automatically satisfied. Similarly, for a fundamental fourth-degree node, the corresponding stereocenter would already have the maximum number of four effective *locations* interacting with the receptor. Therefore,

no additional constraints need be imposed with respect to it. It follows that for all acyclic ligands, the minimum number of interactions with ligand *locations* to determine stereoselectivity is given by $L = 2n_1 + n_2$. The number of second-degree nodes (n_2) in a tree is variable, but the number of first-degree nodes (n_1) can be related to the number of third-degree nodes (n_3) and fourth-degree nodes (n_4) by a simple topological analysis. An unbranched tree has $n_1 = 2$. In a branched tree, each third-degree node contributes an additional first-degree node, while each fourth-degree node contributes two additional first-degree nodes, so that $n_1 = n_3 + 2n_4 + 2$. Therefore, we define $n' = n_1 + n_2 + n_3 + 2n_4 = n_4 + \sum n_i$. In order for stereoselectivity to occur, the minimum number of ligand *locations* interacting with a receptor should be $L = 2n_1 + n_2 = n_1 + n_2 + (n_3 + 2n_4 + 2) = n' + 2$.

The variable n' builds into it information about the number of stereocenters in the molecule as well as the structure of the molecule. Note that in the most general case, $n' \geq N$, so that the minimum number of ligand *locations* that is necessary to determine stereoselectivity depends not only on the number of stereocenters, but also on their distribution in the overall structure of the molecule. In specific cases, interactions with a higher number of ligand *locations* might be necessary for stereoselectivity. One reason would be the possibility of bringing more than three *locations* in the molecule into coplanar arrangements. With increasing *N* however, it would be increasingly difficult to constrain all $n' + 2$ *locations* in a molecule in a coplanar arrangement, so that the need for additional constraints is likely to be more significant for acyclic molecules that have a small number of stereocenters or for a smaller subset of stereocenters in a large acyclic

molecule with multiple stereocenters. Interactions with a larger number of ligand locations may also be necessary in a case where two adjacent nodes in a tree representation do not correspond to adjacent stereocenters in the corresponding molecule, but are actually separated by one or more intervening atoms. As already noted earlier in this discussion, even the flexibility offered by a single methylene group can have a significant influence on the bound conformation of the ligand, so that stereoselectivity requirements might call for more interactions than the minimum postulated above.

A ligand that has multiple stereocenters distributed in cyclic structures cannot be represented as a tree, but further generalizations of the above analysis can be explored through a graph representation. A preliminary Gedanken experiment is presented below. None of the stereocenters in a ring can be a first-degree node, because of the cyclicity of the molecule. In the simplest case, all stereocenters in a ring would be second-degree nodes, and a stereoselective receptor would have to interact with at least one *location* on each such stereocenter. This would suggest that for a molecule with N stereocenters distributed in a simple ring, interactions with the receptor at a minimum of N ligand *locations* are necessary to determine stereoselectivity. Experimental observations of sugar-binding proteins may be cited here, to gain more insight into the behavior of real systems. In the case of L-arabinose binding to arabinose binding protein, and in D-glucose/D-galactose binding to glucose/galactose binding protein (Fig. 5. 7), crystal structures (Quiocho and Vyas 1984; Vyas et al. 1988) show that each –OH group in the β-anomer of the sugar interacts with water molecules and with different protein residues, through the formation of hydrogen bonds. There are as many –OH groups as there are stereocenters in the ring, so that each hydroxyl group forms one ligand *location*. In

addition, the oxygen atom in the pyranose ring of the sugar also forms hydrogen bonds with protein residues and with water molecules, so that the total number of ligand *locations* interacting with the receptor in each case is $N + 1$. This is one more than the minimum number of *locations* predicted above, and may be explained as follows. Cyclic structures have certain preferred conformations (e.g., pyranose and furanose forms of sugars), with ligand *locations* occupying specific axial or equatorial positions with respect to the ring. However, it is fairly easy to interconvert the α- and β- forms of the pyranose ring, so that in solution, the sugar molecule usually exists as an equilibrium mixture of anomers, in which the stereochemistry of one carbon atom in the ring is inverted. The interaction of the ring oxygen with protein residues would result in additional stabilization of the anomer that is bound to the protein, and may enhance the stereoselectivity of the receptor. Stereochemical requirements for bicyclic structures and fused rings may be expected to be more complicated. An extension of the SR model to cover these complex structures is not attempted here, but would be of great significance for drug design and for understanding interactions of proteins receptors with hormones, steroids, toxins and other biologically important molecules.

Conclusions

The proposed stereocenter-recognition (SR) model for ligand-receptor stereoselectivity differs from previously proposed models in three significant ways. Firstly, it provides general principles for the selective recognition of ligands with multiple stereocenters, taking into account the minimum number of ligand *locations* at each stereocenter necessary for recognizing the stereochemistry at that center. The

widely cited three-point interaction model has been shown to be limited in its application to molecules with a single chiral center. The TPI model is a special case of the SR model proposed here. For molecules with multiple stereocenters, the SR model introduces the concept of three "effective" interactions per stereocenter, taking into account the number of such centers and their topological distribution. Secondly, a general description of ligand *location*, defined according to sound stereochemical principles, has been adopted. As carbon is tetravalent, each stereocenter has a maximum of four *locations* attached to it. In the context of ligand-receptor interactions, ligand *locations* include not only functional groups entering into favorable binding interactions with a receptor, but also groups that can potentially enter into unfavorable interactions such as repulsion and steric hindrance. Finally, in the SR model, a receptor *site* can be either a specific binding functionality or a morphological feature involving a large part of the receptor's surface, interacting with one or more ligand *locations*. Therefore, the total number of receptor *sites* interacting with a ligand can be different from the total number of ligand *locations* that enter into these interactions. As each ligand *location* can typically enter into multiple interactions, not all of which need to be binding in nature, the number of identifiable "points of attachment" can be different from the *minimum* number of ligand *locations* required to determine stereoselectivity. A receptor that is stereoselective has to offer at least as many interactions as the minimum number of ligand *locations* required for unique recognition. Finally, although the SR model has been discussed largely in terms of binding stereoselectivity, it can equally well be applied to other situations, such as enzymatic catalysis or signal transduction in immunological and neurological pathways. Finally, it should be noted that the number of stereoisomers increases

exponentially (2^N) with N, the number of stereocenters in the molecule, but the minimum required number of interactions with ligand *locations* increases only linearly with N.

The SR model has potential uses in a large number of applications. If the three-dimensional structure of a receptor and its naturally binding ligand are known, the model may be used to rationally design unnatural substrates, inhibitors or drug molecules. The observation that enantiomers may bind to the same protein residues, but in mirror image orientations, can be exploited to investigate a larger pool of potential candidates as drugs or inhibitors for known pharmacological targets. Specific binding sites in proteins can be identified and targeted for mutagenesis, in order to increase or even reverse native selectivities, and thereby obtain tailor-made stereoselectivity profiles. The SR model may also be applied to the design of artificial biomimetic receptors for a targeted stereoisomer of a molecule with multiple stereocenters and perhaps to the *de novo* design of proteins with desired stereoselectivity characteristics.

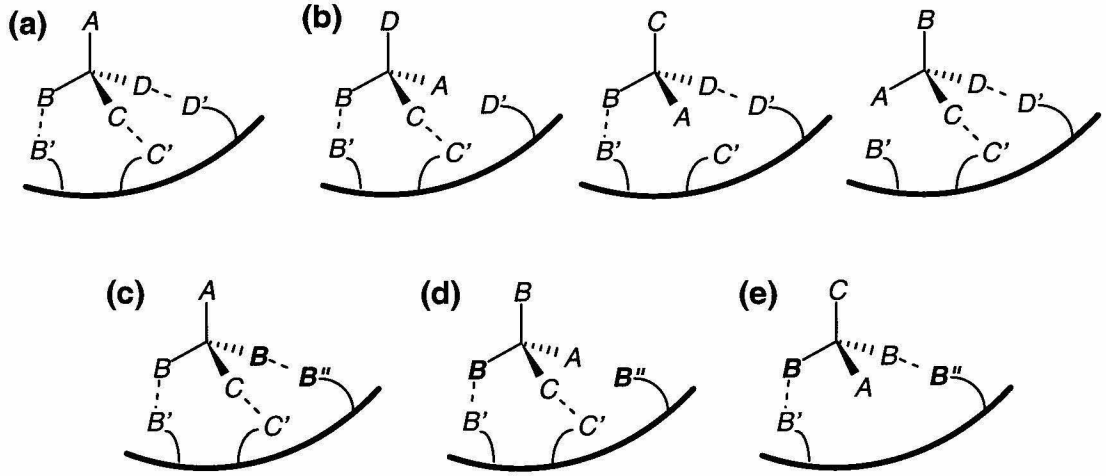

Figure 5. 1. The three-point attachment (TPA) model. **(a)** Groups *B*, *C* and *D* of one enantiomer simultaneously bind to corresponding receptor sites *B'*, *C'* and *D'*. **(b)** In the opposite enantiomer, only two out of the same three groups can bind to their corresponding sites in the receptor, but the third group is unable to bind to its corresponding receptor site. **(c)** Two enantiotopic groups (*B* and ***B***) of a prochiral molecule bind to distinct sites *B'* and ***B"***, while group *C* binds to the receptor at *C'*. If only one of the two sites, *B'* and ***B"***, is a catalytic site in an enzyme, the reaction will proceed in an enantiospecific manner. **(d)** If ***B*** binds at *B'*, then *B* cannot simultaneously bind at ***B"***, so long as the molecule is also anchored at *C'*. **(e)** In the absence of the third binding site (*C'*) in the receptor, resulting in a two-point binding, there will be a loss of enantiospecificity, as ***B*** can bind to *B'*, while *B* can simultaneously bind to ***B"***. Thus, a two-point interaction will not result in an enantiospecific reaction.

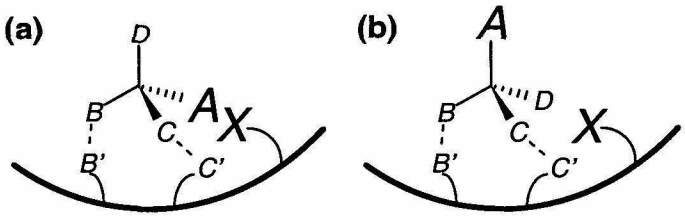

Figure 5. 2. The influence of non-binding interactions. A steric interaction is shown here. **(a)** Groups *B* and *C* on the ligand bind to sites *B'* and *C'* on the receptor, but the bulky group *A* faces steric hindrance from some bulky group *X* in the receptor. In the general case, *X* may simply be a topological or morphological feature of the receptor surface, and need not be a specific functional group. **(b)** The opposite enantiomer is still able to bind at *B'* and *C'*, but the group *D* is not sterically hindered by *X*. The absence of steric hindrance would result in stronger binding, and enantioselectivity would be a result of two binding interactions combined with a third non-binding interaction.

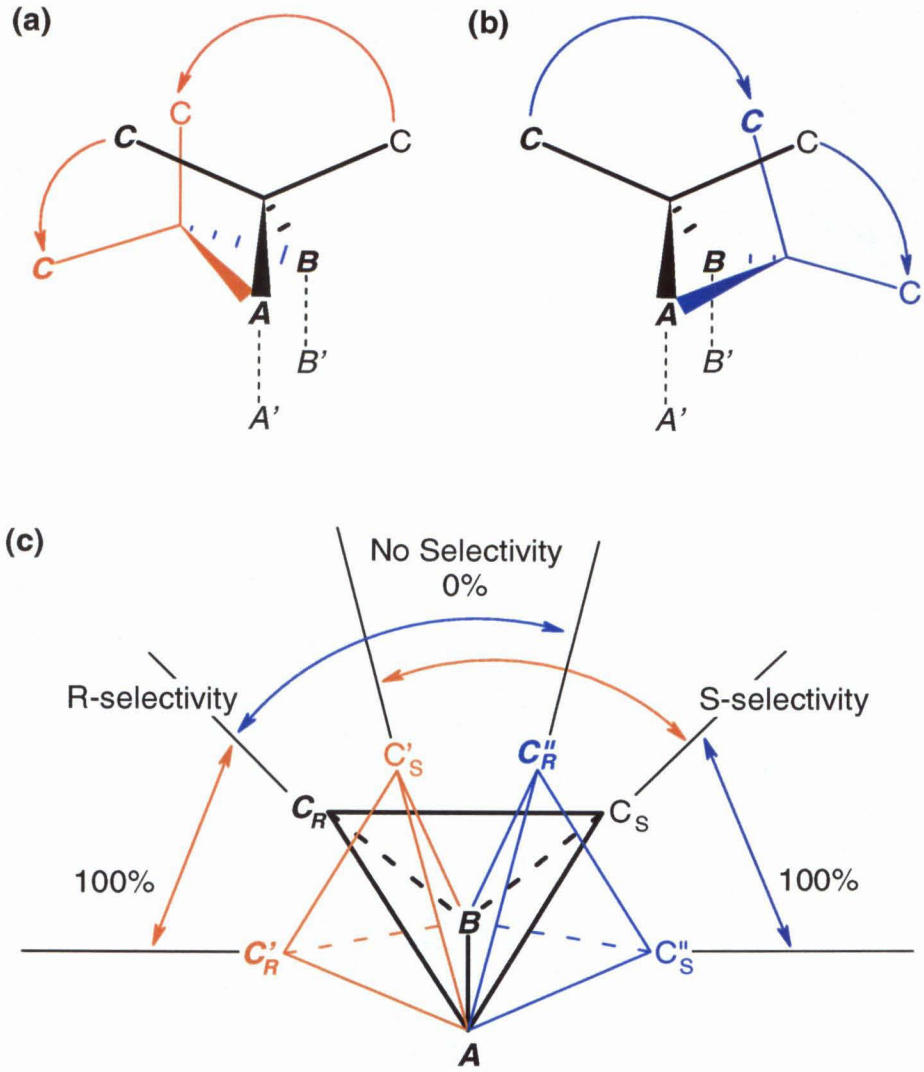

Figure 5. 3. The rocking tetrahedron model. With two-point attachment at groups *A* and *B*, a prochiral molecule can rock either to the left **(a)** or to the right **(b)**, in a pendular motion. The enantiotopic groups are differentiated as plain text and bold-italic text, and the trajectories swept by them are indicated by arrows. The various spatial regions in which different enantioselectivity profiles may be expected are shown in **(c)**, with the enantiotopic groups labeled according to an arbitrarily assigned priority rule $A > B > C$.

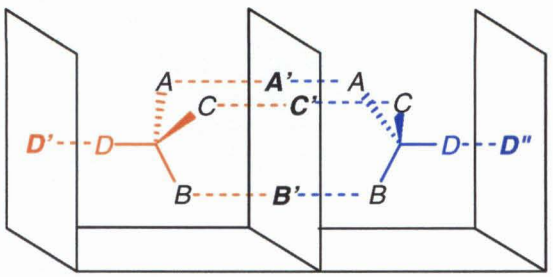

Figure 5. 4. The four location (FL) model. Binding sites, *A'*, *B'* and *C'* are present in a receptor such that two opposite enantiomers of the ligand can bind, but on opposite sides of the same surface. This necessitates the presence of a fourth binding site (*D'* or *D''*), to distinguish between enantiomers. Alternatively, there must be other conditions preventing the approach of the ligand towards one side of the plane determined by the three binding sites in the receptor.

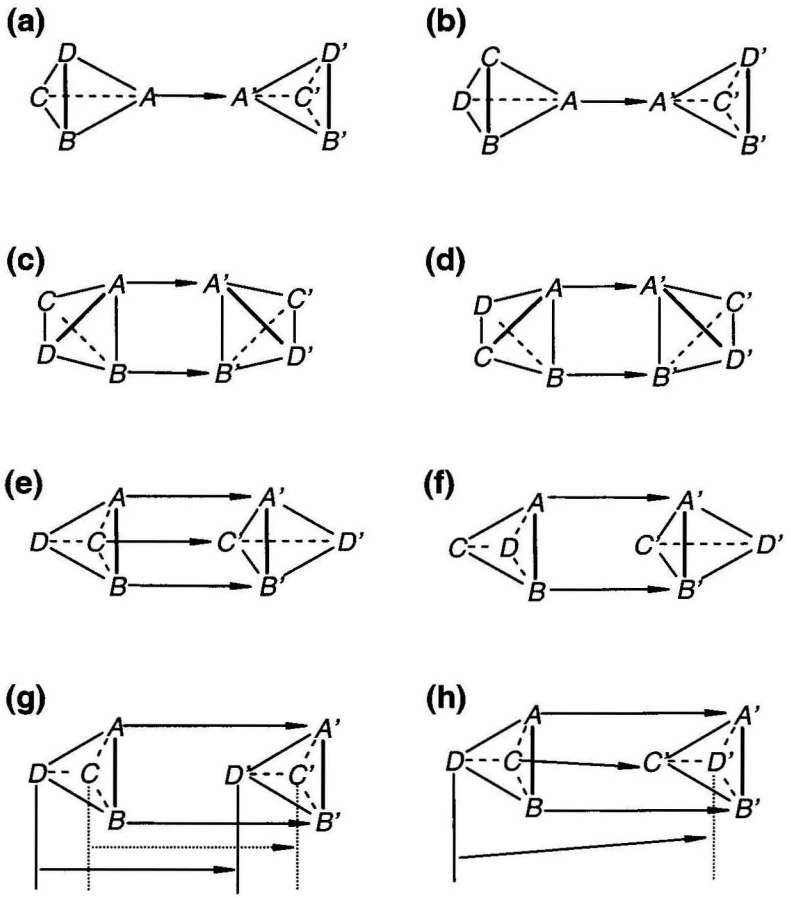

Figure 5. 5. Different kinds of interactions between two asymmetric tetrahedra. Interactions that are purely vertex-to-vertex **(a, b)** or edge-to-edge **(c, d)** are not chirally selective. A face-to-face interaction **(e, f)** allows for chiral recognition (Salem et al. 1987). However, these scenarios implicitly rule out possibilities like vertex-to-face interactions **(g, h)** between two asymmetric tetrahedra. If these are taken into account, all four pairs of vertices in the two tetrahedra have to be formally accounted for (Topiol and Sabio 1989).

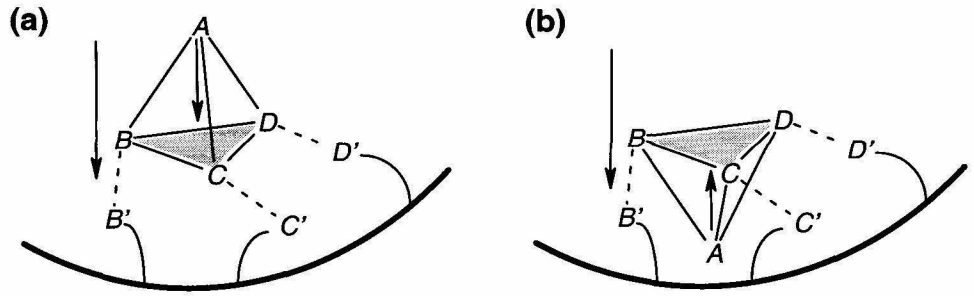

Figure 5. 6. Implicit assumptions in the TPI model: Directionality of approach and bound orientation of the ligand. Vertices *B*, *C* and *D* of a chiral tetrahedron interact with receptor sites *B'*, *C'* and *D'* respectively. In both **(a)** and **(b)**, the arrows outside the tetrahedra show the direction of approach of the ligand molecule towards the receptor surface. The arrows inside the tetrahedra show the normal from vertex *A* to face *BCD*. In **(a)**, the normal to face *BCD* from vertex *A* is aligned along the direction of approach of the ligand. In **(b)**, the normal to face *BCD* from vertex *A* lies opposite to the direction of approach of the ligand towards the receptor surface. In most cases where a TPI model is cited for enantioselectivity, the situation depicted in **(b)** is excluded, usually for steric reasons.

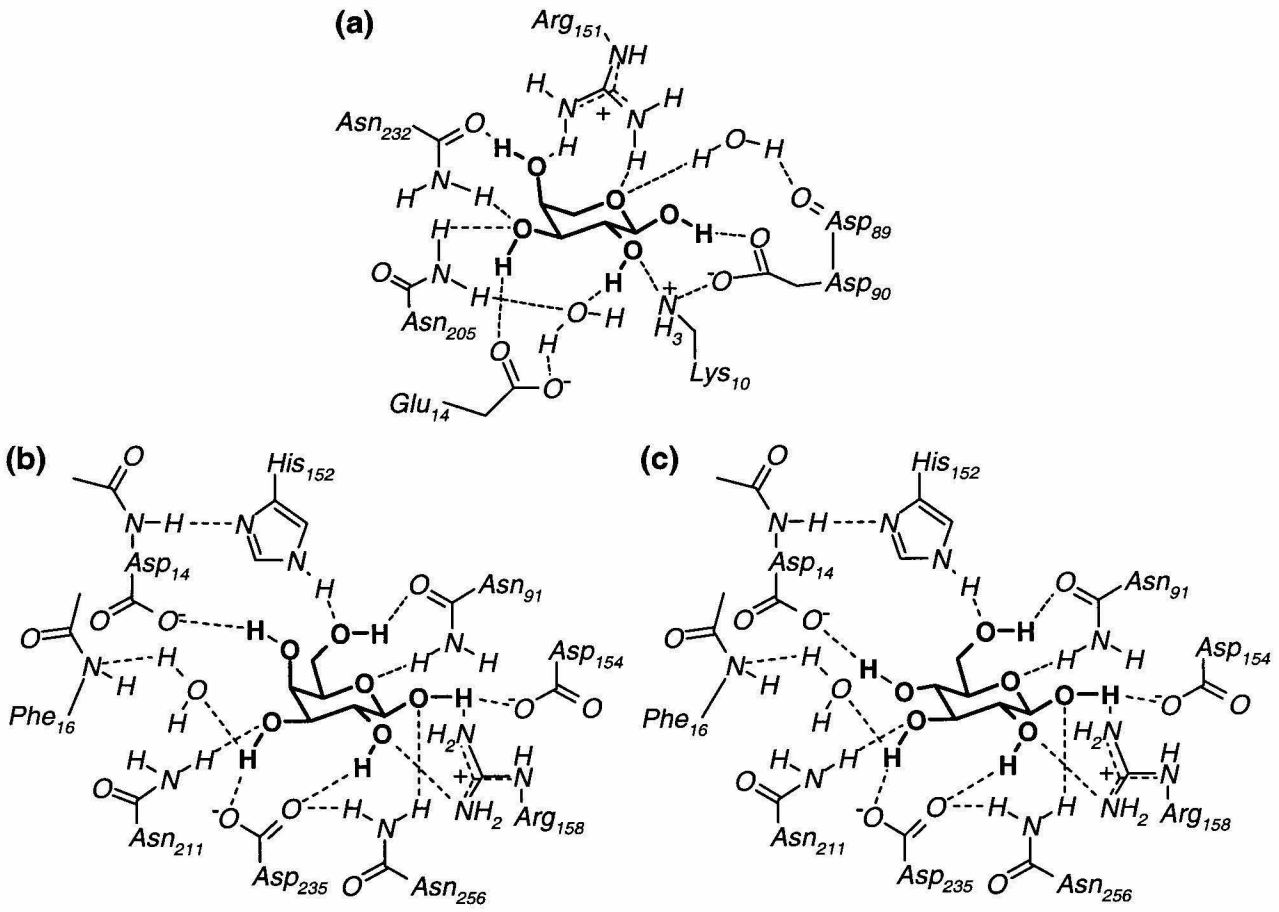

Figure 5. 7. Complexes of sugars bound to sugar binding proteins. **(a)** L-arabinose (four stereocenters) and L-arabinose binding protein (ABP); **(b)** D-galactose (five centers) with galactose/glucose binding protein (GGBP), and **(c)** D-glucose (five centers) with GGBP. In each case, the oxygen atom in the sugar pyranose ring and each hydroxyl residue in the sugar molecule enter into multiple interactions with protein residues and with water molecules in the crystal. D-glucose and D-galactose bind in an almost identical geometry to GGBP, but the epimeric difference at the C4 carbon in the pyranose structure results in a measurable energetic difference in the binding of that –OH group to the Asp14 residue.

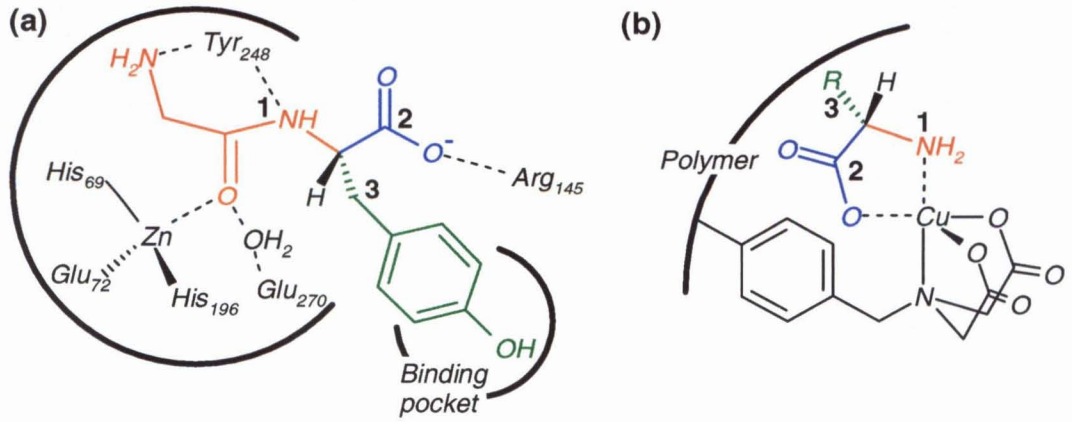

Figure 5. 8. Examples of multiple interactions between ligand *locations* and receptor *sites*. Each ligand *location* is depicted in a single color. **(a)** A single ligand *location* may consist of multiple functional groups, interacting with multiple *sites* distributed over a large surface contour in the receptor. The amide nitrogen, the amide carbonyl and the free amine group in glycyl-L-tyrosine together constitute a single *location*, interacting with Tyr-248, Zn^{2+}, H_2O and Glu-270 in the active site of carboxypeptidase A. **(b)** A single receptor *site* may interact with more than one ligand *location*. The amine and the carboxylate groups in an amino acid constitute two different *locations* attached to the chiral α-carbon, both interacting with the same metal ion through a chelation interaction.

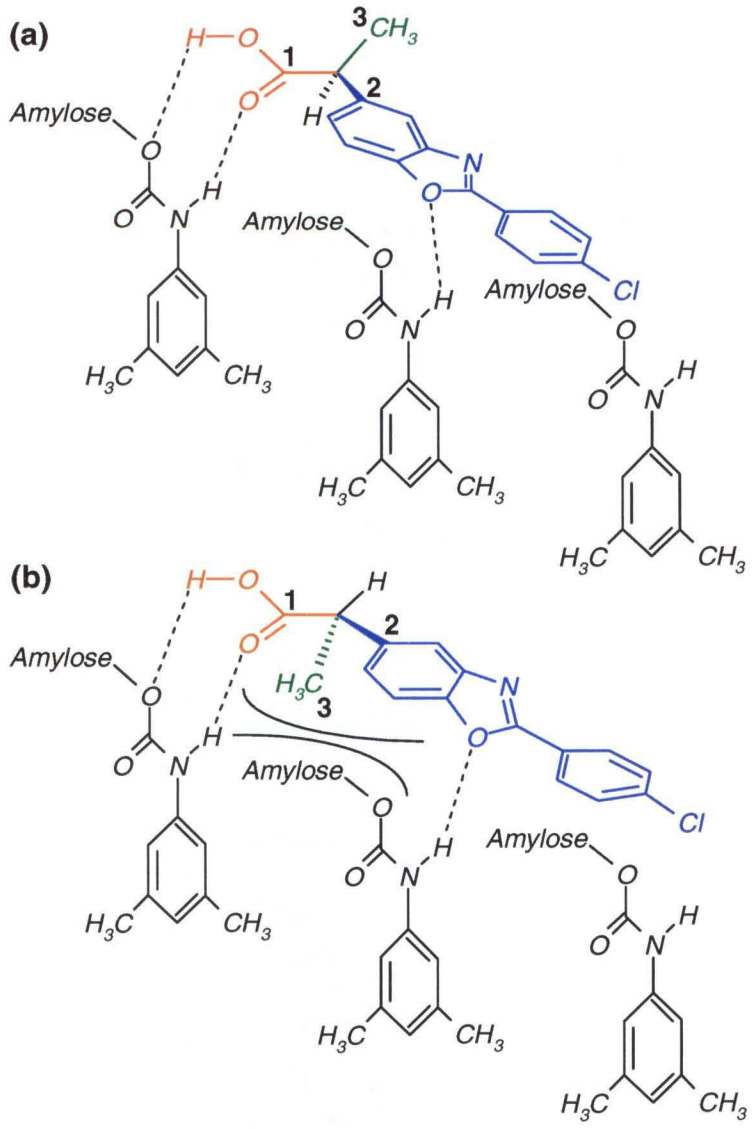

Figure 5. 9. Benaxoprofen separations on an amylose based chiral adsorbent. The binding of S-benaxoprofen **(a)** is energetically favorable, as it is not sterically hindered. The binding of the R enantiomer occurs in a strained conformation, as the methyl group is in a sterically hindered position **(b)**. Thus, steric hindrance destabilizes the overall binding, although the same set of chemical interactions is possible with the adsorbent.

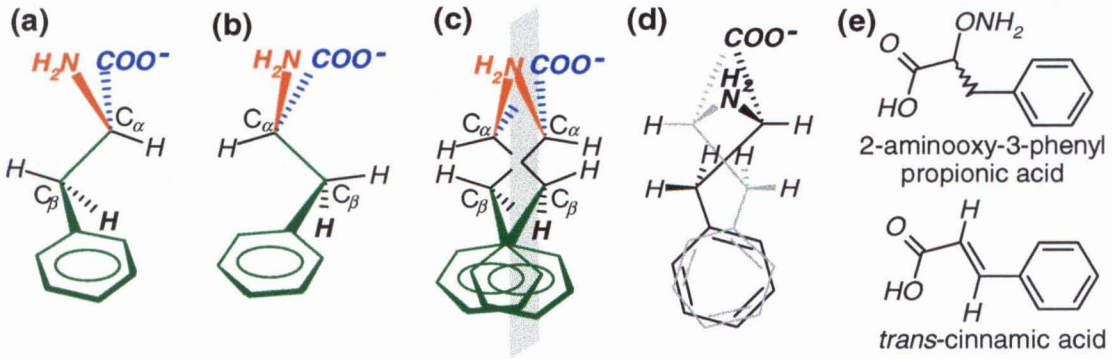

Figure 5. 10. Mirror image packing of enantiomers proposed for phenylalanine ammonia-lyase. The enzyme binds to both L-phenylalanine, the natural susbtrate **(a)**, and D-phenylalanine, an inhibitor **(b)**, with comparable binding strengths (Hanson 1981). If both enantiomers of the amino acid are simultaneously docked into the enzyme binding site, as shown in **(c)**, the following four groups would lie on a hypothetical mirror plane (gray rectangle): the amine nitrogen, the carboxylate carbon, the C_γ carbon atom from the phenyl ring and a hydrogen atom on the methylene carbon. The phenyl rings from both enantiomers would overlap significantly, and in each enantiomer, the chiral carbon atom and the methylene carbon atoms would lie on opposite sides of the mirror plane. **(d)** A better overlap of the phenyl rings can be achieved with slight adjusments in the dihedral angles, so that the hydrogen atom from the methylene group no longer lies on the mirror plane, but retaining the spatial positions of the amine and carboxylate groups. D-phenylalanine is shown in grey, and L-phenylalanine in black. **(e)** Both enantiomers of 2-aminooxy-3-phenylpropionic acid are superinhibitors of the enzyme. Trans-cinammic acid is the reaction product resulting from deamination of L-phenylalanine.

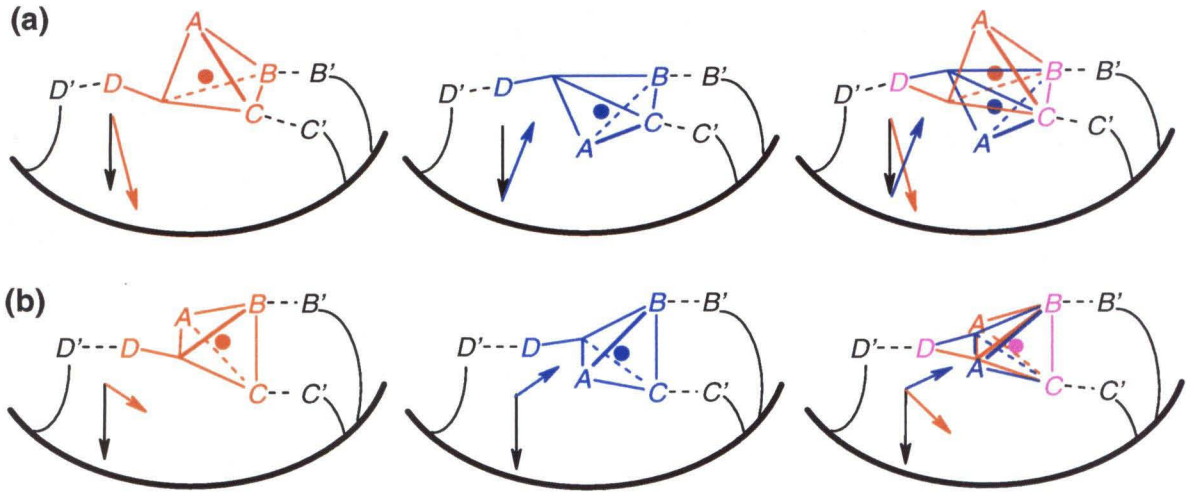

Figure 5. 11. Mirror image orientations of bound ligand enantiomers. The ligand shown has the carbon of a methylene group occupying a vertex of an asymmetric tetrahedron, and further attached to a group *D*. The colored dots show the chiral center in each case, and the colored arrows depict the orientation vectors, determined by the normal from vertex *A* of the tetrahedron to the triangular face determined by *B*, *C* and the methylene carbon. The black arrow shows the direction of approach of the ligand molecule towards the receptor surface, while groups *B*, *C* and *D* determine a mirror plane that relates the spatial coordinates of group A in the two enantiomers. **(a)** The two enantiomers bind in mirror image orientations with the chiral centers at different spatial coordinates. The respective orientation vectors have positive or negative components along the direction of approach, as also orthogonal components. **(b)** The two enantiomers bind in mirror image orientations such that the chiral centers have identical spatial coordinates, but both orientation vectors are completely orthogonal to the direction of approach.

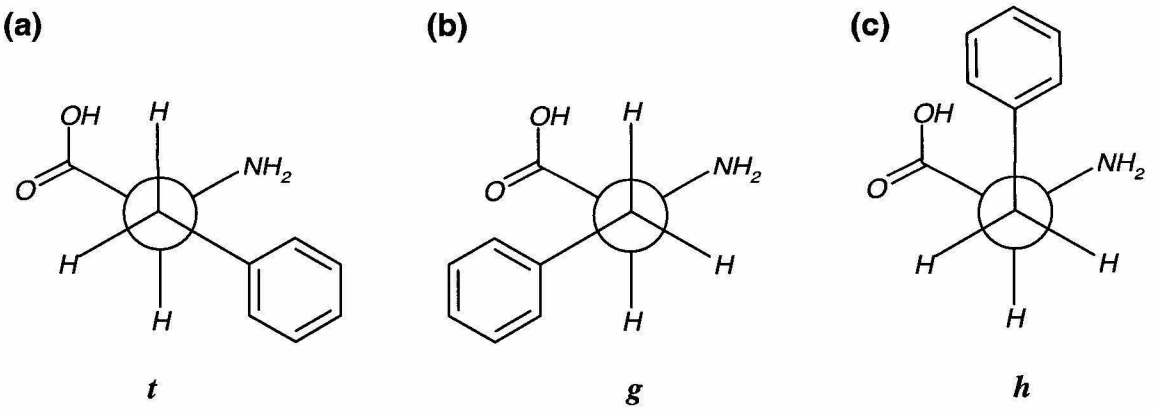

Figure 5. 12. Newman projections of staggered conformations of phenylalanine, viewed down the C_β-C_α bond. The L- enantiomer is shown, the corresponding conformations of D-phenylalanine being mirror images of the ones shown here. **(a)** In the ***t*** rotamer, the phenyl ring lies *trans* to the carboxylate group, and *gauche* to the amine group. **(b)** The ***g*** rotamer has the phenyl ring *gauche* to the carboxylate group, and *trans* to the amine group. This conformation has been ruled out for phenylalanine ammonia-lyase, as it cannot give rise to an anti-elimination mechanism. However, both ***t*** and ***g*** rotamers can give rise to the mirror image packing model proposed by Hanson (1981). **(c)** In the ***h*** rotamer, the phenyl group is in a hindered position, lying *gauche* to both the amine and the carboxylate groups. This rotamer has both the chiral carbon and the methylene carbon on the same side of these three groups, and cannot give rise to the proposed mirror image packing in the active site of phenylalanine ammonia-lyase.

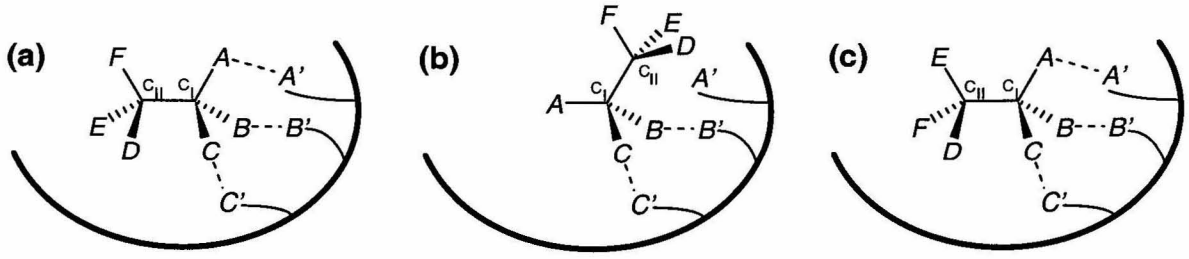

Figure 5. 13. Receptor interactions with three *locations* distributed in a (3-0) configuration in a ligand with two adjacent stereocenters. **(a)** *A*, *B* and *C*, the three *locations* interacting with receptor *sites A'*, *B'* and *C'* respectively, are all directly attached to the stereocenter C_I. **(b)** The opposite enantiomer can interact only at two out of the three *locations* on C_I. The ligand *location* required for an interaction with the third receptor *site* occupies a different spatial position. Enantioselectivity may be possible in this case. **(c)** However, the diastereomer incorporating opposite stereochemistry at C_{II} can interact with the receptor at the same three receptor *sites* as the stereoisomer shown in **(a)**. An interchange of the positions of groups *E* and *F* on the second stereocenter does not substantially alter the binding geometry at C_I. In this case, stereoselectivity would be primarily due to the intrinsic thermodynamic differences between diastereomers of the ligand, rather than the number of ligand *locations* interacting with the receptor.

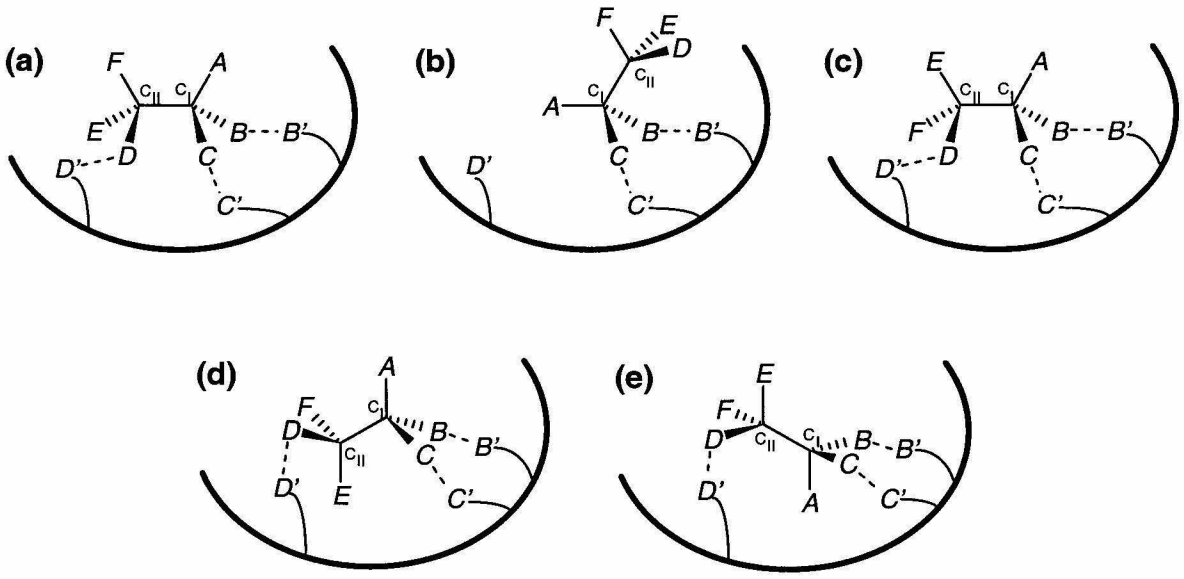

Figure 5. 14. Receptor interactions with three *locations* in the (2-1) configuration in a ligand with two adjacent stereocenters. **(a)** Of the three *locations* interacting with receptor *sites A'*, *B'* and *C'* respectively, *B* and *C* are attached to the stereocenter C_I, while *D* is attached to C_{II}. **(b)** The opposite enantiomer interacts at the two ligand *locations* attached to C_I, but the *location* at C_{II} now occupies different spatial coordinates, disrupting the interaction with the third receptor *site*. **(c)** However, the diastereomer incorporating opposite stereochemistry at C_{II} can interact with the receptor at the same three receptor *sites* as the stereoisomer shown in **(a)**, leading to loss of stereoselectivity between diastereomers. Moreover, mirror image binding orientations **(d,e)** of two enantiomers are possible in this distribution of ligand *locations*, which would diminish receptor enantioselectivity also. The stereoisomer shown in **(d)** is identical to the one shown in **(a)**, while the one shown in **(e)** is its enantiomer.

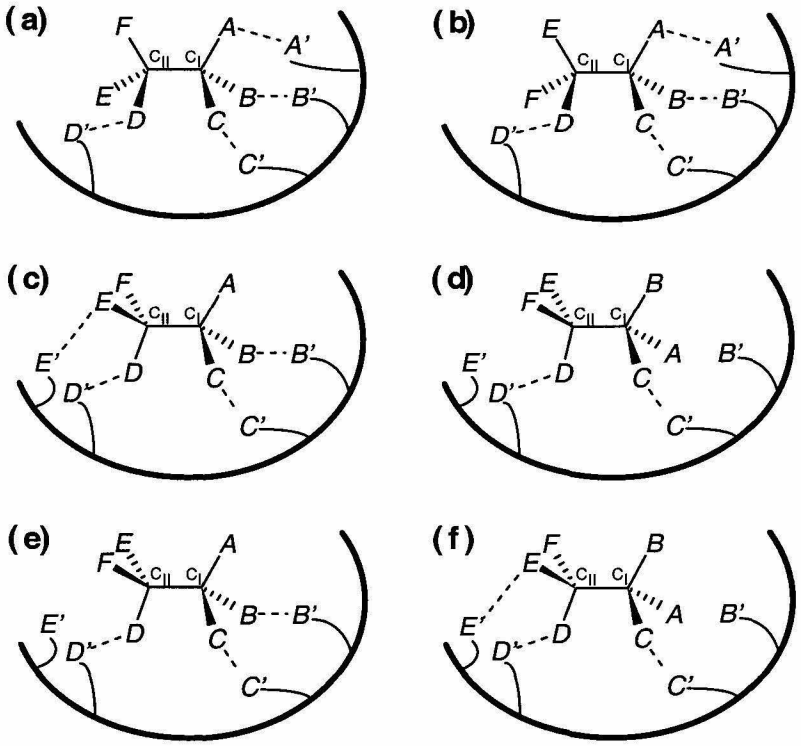

Figure 5. 15. Receptor interactions with four *locations* in a ligand with two adjacent stereocenters. **(a,b)** Interactions with a (3-1) distribution of ligand *locations* would fail to distinguish between two diastereomers that have opposite stereochemistry at C_{II}. **(c-f)** Distributing receptor interactions with four *locations* in a (2-2) configuration in the ligand can result in unique stereoselectivity. The stereoisomer shown in **(d)** is the enantiomer of the one in **(c)**, while those shown in **(e)** and **(f)** are the two diastereomers.

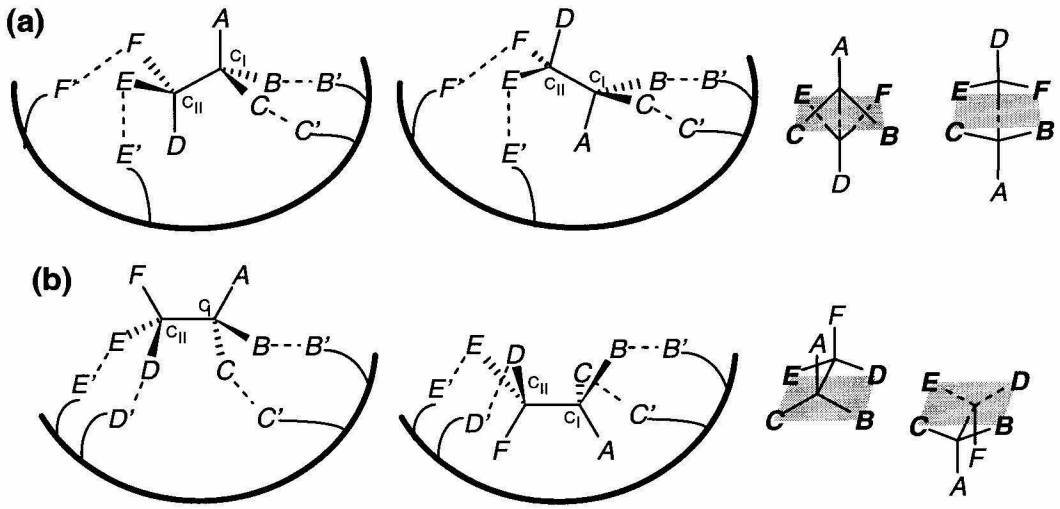

Figure 5. 16. Mirror image binding orientations in a (2-2) configuration of ligand *locations*. This is possible if the bound rotamer conformation of the ligand puts the four *locations* in a coplanar geometry. **(a)** The ligand binds in a staggered conformation, with the two stereocenters on opposite sides of the plane determined by the four *locations B*, *C*, *E* and *F* (shown as a grey quadrilateral). This plane intersects the bond between C_I and C_{II}. In one stereoisomer, the stereocenter C_I and the group *A* on it lie above this plane, but C_{II} and group *D* are below the plane, while in the enantiomer, the situation is reversed. **(b)** The ligand binds in an eclipsed conformation, with both stereocenters and the bond between them lying on the same side of the plane determined by *B*, *C*, *D* and *E*. In one stereoisomer, both stereocenters lie above this plane, while in its enantiomer, both stereocenters lie below the plane.

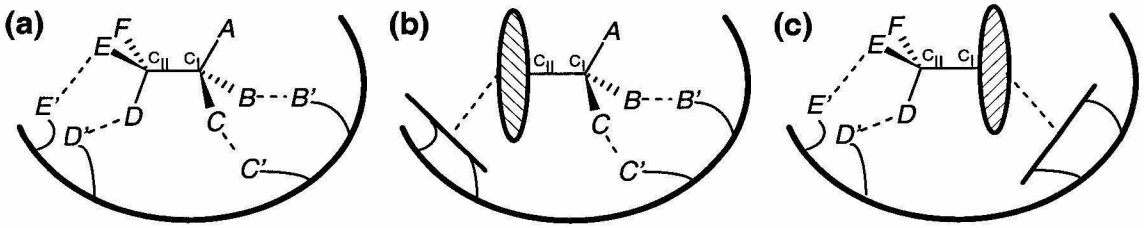

Figure 5. 17. Three effective *locations* per stereocenter in the (2-2) configuration of ligand *locations*. **(a)** Groups *B* and *C* are attached to C_I, while *D* and *E* are at C_{II}. **(b)** The sum of the interactions at *D* and *E*, which are attached to C_{II}, counts as one interaction with respect to C_I, because C_{II} is covalently linked to C_I. Thus, C_{II} and the *locations* attached to it together constitute the third effective *location* with respect to C_I. **(c)** Similarly, the sum of interactions at C_I constitutes one interaction with respect to C_{II}. C_I and its *locations* together constitute the third effective *location* with respect to C_{II}.

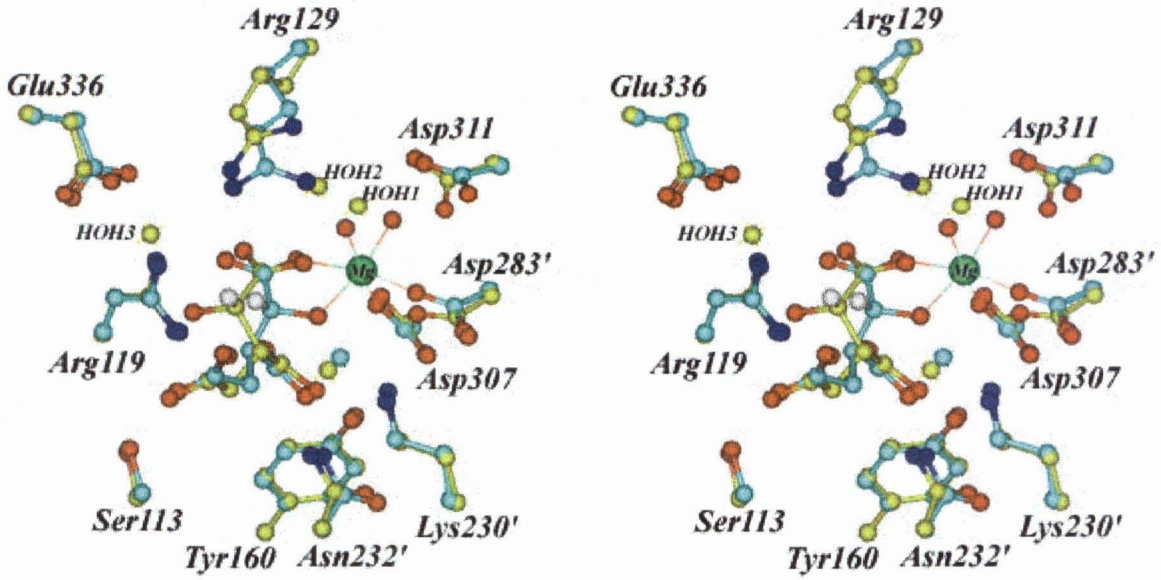

Figure 5. 18. Stereoviews of the superimposed structures of isocitrate stereoisomers bound to isocitrate dehydrogenase (IDH). The binding of D-isocitrate to IDH residues in the presence of metal ions is shown in blue, while the binding of L-isocitrate in the absence of metal ions is shown in yellow. The substituents on the C3 carbon bind to the same sets of enzyme residues, but the substituents on the C2 carbon bind differently in the two cases. Note that bond rotation plays a significant role in the interaction of the Arg129 residue with the carboxylate substituent on the C2 carbon. The other enzyme residues interacting with the two isocitrate stereoisomers occupy almost identical positions in the two cases.

(*Reproduced with permission from* Mesecar, A.D. and Koshland Jr., D.E. 2000. *Nature* **403:** 614-615.)

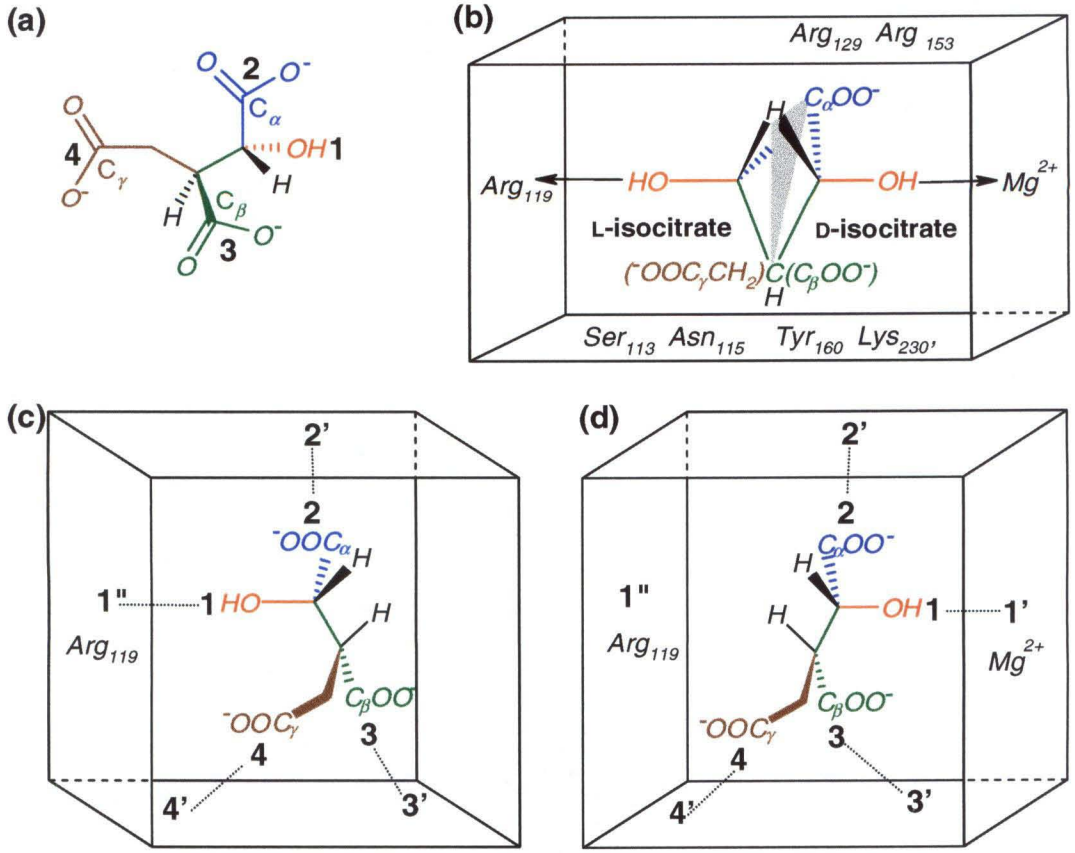

Figure 5. 19. Interactions of isocitrate with IDH. Four *locations*, –OH (**1**), $-C_\alpha OO^-$ (**2**), $-C_\beta OO^-$ (**3**) and $-CH_2C_\gamma OO^-$ (**4**), are distributed on two stereocenters in isocitrate, in a (2-2) configuration **(a)**, leading to three effective *locations* on the chiral C2 carbon. A hypothetical mirror plane may be drawn **(b)** through –H, $-C_\alpha OO^-$ and the chiral C3 carbon, with the C2 carbon of the (2S,3R) and (2R,3S) stereoisomers on opposite sides. In the absence of Mg^{2+}, the –OH group of (2S,3R)-isocitrate binds to the Arg119 residue **(c)**. In the presence of Mg^{2+}, the –OH group of (2R,3S)-isocitrate binds to the metal **(d)**. The other three ligand *locations* bind to the same sets of enzyme residues.

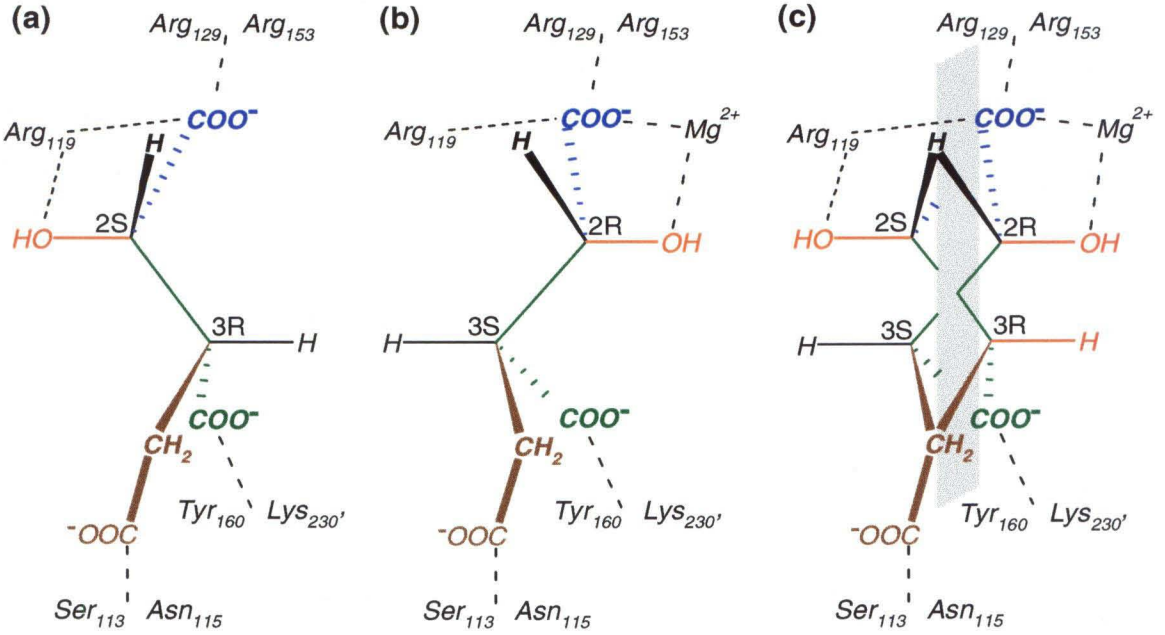

Figure 5. 20. Idealized mirror-image orientations of isocitrate stereoisomers bound to IDH. (2S,3R)-isocitrate binds to the metal-free enzyme, such that the $-COO^-$ and –OH groups on the chiral C2 carbon to interact with Arg119. The $-COO^-$ group also interacts with Arg129 and Arg153 in the enzyme **(a)**. (2R,3S)-isocitrate binds to the metal-containing enzyme, such that the interactions of the $-COO^-$ group on the chiral C2 carbon are retained, but the –OH group binds to the metal ion **(b)**. A hypothetical plane may be drawn through the four groups shown in **(c)**, with the two stereocenters in each stereoisomer lying on opposite sides. Note that the torsional flexibility offered by the methylene group allows the carboxylate in the $-CH_2COO^-$ group to lie on the same side of this hypothetical plane. Also note that the –OH group in the isocitrate stereoisomers lies outside this hypothetical plane.

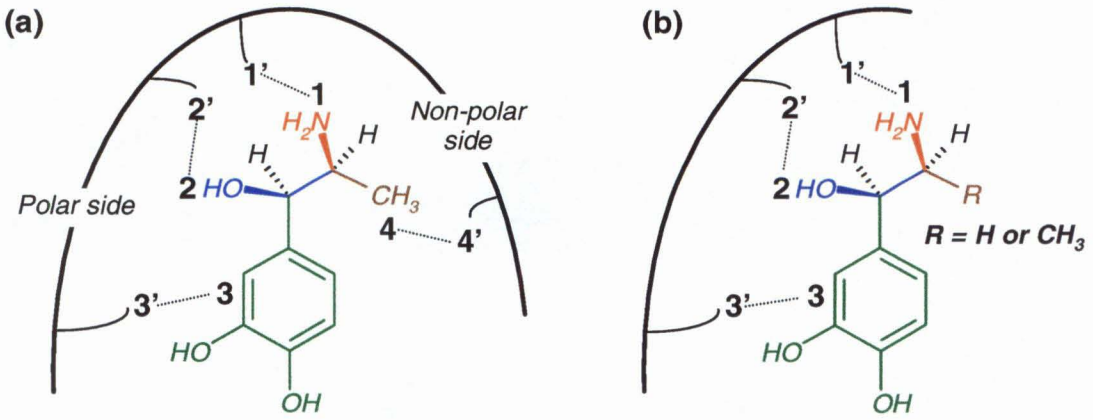

Figure 5. 21. Interactions of (1R,2S)-α-methylnoradrenaline with adrenergic receptors. The drug molecule has four *locations* distributed in a (2-2) configuration, interacting with α_2-adrenergic receptors **(a)**. The $-NH_2$ (**1**) group on one stereocenter and the –OH (**2**) and catechol (**3**) groups on another stereocenter bind to receptor *sites* **1'**, **2'** and **3'** on the polar side of a receptor surface. The $-CH_3$ (**4**) group either binds to a *site* **4'** on the non-polar side (Ruffolo 1983) or sterically affects the binding of the other three groups (Triggle 1976). On the other hand, α_1-adrenergic receptors **(b)** seem to interact with the $-NH_2$, –OH and catechol groups only, and not with the methyl group. Therefore, both (1R)-noradrenaline and (1R,2S)-α-methylnoradrenaline have equipotent drug action at these receptors.

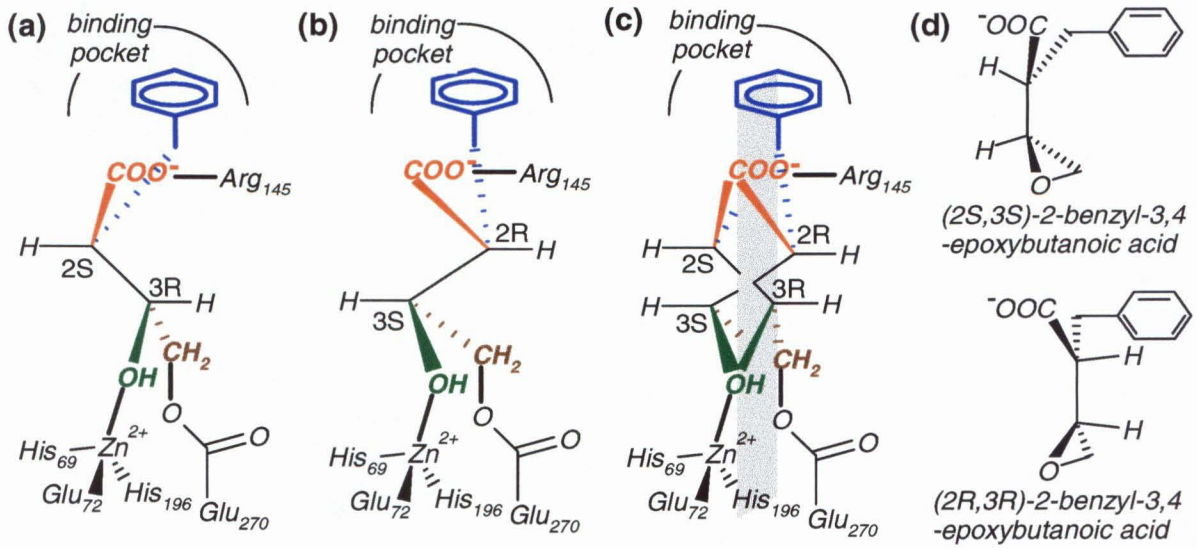

Figure 5. 22. Inactivation of carboxypeptidase A. (2S,3R)- 2-benzyl-3,4-epoxybutanoic acid **(a)** inactivates the enzyme by means of covalent bond formation at the active site. An ester linkage is formed between the $-CH_2$ group in the epoxide ring of the inhibitor and the Glu270 residue in the enzyme, while the epoxy oxygen is converted to a hydroxyl group. The (2R,3S)- stereoisomer **(b)** also has the same set of interactions with the enzyme, and also irreversibly inactivates the enzyme. In the enzyme-inactivator complex, a hypothetical mirror plane relating these two isomers can be drawn **(c)** through the carbon atoms of the carboxylate group and the benzyl group on the C2 carbon and the ester methylene carbon and the hydroxyl oxygen atom on the C3 carbon. For the (2R,3R) and (2S,3S) stereoisomers, a similar arrangement can only be achieved in an unfavorable eclipsed conformation, as shown in **(d)**, with the corresponding *locations* on the C2 carbon being placed relatively farther apart from those on the C3 carbon.

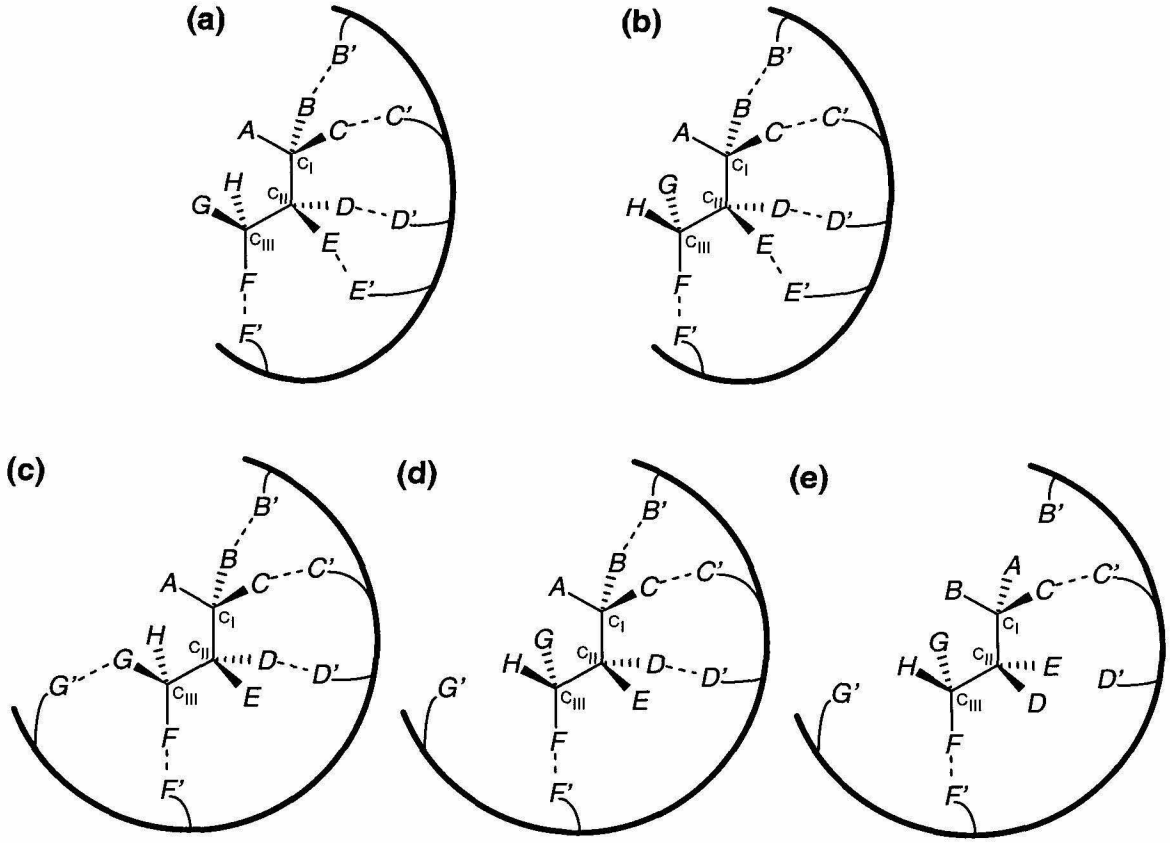

Figure 5. 23. Receptor interactions with five *locations* in a ligand with three consecutive stereocenters. The ligand stereoisomer shown in **(b)** and **(d)** has the opposite chirality at the C_{III} carbon, as compared to the one shown in **(a)** and **(c)**. In **(a)** and **(b)**, ligand *locations* are in the (2-2-1) configuration (*B* and *C* on C_I; *D* and *E* on C_{II}; *F* on C_{III}), and diastereomers with inverted stereochemistry at the C_{III} carbon remain unresolved. When ligand *locations* are in the (2-1-2) configuration (*B* and *C* on C_I; *D* on C_{II}; *F* and *G* on C_{III}), the receptor can distinguish between diastereomers **(c)** and **(d)** and also between enantiomers **(c)** and **(e)**.

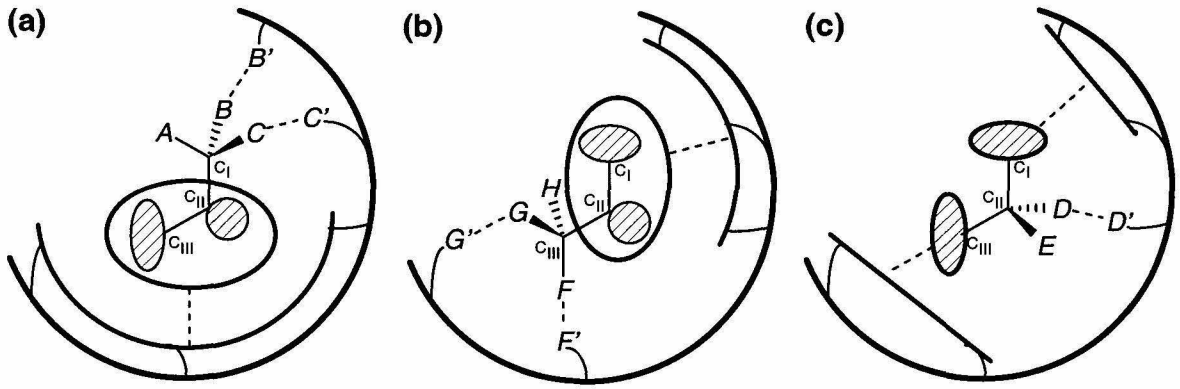

Figure 5. 24. Three effective *locations* per stereocenter in a ligand with three stereocenters. **(a)** Groups *B* and *C* form two *locations* at C_I, while all the *locations* at C_{II} and C_{III} together act as an effective third *location* with respect to C_I. **(b)** Similarly, groups *F* and *G* are two *locations* at C_{III}, while all the locations at C_I and C_{III} together act as an effective third *location* with respect to C_{III}. **(c)** Group D forms one *location* at C_{II}, while the *locations* at C_I together act as an effective second *location* and the *locations* at C_{III} form the effective third *location* with respect to C_{II}.

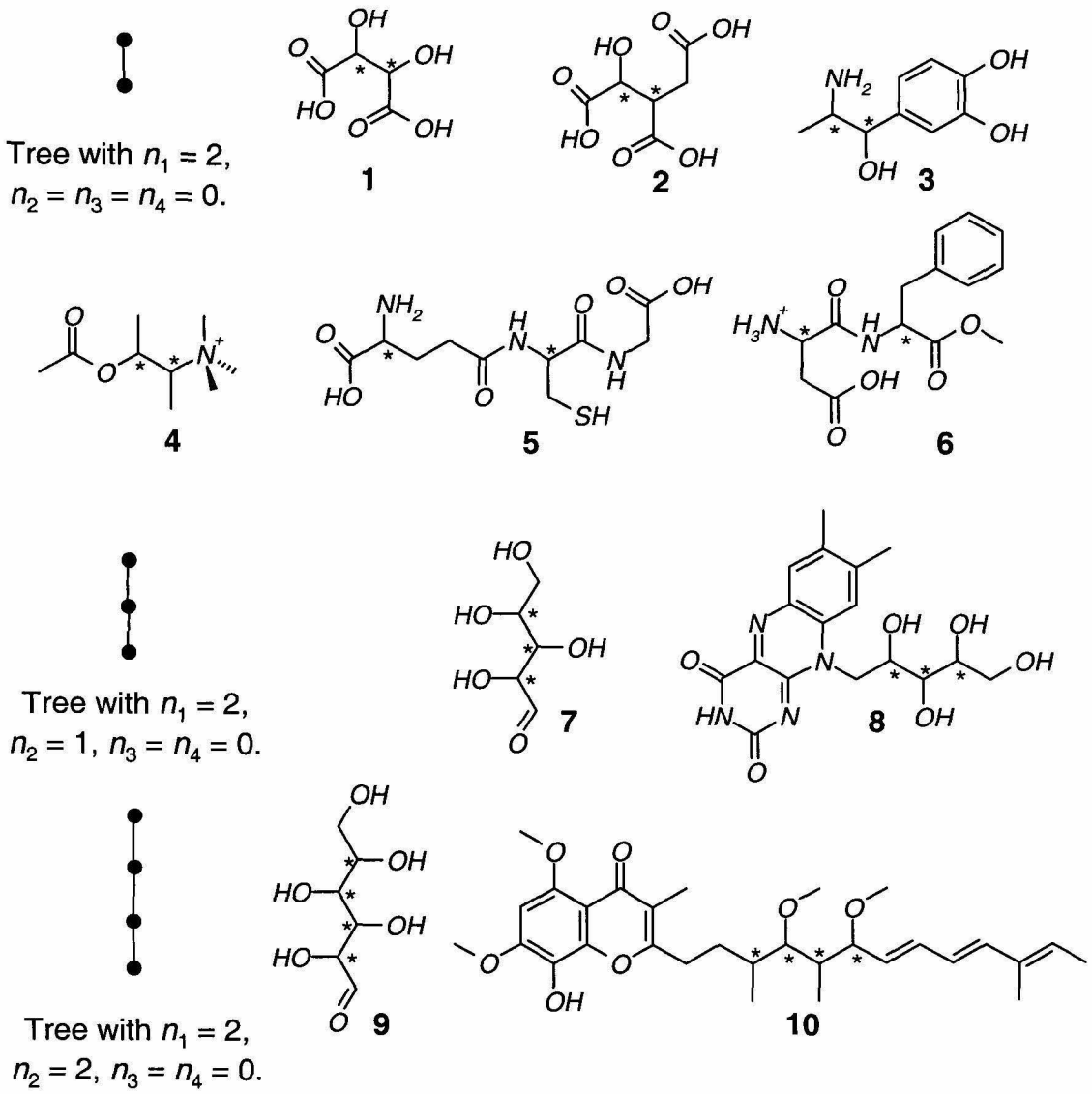

Figure 5. 25. Examples of tree representations of molecules with multiple stereocenters in acyclic structures. The stereocenters are indicated with asterices. **1** = tartaric acid, **2** = isocitric acid, **3** = α-methylnoradrenaline, **4** = α,β-dimethylacetylcholine, **5** = glutathione, **6** = aspartame, **7** = aldopentose, e.g., ribose, arabinose and xylose, **8** = riboflavin (vitamin B2), **9** = stigmatellin A, **10** = aldohexose, e.g., glucose, mannose and galactose.

References

Ács, M. 1995. *Acta. Chim. Hung.- Models in Chemistry.* **132:** 409-434.

Ahn, S., Ramirez, J., Grigorean, G., and Lebrilla, C.B. 2001. *J. Am. Soc. Mass Spectrom.* **12:** 276-287.

Amrhein, N., Gödekke, K.-H., and Kefeli, V.I. 1976. *Ber. Dtsch. Bot. Ges.* **89:** 246-259.

Andelman, D. and Orland, H. 1993. *J. Am. Chem. Soc.* **115:** 12322-12329.

Arnett, E.M., and Zingg, S.P. 1981. *J. Am. Chem. Soc.* **103:** 1221-1222.

Bentley, R. 1978. *Nature.* **276:** 673-676.

Bentley, R. 1983. *Trans. NY Acad. Sci. Ser. II* **41:** 5-24.

Bergmann, M., Zervas, L., and Fruton, J.S. 1936. *J. Biol. Chem.* **115:** 593-611.

Bergmann, M. and Fruton, J.S. 1937. *J. Biol. Chem.* **117:** 189-202.

Booth, T.D. and Wainer, I.W. 1996. *J. Chromatogr. A.* **737:** 157-169.

Booth, T.D., Wahnon, D., and Wainer, I.W. 1997. *Chirality.* **9:** 96-98.

Cahn, R.S., Ingold, C., and Prelog, V. 1966. *Angew. Chem. Int. Ed. Engl.* **5:** 385-415.

Caira, M.R., Clauss, R., Nassimbeni, L.R., Scott, J.L., and Wildervanck, A.F. 1997. *J. Chem. Soc. Perkin Trans.* **2:** 763- 768.

Copeland, R.A. 2000. *Enzymes: A practical introduction to structure, mechanisms and data analysis*, 2nd ed. pp. 149-150. John Wiley and Sons, New York, NY.

Cushny, A.R. 1926. *Biological relations of optically isomeric substances.* Williams and Wilkins, Baltimore, MD.

Dalgliesh, C.E. 1952. *J. Chem. Soc.* **132:** 3940-3942.

Davankov, V.A. and Kurganov, A.A. 1983. *Chromatographia.* **17:** 686-690.

Davankov, V.A. 1997. *Chirality.* **9:** 99-102.

DeTar, D.F. 1981. *Biochemistry.* **20:** 1730-1743.

Easson, L. and Stedman, E. 1933. *Biochem. J.* **27:** 1257-1266.

Fersht, A. 1999. *Structure and mechanism in protein science: A guide to enzyme catalysis and protein folding*, ed. pp. 248-249. W. H. Freeman and Company, New York, NY.

Fischer, E. 1894. *Ber. Dtsch. Chem. Ges.* **27:** 2985-2993.

Gerlt, J.A., Kenyon, G.L., Kozarich, J.W., Neidhart, D.J., Petsko, G.A. and Powers, V.M. 1992. *Curr. Opin. Struct. Biol.* **2:** 736-742.

Glavas, S. and Tanner, M.E. 1999. *Biochemistry.* **38:** 4106-4113.

Hanson, K.R. 1981. *Arch. Biochem. Biophys.* **211:** 575-588.

Havir, E.A. and Hanson, K.R. 1968. *Biochemistry.* **7:** 1904-1914.

Jennings, G.T., Minard, K.I., and McAlister-Henn, L. 1997. *Biochemistry.* **36:** 13743-13747.

Koshland Jr., D.E. 1958. *Proc. Natl. Acad. Sci.* **44:** 98-104.

Koshland Jr., D.E., Neméthy, G., and Filmer, D. 1966. *Biochemistry.* **5:** 365-385.

Kuroda, Y., Kato, Y., Higashioji, T., and Ogoshi, H. 1993. *Angew. Chem. Int. Ed. Engl.* **35:** 723-725.

Lee, S.S., Li, Z.-H., Lee, D.H., and Kim, D.H. 1995. *J. Chem. Soc. Perkin Trans.* **1:** 2877-2882.

Mackenzie, N.E., Fagerness, P.E., and Scott A.I. 1985. *J. Chem. Soc. Chem. Comm.* **10:** 635-637.

Mesecar, A.D. and Koshland Jr., D.E. 2000a. *IUBMB Life.* **49:** 457-466.

———. 2000b. *Nature.* **403:** 614-615.

Mislow, K. 1962. Stereoisomerism. In *Comprehensive Biochemistry,* v. 1 (eds. M. Florkin and E.H. Stotz). pp. 192-243. Academic Press, New York, NY.

Morris, N.M., Greally, B.R., and Cairns, P.M. 1996. *J. Liq. Chromatogr. R. T.* **19:** 489-502.

Nederkoorn, P.H.J., vanGelder, E.M., denKelder G.M.D.O., and Timmerman, H. 1996. *J. Comput. Aid. Mol. Des.* **10:** 479-489.

Nesterenko, P.N., Krotov, V.V., and Staroverov, S.M. 1994. *J. Chromatogr. A.* **667:** 19-28.

Nickolau, K.C., Boddy, C.N.C., and Siegel, J.S. 2001. *Angew. Chem. Int. Ed. Engl.* **40:** 701-704.

Ogston, A.G. 1948. *Nature.* **163:** 963-963.

Parascandola, J. and Jasensky, R. 1974. *Bull. Hist. Med.* **48:** 199-220.

Pirkle, W.H., Welch, C.J., and Hyun, M.H. 1983. *J. Org. Chem.* **48**: 5022-5026.

Pirkle, W.H. and Pochapsky, T.C. 1986. *J. Am. Chem. Soc.* **108:** 5627-5628.

Pirkle, W.H. 1997. *Chirality.* **9:** 103.

Popjak, G. and Cornforth, J.W. 1966. *Biochem. J.* **101:** 553-568.

Quiocho, F.A. and Vyas, N.K. 1984. *Nature.* **310:** 381-386.

Reetz, M.T., Huette, S., and Goddard, R. 1999. *Eur. J. Org. Chem.* **1999:** 2475-2478.

Ruffolo Jr., R.R. 1983. Stereoselectivity in adrenergic agonists and adrenergic blocking agents. In *Stereochemistry and Biological Activity of Drugs* (eds. E.J. Ariens, W. Soudjin, P.B.M.W.M. Timmermans), pp. 103-125. Blackwell Scientific, Oxford, UK.

Ryu, S.-E., Choi, H.-J., and Kim, D.H. 1997. *J. Am. Chem. Soc.* **119:** 38-41.

Salem, L., Chapuisat, X., Segal, G., Hiberty, P.C., Minot, C., Leforestier, C., and Sautet, P. 1987. *J. Am. Chem. Soc.* **109:** 2887-2894.

Shallenberger, R.S. 1983. *Food Chem.* **12:** 89-107.

Silverman, R.B. 1992. *The organic chemistry of drug design and drug action.* pp. 74-86. Academic Press, New York, NY.

Sokolov, V.I. and Zefirov, N.S. 1991. *Dokl. Akad. Nauk. SSSR.* **319**: 1382-1383.

Soundar, S., Danek, B.L., and Colman, R.F. 2000. *J. Biol. Chem.* **275:** 5606-5612.

Suami, T. and Hough, L. 1993. *Food Chem.* **46:** 235-238.

Sun, S. and Toney, M.D. 1999. *Biochemistry.* **38:** 4058-4065.

Sundaresan, V., Ru, M.T., and Arnold, F.H. 1997. *J. Chromatogr. A.* **775:** 51-63.

Topiol, S. and Sabio M. 1989. *J. Am. Chem. Soc.* **111:** 4109-4110.

———. 1996. *Enantiomer.* **1:** 251-265.

Triggle, D.J. 1976. Structure-activity relationships: Chemical constitution and biological activity. In *Chemical Pharmacology of the Synapse* (eds., D.J. Triggle and C.R. Triggle), pp. 233-430. Academic Press, New York, NY.

Vestues, P.I. and Martin, R.B. 1980. *J. Am. Chem. Soc.* **102:** 7906-7909.

Vyas, N.K., Vyas, M.N., and Quiocho, F.A. 1988. *Science.* **242:** 1290-1295.

Welch, C.J. 1994. *J. Chromatogr. A.* **666:** 3-26.

Wilcox, P.E., Heidelberger, C., and Potter, V.R. 1950. *J. Am. Chem. Soc.* **72:** 5019-5024.

Yun, M., Park, C., Kim, S., Nam, D., Kim, S.C., and Kim, D.H. 1992. *J. Am. Chem. Soc.* **114:** 2281-2282.